獸醫學博士 學位論文

Elucidation of canine immune response to *Mycobacterium avium* complex infection

개에서의 *Mycobacterium avium* complex 감염에 대한 숙주 면역반응 규명

2022년 2월

서울대학교 대학원

수의학과 수의병인생물학 및 예방수의학 전공

김 수 지

Elucidation of canine immune response to *Mycobacterium avium* complex infection

A Dissertation
Submitted to the Faculty of Graduate School of Seoul National University in Partial Fulfillment of the Requirements for the Degree of Doctor of Philosophy in Veterinary Pathobiology and Preventive Medicine

Department of Veterinary Medicine
(Major: Veterinary Pathobiology and Preventive Medicine)
The Graduate School
Seoul National University

By
Suji Kim

2022

Elucidation of canine immune response to *Mycobacterium avium* complex infection

지도교수 : 유 한 상

이 논문을 수의학박사 학위논문으로 제출함
2021년 12월

서울대학교 대학원
수의학과 수의병인생물학 및 예방수의학 전공
김 수 지

김수지의 수의학박사 학위논문을 인준함
2022년 1월

위 원 장 _____ (인)

부위원장 _____ (인)

위 원 _____ (인)

위 원 _____ (인)

위 원 _____ (인)

Abstract

Elucidation of canine immune response to *Mycobacterium avium* complex infection

Suji Kim

(Supervisor: Prof. Han Sang Yoo, D.V.M., Ph.D)

Department of Veterinary Medicine

The Graduate School

Seoul National University

Nontuberculous mycobacteria (NTM) are ubiquitous bacteria that are widely distributed in natural environments such as soil, water, and dust. *Mycobacterium avium* complex (MAC), to which *M. avium* and *M. intracellulare* belong, is a major opportunistic pathogen causing chronic lung disease in humans. MAC can infect a wide range of hosts, including dogs and there have been sporadic reports of MAC-induced mycobacteriosis in dogs. However, in most cases, infected dogs were euthanized or died due to clinical deterioration, a lack of response to therapy, and poor prognosis. Nevertheless, the underlying mechanisms of MAC infection in dogs

have not yet been studied. In addition, dogs represent a reservoir of zoonotic diseases caused by *Mycobacterium tuberculosis*-complex (MTBC) such as *M. tuberculosis*, *M. bovis* and *M. microti*. The zoonotic potential of MAC has not been elucidated in dogs; however, the zoonotic aspects of MAC transmitted by domestic animals and wildlife have a major impact on human health. Therefore, investigating the canine immune response to MAC infection is important for diagnosis and treatment and can help to control potential zoonotic transmission between humans and dogs.

M. avium subsp. *hominissuis* (MAH) has been identified as a major causative agent of canine mycobacteriosis by members of the MAC family. In this study, the host immune response against MAH infection was investigated by transcriptome analysis of canine peripheral blood mononuclear cells (PBMCs). Transcriptome profiling revealed that MAH infection induced a T cell immune response related to Th1 and Th17 cells. The expression of Th1-associated genes was identified in early infection, while that of Th17-associated genes increased 12 hours after infection. The expression of apoptosis-related genes decreased and the abundance of intracellular MAH increased within macrophages after 24 h. The results showed that MAH induces Th1 and Th17 immune responses and can survive within canine macrophages by avoiding apoptosis signaling.

Although MAH appears to be the predominant pathogenic subspecies in canine cases, most case reports have not described the species and subspecies. The identification of species in canine mycobacteriosis is difficult due to sample

acquisition, unspecific clinical signs and long incubation periods. However, different treatment regimens are required for each species of MAC because they exhibit differential pathogenicity and antibiotic susceptibilities. In particular, *M. intracellulare* is a major causative agent of MAC lung disease along with *M. avium*, and it mainly occurs from environmental sources rather than by infected individuals. In Korea, it was reported that *M. intracellulare* accounted for the majority of NTM distributed in animal shelters and parks. Therefore, companion animals might easily come in contact with *M. intracellulare*. In this study, the host immune response to *M. intracellulare* infection was investigated by coculture systems of canine T helper cells and autologous monocyte-derived macrophages (MDMs). Transcriptome analysis revealed that canine MDMs differentiated into M1-like macrophages and secreted molecules that induced Th1/Th17 cell polarization. The coculture systems showed that Th17 cells predominantly responded to *M. intracellulare* infection through macrophage activation in dogs.

New species and subspecies of MAC are still being identified and pose new threats to disease control. These new species and subspecies of MAC exhibit genetic diversity and evolution with respect to antimicrobial susceptibility, host specificity, and pathogenicity. It is important to understand the genomic characteristics of newly identified species for the control of diseases caused by MAC. The genetic characteristics of MAC have been elucidated with the development of whole genome sequencing. However, *M. intracellulare* is poorly understood compared to the other MAC species.

In Korea, *M. intracellulare* strains newly isolated from animal shelters and parks indicated various antimicrobial resistance patterns for each species. In this study, the genomic characteristics of these *M. intracellulare* isolates were investigated by single-molecule real-time (SMRT) sequencing. The comparative analysis of *M. intracellulare* isolates showed genetic diversity and evolution in relation to virulence factors such as mammalian cell entry and the type VII secretion system. These genetic differences were also associated with cytokine induction and survival in alveolar macrophages. Genetic variation of these environmental isolates will pose a new threat to dogs that are easily exposed to environmental sources.

Investigating the host immune response is important for disease prevention and treatment development as MAC infection has been reported in dogs. The findings from this study will contribute to a better understanding of the pathogenesis and susceptibility of MAC in dogs and the control of potential zoonotic transmission.

K**eywords:** *Mycobacterium avium* complex, Cellular immune response, Dog, Transcriptome analysis, Whole genome sequencing

Student Number: 2016-21760

Contents

List of Figures

List of Tables

List of Abbreviations

AMR	Antimicrobial resistance gene
BLAST	Basic local alignment search tool
CD	Cluster of differentiation
CFU	Colony forming unit
COG	Clusters of Orthologous Group
DEG	Differentially expressed gene
ELISA	Enzyme-linked immunosorbent assay
GAPDH	Glyceraldehyde-3-phosphate dehydrogenase
GO	Gene ontology
IFN-γ	Interferon-gamma
IL	Interleukin
IPA	Ingenuity pathway analysis
LPS	Lipopolysaccharide
M1	Classically activated macrophages
M2	Alternatively activated macrophages
MAC	*Mycobacterium avium* complex
MCE	Mammalian cell entry
M-CSF	Macrophage colony-stimulating factor
MDM	Monocyte-derived macrophages

MOI	Multiplicity of infection
NTM	Non-tuberculous mycobacteria
OD	Optical density
PBMC	Peripheral blood mononuclear cell
PCR	Polymerase chain reaction
PMA	Phorbol 12-myristate 13-acetate
PPI	Protein-protein interaction
RLU	Relative light unit
RNA-Seq	RNA sequencing
RT-qPCR	Reverse transcription quantitative real-time PCR
SMRT	Single-molecule real-time
T7SS	Type VII secretion systems
Th	Helper T cells
TNF	Tumor necrosis factor
VF	Virulence factor

General Introduction

Nontuberculous mycobacteria (NTM) are opportunistic bacteria that are highly abundant in environmental niches such as soil and water sources (Falkinham, 2015). *Mycobacterium avium* complex (MAC) is one of the most prevalent pathogenic NTM that cause chronic pulmonary disease worldwide (Huchzermeyer & Michel, 2001; Prevots & Marras, 2015; Stout, Koh, & Yew, 2016). MAC has a wide range of host susceptibilities, including in companion animals (Campora, Corazza, Zullino, Ebani, & Abramo, 2011; Pavlik, Svastova, Bartl, Dvorska, & Rychlik, 2000). Canine mycobacteriosis caused by MAC has been reported in multiple organs with granulomatous inflammation (Campora et al., 2011; Horn, Forshaw, Cousins, & Irwin, 2000; M.-C. Kim, Kim, Kang, Jang, & Kim, 2016). Dogs with mycobacteriosis caused by MAC usually have poor prognoses due to the difficulty of diagnosis and nonspecific clinical signs (Ghielmetti & Giger, 2020). However, the underlying mechanism of MAC infection in dogs has not yet been elucidated. *M. avium* subsp. *hominissuis* (MAH) is the most common etiological agent in canine mycobacteriosis caused by MAC (Ghielmetti & Giger, 2020; Marianelli, Ape, & Rossi Mori, 2020). Therefore, this study investigated the canine immune response to MAC infection with MAH as a representative causative agent. To understand the mechanism of MAH infection, gene expression on canine peripheral blood mononuclear cells (PBMCs) was analyzed according to the infection time. Intracellular survival and replication in canine monocyte-derived macrophages

(MDMs) were also identified to determine whether MAH evades the host immune response.

Unlike *M. avium* subsp. *hominissuis*, other MAC species have rarely been reported in dogs (Cucchi et al., 2009; Kontos, Papadogiannakis, Mantziaras, Styliara, & Kanavaki, 2014; O'Toole, Tharp, Thomsen, Tan, & Payeur, 2005; Zeiss, Jardine, & Huchzermeyer, 1994). However, many cases of canine MAC infection have not been identified at the species and subspecies levels due to low disease awareness, and the time-consuming and laborious detection methods. In addition, many cases are unreported because of the absence of epidemiological data for a non-notifiable disease, the negligible impact of additional case reports, and misdiagnoses. Furthermore, some *Mycobacterium* species can be transmitted from domestic dogs to humans, and an infected dog can act as a reservoir for human infection even though it can be a negligible pathogen in canine cases (Bonovska, Tzvetkov, Najdenski, & Bachvarova, 2005; Olea-Popelka et al., 2017). For this reason, it is important to investigate the canine immune response to other members of MAC in dogs, which will aid in the diagnosis and treatment as well as control the potential zoonotic risk.

M. intracellulare, a major pathogenic species of MAC along with *M. avium*, is widely distributed in the environment (Diel et al., 2018). MAC infection mainly occurs by exposure to environmental sources due to its ubiquitous nature (Shin, Shin, & Shin, 2020). In Korea, *M. intracellulare* accounted for the majority of NTM

isolates from soils in animal shelters and parks (Park et al., 2020). Most *M. intracellulare* isolates were multidrug-resistant strains and each isolate showed various antibiotic susceptibilities. Therefore, *M. intracellulare* and newly isolated strains could be a potential threat to dogs because they are prone to contact environmental sources. For this reason, the host immune response to *M. intracellulare* infection was investigated with canine macrophages and T lymphocytes, and the characteristics of *M. intracellulare* isolates were analyzed using whole genome sequencing.

Mycobacterium is an intracellular pathogen that primarily affects macrophages (Thegerström et al., 2012). Macrophages are the first line of defense against pathogen invasion and undergo apoptotic cell death to minimize tissue injury and decrease pathogen viability (Behar, Divangahi, & Remold, 2010). However, *Mycobacterium* survives and replicates within macrophages by preventing the phagosome maturation process (Early, Fischer, & Bermudez, 2011; O'Sullivan, O'Leary, Kelly, & Keane, 2007; Rojas, Barrera, & García, 1998). Macrophage plasticity is key for mycobacterial control (Refai, Gritli, Barbouche, & Essafi, 2018). M1 macrophages enhance microbicidal activity by releasing proinflammatory cytokines, while M2 macrophages produce anti-inflammatory cytokines that cause persistent mycobacterial infection (Murray et al., 2014; Thiriot, Martinez-Martinez, Endsley, & Torres, 2020). Macrophages have mainly exhibited a transformation from the M1 phenotype to the M2 phenotype during mycobacterial infection (Lugo-Villarino, Vérollet, Maridonneau-Parini, & Neyrolles, 2011; Refai et al., 2018).

However, some studies recently reported that macrophages polarize to a unique phenotype after mycobacterial infection (Tomioka et al., 2012). In particular, mouse macrophages exhibit a novel polarization that downregulates Th1/Th2 cell production while driving Th17 polarization after MAC infection (Tatano, Shimizu, & Tomioka, 2014).

T cell immune responses are important in regulating MAC infection. In particular, the Th1/Th17 balance is crucial for protection against mycobacterial infection (Matsuyama et al., 2014; Wang et al., 2012). The T helper 1 (Th1) response is essential for controlling mycobacterial infection by increasing macrophage bactericidal capacity (Haverkamp, Van Dissel, & Holland, 2006). The T helper 17 (Th17) response is involved in the antimycobacterial response by accelerating the accumulation of Th1 cells (Gopal et al., 2012; Ouyang, Kolls, & Zheng, 2008; Shu et al., 2018). However, the Th17 response has pathological effects during MAC infection under Th1-diminished conditions (Matsuyama et al., 2014; Lichen Xu et al., 2016). Th17 development induces excessive neutrophilic pulmonary inflammation by reducing Th1 responses and can increase susceptibility to systemic MAC infection. Inflammation and neutrophil recruitment driven by Th17 cells play a pivotal role in granuloma formation and mycobacterial disease development (Cardona & Cardona, 2019; Torrado & Cooper, 2010). In particular, IL-17 plays a crucial role in chronic inflammation and is important for the formation and maintenance of granulomas in mycobacterial infection sites (Q. Li et al., 2016; Ostadkarampour et al., 2014).

Whole-genome sequencing of MAC provides insight into not only the genetic differences between species and strains but also genomic characterization, including virulence and pathogenesis. However, genome sequencing of MAC was predominantly performed in *M. avium* (Bannantine, Conde, Bayles, Branger, & Biet, 2020; J. Lim et al., 2021; Uchiya et al., 2017). The complete sequences of *M. intracellulare* still need to be constructed. In particular, for *M. intracellulare*, differentiating the subspecies and related species is difficult using conventional methods because they are closely related genetically (Pranada, Witt, Bienia, Kostrzewa, & Timke, 2017; Van Ingen et al., 2012). Some *M. intracellulare* strains, which were previously identified by sequence-based typing analyses, were recently reclassified as *M. intracellulare*-related strains such as *M. indicus pranii*, *M. yongonense*, *M. paraintracellulare*, and *M. chimaera* (S.-Y. Kim et al., 2015; S.-Y. Kim et al., 2017). However, taxonomic controversies remain in *M. intracellulare* and related strains (van Ingen, Turenne, Tortoli, Wallace Jr, & Brown-Elliott, 2018). A recent report revealed some discrepant cases in previously classified *M. intracellulare* clinical strains by whole genome sequencing (Tateishi et al., 2021). In this study, the genomic characteristics of six *M. intracellulare* isolates from the environment in Korea were analyzed by single-molecule real-time sequencing. The complete genomes of *M. intracellulare* isolates were compared with that of *M. intracellulare* ATCC13950 to identify genetic differences between the isolates and reference strain. Pangenome analysis provided genetic differences regarding the virulence and pathogenesis of *M. intracellulare* isolates. Phylogenetic analysis of

MAC species and isolates indicated that some strains should be reclassified as either *M. chiamera* or *M. paraintracellulare*.

This study revealed the host immune response to MAC infection in dogs and analyzed the genetic characterization of newly isolated *M. intracellulare* from animal shelters and parks. This study will help us understand the pathogenesis of MAC and develop diagnostics techniques and treatments for dogs.

Literature Review

Pathogenic mycobacteria are composed of the following three major groups: *Mycobacterium tuberculosis* complex, *Mycobacterium leprae*, and nontuberculous mycobacteria (NTM). NTM are ubiquitous in the environment and can cause a wide range of mycobacterial infections. NTM are classified into slow growers, which include *Mycobacterium avium* complex (MAC), and rapid growers, which include *Mycobacterium abscessus*, *Mycobacterium chelonae*, and *Mycobacterium fortuitum*. Slow-growing mycobacteria grow for more than 7 days, whereas rapid-growing mycobacteria grow on culture media within 7 days (Henkle, Hedberg, Schafer, & Winthrop, 2017).

Mycobacterium avium complex

Mycobacterium avium complex (MAC) is the most common nontuberculous mycobacteria (NTM) that cause pulmonary disease. MAC pulmonary disease is important as a chronic and debilitating disease associated with high mortality (Kendall & Winthrop, 2013; Saleeb & Olivier, 2010). In the United States, the incidence and prevalence of pulmonary disease (PD) caused by mycobacteria increased predominantly due to *M. avium* complex (Prevots & Marras, 2015). Although pulmonary diseases caused by other NTM species are stable in Japan, the incidence of pulmonary MAC disease is rapidly increasing (Namkoong et al., 2016).

In Korea, *M. avium* and *M. intracellulare* are the most common etiologies of NTM-PD (Ko et al., 2018; Ryu, Koh, & Daley, 2016). Accurate diagnosis is becoming more important as the incidence of NTM-PD by MAC increases worldwide. However, MAC diagnoses are often delayed due to the nonspecific presentation of MAC-PD and radiological findings that overlap with those of other pulmonary diseases (Maiga et al., 2012). In addition, respiratory specimens must be collected to avoid misdiagnosis, and the antimicrobial susceptibility must be tested. However, it can take weeks to months to identify the species due to the characteristics of MAC. Moreover, the number of MAC species is growing because of newly identified species, including *M. chimaera*, *M. vulneris*, and *M. yongonense* (Daley, 2017). Therefore, the identification of precise species is important because of different sources of environmental exposure (Wallace Jr et al., 2013), various degrees of pathogenicity (Koh et al., 2012), and even differences in treatment outcomes among MAC species (Boyle, Zembower, & Qi, 2016; Boyle, Zembower, Reddy, & Qi, 2015). In particular, careful consideration is needed due to the length, complexity, and toxicity of the treatment regimen.

I. Differentiation of *Mycobacterium avium* complex

MAC species are detected by several methods, including high-pressure liquid chromatography (HPLC), line probe assays, single and multigene sequencing, and matrix-assisted laser desorption ionization-time of flight (MALDI-TOF) mass

spectrometry (van Ingen, 2015). DNA probes can be easily used to differentiate MAC species, but only a few MAC species have available probes (Griffith et al., 2007; Tortoli, Pecorari, Fabio, Messinò, & Fabio, 2010). HPLC also has the least ability to discriminate between species and subspecies although it is the least expensive approach. MALDI-TOF has recently been accepted to have good discriminatory power, but it is unable to distinguish within subspecies, including the *M. abscessus* complex. Therefore, multigene sequencing is considered the best discriminatory method. For example, the *hsp65* and *rpoB* genes can distinguish subspecies, and multigene sequencing of MAC has made it possible to distinguish new species (Bang et al., 2008; B.-J. Kim et al., 2013; Murcia, Tortoli, Menendez, Palenque, & Garcia, 2006; Salah, Cayrou, Raoult, & Drancourt, 2009; van Ingen, Boeree, et al., 2009; van Ingen, Lindeboom, et al., 2009). However, for *M. intracellulare*, differentiating the subspecies and related strains by single- and multiple-gene sequencing is difficult because they are closely related genetically. On the other hand, recent whole genome sequencing revealed that the newly identified species *M. yongonense* and *M. indicus pranii* should be reclassified as a subspecies of *M. intracellulare* (Castejon, Menéndez, Comas, Vicente, & Garcia, 2018). In addition, a recent report showed some discrepant cases in clinical *M. intracellulare* strains. The study suggested that genomic diversity among *M. intracellulare*, *M. paraintracellulare*, *M. indicus pranii* and *M. yongonense* remains at the subspecies or genovar levels but does not reach the species level by whole genome sequencing (Tateishi et al., 2021). Whole genome sequencing has led to a reconsideration of the

classification of *M. intracellulare*. However, whole genome sequencing of *M. intracellulare* still needs to be performed, while whole genome sequencing of *M. avium* was predominantly performed within MAC species (Bannantine et al., 2020; J. Lim et al., 2021; Uchiya et al., 2017).

II. Host immune response to *Mycobacterium avium* complex

Immunity to mycobacterial infection requires an effective interplay between myeloid cells (monocytes, macrophages, and dendritic cells) and lymphoid cells (T cells and natural killer cells) (Wu & Holland, 2015). In particular, macrophages play a pivotal role in controlling MAC infection as a primary reservoir for mycobacterial growth (Cambier, Falkow, & Ramakrishnan, 2014). MAC infected macrophages undergo apoptotic cell death to minimize tissue injury and decrease pathogen viability (Behar et al., 2010; Thegerström et al., 2012). However, MAC inhibits the apoptosis of macrophages via several mechanisms involving TNF-, caspase-, NO-, and cathepsin-related mechanisms and persistence within macrophages (M. Chen, Gan, & Remold, 2006; Early et al., 2011; Kabara & Coussens, 2012; O'Sullivan et al., 2007; Rojas et al., 1998; Sharbati et al., 2011). Macrophage plasticity, involving polarization to the classical (M1) or alternative (M2) phenotypes, is key for mycobacterial control (Refai et al., 2018). M1 macrophages release proinflammatory cytokines that enhance microbicidal activity, while M2 macrophages produce anti-inflammatory cytokines that cause persistent infection (Murray et al., 2014; Thiriot

et al., 2020). During MAC infection, macrophages have been reported to exhibit transformation from the M1 to M2 phenotype over time (Lugo-Villarino et al., 2011; Refai et al., 2018). However, recent studies have shown that *Mycobacterium*-infected macrophages polarize to a unique macrophage population that is distinguished to both the M1 and M2 subsets (Tomioka et al., 2012). Moreover, other novel polarized populations have also been reported to downregulate the Th1/Th2 cell population while driving Th17 polarization (Tatano et al., 2014).

MAC has shown the importance of CD4 and CD8 T cells and their associated cytokines in controlling infection. In particular, $CD4^+$ T cells are the most dominant in mycobacterial infection (Appelberg, Leal, Pais, Pedrosa, & Flórido, 2000). Of the $CD4^+$ subsets, the Th1/Th17 balance is thought to be important for protection against mycobacterial infection (Matsuyama et al., 2014; Wang et al., 2012). The T helper 1 (Th1) response plays a critical role in mycobactericidal activities in the early stage of infection. Th1 cells are involved in the clearance of mycobacteria by producing cytokines (Haverkamp et al., 2006; Patel et al., 2005; Thegerström et al., 2012). Tumor necrosis factor (TNF) induces antigen-specific $CD4^+$ cells that produce IFN-γ early during infection. IFN-γ inhibits mycobacterial growth by IFN regulatory factors induced by infection (Keane et al., 2001; Patel et al., 2005; Vila-del Sol, Punzón, & Fresno, 2008). These cytokines are essential for protecting against MAC early during infection by inducing cell-mediated immune responses.

Th17 cells participate in the antimycobacterial response by accelerating the accumulation of Th1 cells at an early stage (Cruz, Ludovico, et al., 2015; Gopal et

al., 2012; Ouyang et al., 2008; Weaver, Elson, Fouser, & Kolls, 2013). Th17 cells produce lineage-specific cytokines (IL-17A, IL-17F, IL-22) as well as other cytokines (IL-6, GM-CSF) and chemokines (CXCL1, CXCL2, CXCL5, CXCL8) to control chronic lung infection (Jasenosky, Scriba, Hanekom, & Goldfeld, 2015; Lombard et al., 2016; Shu et al., 2018). In particular, IL-17 promotes the migration of neutrophils to inflamed sites for the early clearance of bacteria by inducing the production of the chemokines CXCL1 and CXCL5 (Shen & Chen, 2018). However, in Th1-diminished conditions, Th17 cells have a pathological role rather than a protective role (Matsuyama et al., 2014; Lichen Xu et al., 2016). Th17 development induces excessive neutrophilic pulmonary inflammation by reducing the Th1 response (Figure 1). Th17 development causes increased susceptibility to systemic MAC infection (Matsuyama et al., 2014). Inflammation and neutrophil recruitment driven by Th17 cells play a pivotal role in granuloma formation and mycobacterial disease development (Cardona & Cardona, 2019; Torrado & Cooper, 2010). IL-17 from Th17 cells also induces mature granuloma formation according to the Th17 cell balance (Q. Li et al., 2016; Ostadkarampour et al., 2014; Yoshida et al., 2010). IL-1β, IL-6, and IL-23 induce the Th17 response and form granulomas with IL-17 (Stark et al., 2005). In addition, IL-17 contributes to the persistence of MAC in macrophages by inhibiting apoptosis (Cruz, Ludovico, et al., 2015; Vázquez et al., 2012). These studies show that IL-17A inhibits p53 of the intrinsic apoptotic pathway by increasing BCL2 levels and decreasing BAX expression, CASP 3 activity, and cytochrome c release.

III. *Mycobacterium avium* complex infection in dogs

MAC is an opportunistic pathogen that has a broad host range including dogs, cats, cattle, goats, domestic rabbits, free-ranging red deer, African elephants, and horses (Glawischnig, Steineck, & Spergser, 2006; Johansen et al., 2007; D. Klotz, Barth, Baumgärtner, & Hewicker-Trautwein, 2018; Kriz et al., 2010; Madarame et al., 2017; Schinköthe, Möbius, Köhler, & Liebler-Tenorio, 2016; Wellenberg, De Haas, Van Ingen, Van Soolingen, & Visser, 2010). Although dogs are known to be resistant to MAC, canine mycobacteriosis caused by MAC has been sporadically reported, and some dog breeds have been recently reported to be susceptible to MAC (Ghielmetti & Giger, 2020). In Korea, the first case of MAC infection in a pet dog was reported in 2016 (M.-C. Kim et al., 2016).

In most canine case reports, the subspecies level of MAC was not identified (Bauer et al., 2002; Cucchi et al., 2009; Etienne et al., 2013; Friend, Russell, Hartley, & Everist, 1979; Horn et al., 2000; Kontos et al., 2014; Miller, Greene, & Brix, 1995; Zeiss et al., 1994), because of financial or technical constraints. Therefore, *Mycobacterium avium* subsp. *hominissuis* has been predominantly reported in MAC-related mycobacteriosis in dogs (Campora et al., 2011; Haist et al., 2008; Hobi, Bettenay, Majzoub, Mueller, & Moser, 2015; Lam et al., 2012); however, other members of MAC can cause mycobacteriosis in dogs. In addition, some cases are thought to be underreported due to unspecific clinical signs and misdiagnoses (Ghielmetti & Giger, 2020).

Clinical signs of mycobacteriosis caused by MAC in dogs are weight loss, lethargy and inappetence with lymphadenopathy, splenomegaly, and gastrointestinal signs. Other less common clinical signs were reported spinal pain, paresis, lameness, subcutaneous swellings, and diffuse alopecia. Most dogs show granulomatous inflammation in various organs including the small and large intestine, spleen, liver, lungs, bone marrow, and various lymph nodes. Finally, most dogs were subjected to humanitarian euthanasia due to the severity of the diseases (Table 1).

The infection source of MAC in dogs has not been reported to date. Epidemiological data are absent because of the nonnotifiable disease status of MAC infection, the negligible impact of additional case reports, and misdiagnoses. In addition, the source and time of infection are difficult to ascertain because of the ubiquitous nature of MAC, different possible transmission routes, broad host range, unspecific clinical signs, and long incubation period of disease. Although it is well known that dogs can serve as an intermediate host to transmit atypical tuberculosis to humans, only one case of MAC members being transmitted from dogs to humans has been reported (van Ingen, Boeree, et al., 2009). Some reports have suggested that the infection route is ingestion from the environment (O'Toole et al., 2005). Therefore, the susceptibility and pathogenicity of MAC in dogs must be investigated.

Table 1. The published cases of *Mycobacterium avium* complex infection in dogs (Adapted from Ghielmetti & Giger, 2020).

Breed	Country	Clinical findings	Detection of MAC	Antimycobacterial treatment	Outcome
Miniature Schnauzer	USA	Lethargy, inappetence, hematochezia, lymphadenopathy, vomiting, diarrhea	LNs, Liver, spleen, GI, BM	None	Euthanased
	USA	Subcutaneous swelling, respiratory difficulty	LNs, liver, spleen, GI, BM, lung	Enrofloxacin, clofazimine, ciprofloxacin, rifampin	No improvement over 6 weeks, euthanased
	Argentina	Lethargy, inappetence, lymphadenopathy, vomiting, diarrhea	LNs	None	Died within short time or euthanased
	Germany	Anorexia, lymphadenopathy, hematochezia, diarrhea	LNs, lung, spleen, liver, GI, thymus, adrenal glands, BM, myocardium	Several unknown antibiotics	Short-term improvement, euthanased
	Germany	Lethargy, weight loss, lymphadenomegaly, diarrhea	LNs, lung	Unknown	Euthanased
	Switzerland	Lethargy, inappetence, lymphadenopathy, vomiting	LNs, liver, spleen	None	Euthanased
Basset Hound	USA	Inappetence, lameness, vomiting, diarrhea, thoracolumbar pain	LNs, GI, lung, spleen, liver, CNS, kidney, thymus, BM, bile duct, adrenal gland, tricuspid valve	Amoxycillin, ethambutol, isoniazid, streptomycin, trimethoprim/sulfamethoxazole	No improvement, euthanased
	USA	Anorexia, lymphadenopathy shivering	LNs, spleen, liver, BM, lung, kidney	Isoniazid	Continued deterioration over 10 m, euthanased
	USA	Weight loss, diarrhea	LNs, spleen, liver, BM, GI, lungs	None	Euthanased

	Italy	Lymphadenopathy, lameness, diffuse alopecia	LN, spleen, liver, BM, lungs	None	Euthanased
	Italy	Anorexia, lymphadenopathy	LNs, Liver	Enrofloxacin, rifampin, clarithromycin	No improvement, euthanased
	Greece	Anorexia, diarrhea, splenomegaly, lymphadenomegaly	LNs	Unknown antibiotics	No improvement, euthanased
Staffordshire Bull Terrier	UK	Weight loss, vomiting, diarrhea	LNs, liver, kidney, prostate, lung	None	Euthanased
	South Africa	Depression, weight loss, uveitis	LNs, spleen, liver, kidney, BM	Doxycycline 1 month	Short-term improvement, euthanased
Labrador Retriever	Canada	Lameness	LNs, spleen, liver, GI, kidney, adrenal gland, lung, CNS, BM,	None	Euthanased
	New Zealand	Anemia, lymphadenopathy, splenomegaly	/	/	/
Great Pyrenees	USA	Weight loss, anemia, diarrhea, lameness	Blood, LNs, spleen, liver, lung, GI, adrenal cortices, BM	Amikacin	Euthanased
Australian Terrier	Australia	Weight loss, lymphadenomegaly, diarrhea,	LNs, spleen, liver	Rifampicin, clarithromcyin, moxifloxacin, doxycycline 52 weeks	Prolonged treatment (79 weeks) euthanased
Golden Retriever	UK	Progressive nasal swelling, lymphadenopathy	Nasal mass	Enrofloxacin, clarithromycin, rifampicin 9 months	Successful treatment
Poodle	South Korea	Lethargy, anorexia, splenomegaly, lymphadenomegaly, skin disease	LN, spleen	Enrofloxacin, clavulanate/amoxicillin, doxycycline, rifampicin	No improvement, euthanased

Australian Shepherd	USA	Multiple subcutaneous nodules, lymphadenopathy	Skin	Rifampicin, clarithromycin 4 months	Successful treatment
Shih Tzu-Poodle-cross	USA	Lethargy, anemia, abdominal pain, lymphadenomegaly, splenomegaly	LNs, spleen, liver, lung, GIT, thymus	Enrofloxacin 2 months	No improvement, euthanased
Maltese-cross	Australia	Diarrhea, hematochezia, lymphadenomegaly	GI	Cephalexin, metronidazole, enrofloxacin	No improvement, euthanased
Yorkshire Terrier	Germany	Lethargy, weight loss, lymphadenomegaly, diarrhea	LNs, lung	Unknown	Euthanased
German Elo	Germany	Lethargy, PU/PD, weight loss, pruritic skin disease	Skin	Doxycycline/metronidazole; rifampicin/pradofloxacin, 4 months	Successful treatment
Crossbreed	France	Anorexia, PU/PD, lymphadenomegaly, diarrhea	Blood, LNs, spleen, liver, lung, GI	Unknown antibiotics	No improvement, euthanased
	USA	Hematochezia, diarrhea	LNs, spleen, liver, GI	Ampicillin	Short-term improvement, euthanased
	USA	Hindlimb paralysis, proprioceptive deficits	Spinal cord, adrenal glan	None	Euthanased
	Italy	weight loss, lymphadenomegaly	LNs, BM	Pradofloxacin, azithromycin, rifampicin	Died during therapy

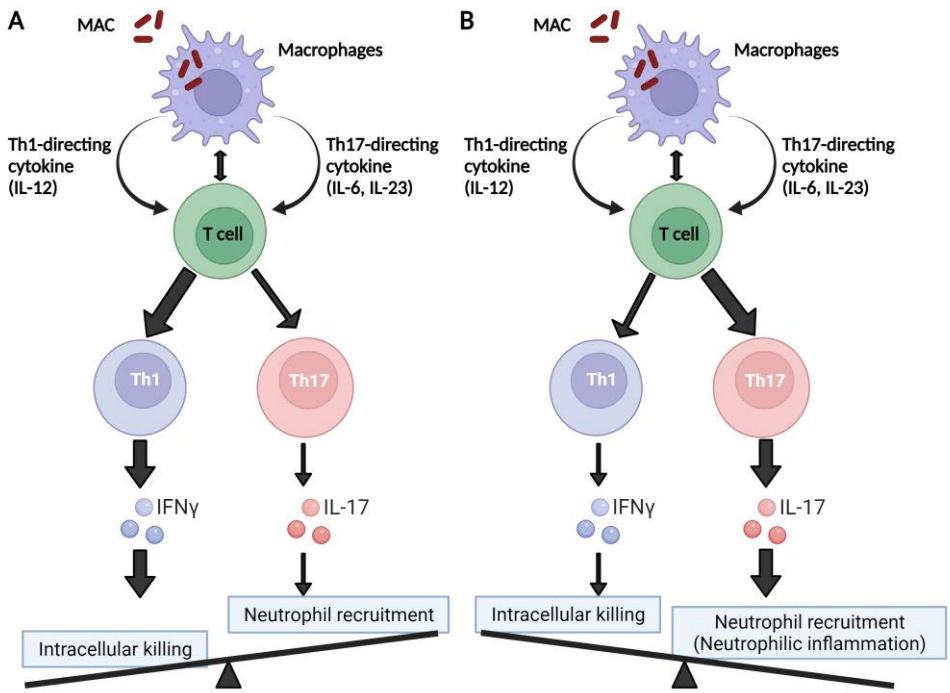

Figure 1. Schematic presentation of the role of Th1/Th17 balance regulated by *Mycobacterium avium* complex infection (Adapted from Matsuyama et al., 2014). Macrophages can produce both Th1- and Th17-directing cytokines by stimulation with MAC. Reduced Th1 responses increase susceptibility to systemic MAC infection, and Th17 development causes excessive neutrophilic pulmonary inflammation. Thus, the fine balance between Th1 and Th17 responses is critical in determining susceptibility and inflammatory responses to MAC.

Chapter I

Mycobacterium avium subsp. *hominissuis* modulates the protective immune response in canine peripheral blood mononuclear cells

Abstract

Mycobacterium avium, an opportunistic intracellular pathogen, is a member of the nontuberculous mycobacteria species. *M. avium* causes respiratory disease in immunosuppressed individuals and a wide range of animals, including companion dogs and cats. In particular, the number of infected companion dogs has increased, although the underlying mechanism of *M. avium* pathogenesis in dogs has not been studied. Therefore, in the present study, the host immune response against *M. avium* subsp. *hominissuis* (MAH) in dogs was investigated by transcriptome analysis of canine peripheral blood mononuclear cells. MAH was shown to induce different immune responses in canine peripheral blood mononuclear cells at different time points after infection. The expression of Th1-associated genes occurred early during MAH infection, while that of Th17-associated genes increased after 12 h. In addition, the expression of apoptosis-related genes decreased and the abundance of intracellular MAH increased in monocyte-derived macrophages after infection for 24 h. These results reveal the MAH induces Th17 immune response and avoids apoptosis in infected canine cells. As the number of MAH infection cases increases, the results of the present study will contribute to a better understanding of host immune responses to MAH infection in companion dogs.

Keywords: *Mycobacterium avium* subsp. *hominissuis*, Peripheral blood mononuclear cells, Host immune response, Dog, Transcriptome analysis

Introduction

Mycobacterium avium is a member of the most common nontuberculous mycobacteria complex that causes chronic respiratory disease in humans (Prevots & Marras, 2015; Yano et al., 2017). Although *M. avium* subsp. *hominissuis* (MAH) primarily infects humans and pigs, it has also been reported to infect several other mammalian species, such as cattle, sheep, horses, cats, and dogs (Campora et al., 2011; Pavlik et al., 2000). Other *Mycobacterium* species have been reported as common etiological agents of canine mycobacteriosis; however, dogs are known to be resistant to *M. avium* (Carpenter et al., 1988; Greene, 2006; Horn et al., 2000; Shackelford & Reed, 1989). Nonetheless, some type of breeds are more susceptible to *M. avium*, and an increasing number of cases of *M. avium* infection in dogs have been reported, several of which have shown granulomatous inflammation in infected organs, such as lung, liver, bone marrow, intestine and lymph nodes (Campora et al., 2011; Ghielmetti & Giger, 2020; Haist et al., 2008; D.-Y. Kim, Cho, Newton, Gerdes, & Richter, 1994; M.-C. Kim et al., 2016). The increase in such cases suggests the possibility of a potential public health risk attributable to *M. avium* infection in dogs. However, the mechanism underlying *M. avium* infection in dogs remains to be elucidated.

Typically, the host immune response attempts to defend against *M. avium* together with macrophages and T lymphocytes early during an infection. T cell immune responses are important in regulating pulmonary *M. avium* complex (MAC)

infection, with T helper 1 (Th1) responses playing an important role in increasing macrophage bactericidal capacity, while T helper 17 (Th17) differentiation induces neutrophilic pulmonary inflammation (Matsuyama et al., 2014; Shu et al., 2018). Th1 cells eradicate mycobacteria by producing various cytokines (Haverkamp et al., 2006). Tumor necrosis factor (TNF) induces antigen-specific $CD4^+$ cells that produce IFN-γ early during an infection. IFN-γ is well known to limit *Mycobacterium* infection by inhibiting outgrowth (Patel et al., 2005). These cytokines are essential for protecting MAC early during an infection by developing cell-mediated immune responses.

Th17 cells are important for establishing a protective immune response to *Mycobacterium* (Kozakiewicz et al., 2013). Th17 cells can accumulate Th1 cells in infected tissues and enhance the antimycobacterial response with Th1 cells (Cruz, Torrado, et al., 2015; Weaver et al., 2013). Th17 cells produce the lineage-specific cytokines IL-17A and IL-17F as well as other cytokines (IL-6 and GM-CSF) and chemokines (CXCL1, CXCL2, CXCL5, and CXCL8) (Jasenosky et al., 2015; Lombard et al., 2016). Importantly, IL-17 enhances the migration of neutrophils to the inflamed sites for the early clearance of bacteria by inducing CXC chemokines during *Mycobacterium* infection. However, Th17 cells have a pathological role rather than a protective role under Th1-diminished conditions after *M. avium* infection (Matsuyama et al., 2014; Lichen Xu et al., 2016). In particular, IL-17 plays crucial roles in chronic inflammation and is important for the formation and maintenance of granulomas in mycobacterial infection sites (Q. Li et al., 2016;

Ostadkarampour et al., 2014). IL-1β, IL-6, and IL-23 induce the Th17 pathway and form granulomas with IL-17 (Stark et al., 2005). In addition, IL-17 contributes to the persistence of *M. avium* in macrophages via the NF-κB and MAPK signaling pathways (Vázquez et al., 2012). These cytokines are important for the immune response to chronic pulmonary *Mycobacterium* infection.

M. avium is an intracellular pathogen that primarily affects macrophages (Thegerström et al., 2012), where infected macrophages undergo apoptotic cell death to minimize tissue injury and decrease pathogen viability (Behar et al., 2010). However, *M. avium* survives intracellularly and replicates within macrophages by preventing the phagosome maturation process (Early et al., 2011). *Mycobacterium* inhibits the apoptosis of macrophages via several mechanisms involving TNF-, caspase-, NO-, and cathepsin-related mechanisms (M. Chen et al., 2006; O'Sullivan et al., 2007; Rojas et al., 1998). In particular, *M. avium* has been reported to inhibit bacterial programmed cell death induced by both the extrinsic pathway through caspase 8 activation and the intrinsic apoptotic pathway through caspase 3 activation (Kabara & Coussens, 2012; Sharbati et al., 2011). Furthermore, IL-17A has also been reported to be associated with the inhibition of apoptosis by a p53-dependent mechanism during *Mycobacterium* infection (Cruz, Ludovico, et al., 2015).

As is the case for *M. avium* infection of several mammalian species, the host response of infected dogs should be studied to estimate the possibility of *M. avium* infection. In the present study, we elucidated the host responses in canine peripheral

blood mononuclear cells and monocyte-derived macrophages upon infection with MAH. Our results revealed that the T cell response shifts from a Th1 to a Th17 cell response according to the time of infection and that the expression of apoptosis-related genes decreased as intracellular MAH proliferates in macrophages. The results of the present study will promote a better understanding of the host immune responses to MAH in dogs and highlight the potential risk of mycobacterial infections in various species.

Materials and Methods

Bacterial strains and cultivation

M. avium subsp. *hominissuis* strain 104 was kindly provided by Prof. SJ Shin from the College of Medicine, Yonsei University in Seoul, Korea. MAH was cultured on Middlebrook 7H11 agar supplemented with OADC (BD Biosciences, CA, USA). After 7 days, the cells were cultured in Middlebrook 7H9 broth for 5 days. Cultures at an optical density of 0.45 at 600 nm (9.2×10^8 CFU/ml) were generated after vigorous vortexing for 30 s to remove clumps.

Blood cell isolation

Blood samples were collected from 6 healthy Beagle dogs in accordance with the Guide for the Care and Use of Laboratory Animals and the Animal Welfare Act in the animal facility of the 2nd Research Center at Genia (Eumsung, Korea). Blood was collected from unanesthetized dogs by professional veterinarians with permission approved by the Institutional Animal Care and Use Committee (IACUC) at Genia (IACUC number; ORIENT-IACUC-19026). Whole blood was diluted 1:3 in RPMI 1640 (Gibco, NY, USA) containing 20% of inactivated fetal bovine serum (FBS; Gibco) and added to a gradient with 1.077 g/mL of histopaque (Sigma Aldrich, Taufkirchen, Germany). Peripheral blood mononuclear cells (PBMCs) were

collected via density gradient centrifugation (400 × g for 30 min) using leucoseptube (Greiner Bio-One, Kremsmünster, Austria). Then, the PBMCs were washed twice with DPBS containing 5% FBS, 1% penicillin/streptomycin, and heparin (2,000 U/mL) and centrifuged at 250 × g for 5 min, after which the cells were resuspended in RPMI 1640 containing 20% FBS and 1% penicillin/streptomycin and cultured for 24 h at 37 ℃.

Cell culture and polarization

PBMCs were seeded into 24-well plates (ThermoScientific, MA, USA) and cultured for 12 h in RPMI 1640 supplemented with 10% FBS, after which they were used for RNA-Seq analysis after MAH stimulation. The protocol described by Goto-Koshino, Yuko, et al. was used to culture canine macrophages from blood-derived monocytes (Goto-Koshino et al., 2011). Adherent cells that strongly adhered to the plastic base of flasks were considered monocytes and collected (Delirezh, Shojaeefar, Parvin, & Asadi, 2013; Heinrich et al., 2017). Canine monocytes were stimulated with 1 μg of PMA to induce macrophage differentiation for an additional 6 days. Then, canine monocyte-derived macrophages (MDMs) were seeded into the wells of plates (ThermoScientific) containing the same medium supplemented with 10% FBS to stabilize the cells.

RNA sequencing

Canine PBMCs were infected with MAH at a multiplicity of infection (MOI) of 1 with DPBS added to one plate as a negative control. Total RNA was isolated at 0, 6, 12, and 24 h after stimulation using an RNeasy Mini kit (Qiagen, Hilden, Germany). After the quality of isolated RNA was assessed using RNA 6000 Nano Chip with an Agilent 2100 bioanalyzer (Agilent Technologies, Amstelveen, The Netherlands), RNA libraries were constructed using a QuantSeq 3'mRNA-Seq Library Prep kit (Lexogen, Inc., Austria). Total RNA was hybridized with an oligo-dT primer including an Illumina-compatible sequence at its 5' end and cDNA library was synthesized using a random primer. The double-stranded library was amplified with the complete adapter sequences and the PCR product was purified. High-throughput sequencing was performed via single-end 75 sequencing using a NextSeq 500 instrument (Illumina Inc., CA, USA).

QuantSeq 3'mRNA-Seq reads were aligned using the index of Bowtie2 (Langmead & Salzberg, 2012), which is generated by aligning genome assembly sequences or representative transcript sequences to genome or transcriptome, and the alignment was also used for the estimation of transcriptional abundance. Differentially expressed genes were determined by counting the reads on the unique and multiple alignments using BEDTools (Quinlan & Hall, 2010) and the read count was processed by quantile normalization method using EdgeR within R (R development Core Team, 2016). Functional genes were classified by DAVID

(http://david.abcc.ncifcrf.gov/) and Medline databases (http://www.ncbi.nlm.nih.gov/). Pathway analysis was performed by Ingenuity Pathway Analysis (Qiagen Inc., https://www.qiagenbioinformatics.com/products/ingenuitypathway-analysis) (Krämer, Green, Pollard Jr, & Tugendreich, 2013).

Quantification of gene expression

Gene expression was quantified by RT-qPCR to verify the RNA-Seq data or by acquiring additional information regarding host immune responses (Figure 2). cDNA was synthesized using a QuantiNova Reverse Transcription Kit (Qiagen), and RT-qPCR was performed using a Rotor-Gene SYBR Green PCR kit (Qiagen). The genes were amplified with a Rotor-Gene Q real-time PCR cycler (Qiagen). Amplification conditions were described in Table 2. The gene expression levels were determined via the $2^{-\Delta\Delta Ct}$ method with glyceraldehyde-3-phosphate dehydrogenase (GAPDH) as a reference gene. The fold change was determined based on the relative gene expression level compared to the control.

Caspase activity assay

Canine monocyte-derived macrophages were stimulated with MAH at an MOI of

1:1 for 6, 12, and 24 h. Caspase activity was monitored by measuring the active forms of caspase 3 and caspase 7 with the Caspase-Glo® 3/7 Assay System (Promega, WI, USA) according to the manufacturer's protocol. To identify the activity of caspases after the induction of apoptosis, cells were treated with hydrogen peroxide (H_2O_2) for 30 min before 24 h of infection with MAH, which is known to stimulate caspase activity (Jones et al., 2000; Kabara & Coussens, 2012). Treatment with 100 μm H_2O_2 for 30 min was used based on time course and dose-response curve studies with uninfected MDMs. Each group was assayed with additional control samples, including cell medium, reagent, MAH and negative control to calculate the RLU values.

Intracellular survival and replication

Bacterial invasion assays with canine monocyte-derived macrophages were performed as described by Bermudez and Sangari (Bermudez & Young, 1994; Sangari, Goodman, & Bermudez, 2000). Canine monocyte-derived macrophages were infected for 2 h with MAH at an MOI of 1. After centrifugation at 400 × g for 5 min, the cells were washed with DPBS and treated with amikacin at a concentration of 200 μg/ml for 2 h to kill extracellular bacteria (Bermudez & Young, 1994; Sangari et al., 2000). The cells were incubated for 4, 12, and 24 h, after which they were washed, and the viable intracellular bacteria were released by incubation after treatment of 1% Triton X-100 (Sigma-Aldrich, MO, USA). Then, the samples

were vigorously vortexed and agitated for 30 s to lyse cells. Bacteria were serially diluted and then plated onto 7H11 agar plates to enumerate viable bacteria.

Quantification of cytokines

Canine IL-17, IL-6, IL-10, IL-12, IL-4, IL-1β, and IFN-γ were detected in the supernatants of canine peripheral blood mononuclear cells at 24 h post MAH infection using DuoSet® and Quantikine® ELISA kits (R&D Systems, Minneapolis, MN, USA), according to the manufacturer's instruction.

Statistical analysis

Statistical significance was analyzed by Student's t-test using GraphPad Prism version 7.00 (Windows, GraphPad Software, La Jolla California USA, www.graphpad.com). Significantly expressed genes were determined at $p < 0.05$. Fold changes are represented by the mean ratio of gene expression in MAH – infected cells/uninfected cells.

Results

Characterization of canine immune responses against *Mycobacterium avium* subsp. *hominissuis* infection by differentially expressed genes

The transcriptomes of canine PBMCs infected with MAH for 0, 6, 12, and 24 h were analyzed by RNA-Seq. Sixteen cDNA libraries from uninfected and MAH – infected cells were sequenced. Approximately 92.87% of clean reads were uniquely mapped onto the canFam 3. A total of 3,366 differentially expressed genes (DEGs) were significantly expressed in canine PBMCs-infected with MAH compared to the uninfected group ($|fold\ \ change| \geq$ 2.0, normalized data (log2) = 4, p-value $<$ 0.05). The DEGs from the cells infected with MAH for 6 and 12 h clustered, while those from cells infected for 24 h were separated from the other groups (Figure 3A). Most DEGs belonged to the GO term categories immune response and inflammatory response compared with 0 h-infection. The percentage of significant DEGs-annotated immune response in the groups infected for 6, 12, and 24 h were 10.57 %, 13.58 %, and 4.91 %, respectively. The percentage of inflammatory response were 11.66 %, 17.94 %, and 12.11% at 6, 12, and 24 h p.i (Figure 3B).

The comparison analysis of canonical pathways showed that signaling pathways were expressed in relation to cellular immune responses against *M. avium* infection (Table 3). The pathways related to the Th1 response (HMGB1 Signaling, Neuroinflammation Signaling pathway, TREM1 Signaling, MIF-mediated

Glucocorticoid Regulation, Dendritic Cell Maturation, and Type I Diabetes Mellitus Signaling) were activated at 6, 12 and 24 h after MAH infection. The Th17 response-related pathways (IL-6 Signaling, IL-23 Signaling Pathway, Role of IL-17F in Allergic Inflammatory Airway Diseases, Th17 Activation Pathway, LXR/RXR Activation, and PPAR Signaling) were commonly expressed at all infection times. Molecules associated with the inhibition of apoptosis were expressed in the pathways Small Cell Lung Cancer Signaling, B Cell Receptor Signaling, and Interferon Signaling.

Proinflammatory cytokines and molecules related to Th1 cells (TNF-α, IL-8, IFN-γ, IL-1β, TREM1, and PTGS2) were upregulated in the pathways HMGB1 Signaling, Neuroinflammation Signaling Pathway, TREM1 Signaling, Type I Diabetes Mellitus Signaling, MIF-mediated Glucocorticoid Regulation, and Dendritic Cell Maturation after 6, 12, and 24 h post infection. Molecules related to the Th17 immune responses (IL-6, IL-23, IL-17A, IL-17F, RORγT, and IL22) were also commonly upregulated in the following signaling pathways; IL-6 Signaling, IL-23 Signaling Pathway, Role of IL-17F in Allergic Inflammatory Airway Diseases, and Th17 Activation Pathway. PPARG, RXRA, NR1H3 and NR1H4, as nuclear receptors that affect the inhibition of Th17 differentiation, were downregulated in the pathways LXR/RXR Activation and PPAR Signaling. In the Small Cell Lung Cancer Signaling pathway, the molecules BIRC2, BCL2L1, and TRAF, which were commonly upregulated at 6, 12, and 24 h, were associated with the inhibition of apoptosis. In relation to apoptosis inhibition, IFI6 of Interferon Signaling and molecules-related to the PI3K/AKT

pathways of B Cell Receptor Signaling were commonly upregulated at 6, 12, and 24 h.

Activation of signaling pathways related to the cellular immune response against *Mycobacterium avium* subsp. *hominissuis* infection

The top 20 canonical pathways showed that canine immune responses changed over time in response to MAH infection. Significant signaling pathways $[-log(p-value) \geq 1.3]$ were related to both the Th1 and Th17 responses at 6 and 12 h, while pathways at 24 h were related to the Th17 immune response. Then, after 6 h of MAH infection, Th1 cell-related pathways (HMGB1 Signaling, Acute Phase Response Signaling, and NF-κB Signaling) were activated. In addition, Th17 immune response-related pathways (LXR/RXR Activation, Role of Macrophages, Fibroblasts and Endothelial Cells in Rheumatoid Arthritis, IL-6 Signaling, STAT3 Signaling, LPS/IL-1 Mediated Inhibition of RXR Function, and PPAR Signaling) were also activated (Table 4).

In canine PBMCs infected with MAH for 12 h, signaling pathways related to Th1 immune responses were activated (HMGB1 Signaling, Acute Phase Response Signaling, Role of Pattern Recognition Receptors in Recognition of Bacteria and Viruses, Toll-like Receptor Signaling, and Hepatic Fibrosis/Hepatic Stellate Cell Activation). In addition, Th17 cell response-related signaling pathways (The

pathways Role of Macrophages, Fibroblasts and Endothelial Cells in Rheumatoid Arthritis, IL-6 Signaling, Differential Regulation of Cytokine Production in Macrophages and T Helper Cells by IL-17A and IL-17F, Role of Hypercytokinemia/hyperchemokinemia in the Pathogenesis of Influenza, Role of Osteoblasts, Osteoclasts and Chondrocytes in Rheumatoid Arthritis, Altered T Cell and B Cell Signaling in Rheumatoid Arthritis, LXR/RXR Activation, and Differential Regulation of Cytokine Production in Intestinal Epithelial Cells by IL-17A and IL-17F) were also activated (Table 5).

Signaling pathways expressed at 24 h post infection showed were associated with the Th17 immune response. In addition, the pathways related to Th17 immune response (Role of Osteoblasts, Osteoclasts and Chondrocytes in Rheumatoid Arthritis, Role of Macrophages, Fibroblasts and Endothelial Cells in Rheumatoid Arthritis, Differential Regulation of Cytokine Production in Macrophages and T Helper Cells by IL-17A and IL-17F, Colorectal Cancer Metastasis Signaling, Differential Regulation of Cytokine Production in Intestinal Epithelial Cells by IL-17A and IL-17F, Role of Cytokines in Mediating Communication between Immune Cells, and Role of Hypercytokinemia/hyperchemokinemia in the Pathogenesis of Influenza) were activated. Furthermore, signaling pathways related to apoptosis (LXR/RXR Activation, LPS/IL-1 Mediated Inhibition of RXR Function, and FXR/RXR Activation) were inhibited in the canine PBMCs infected with *M. avium* for 24 h (Table 6).

Increase of Th17-related molecules in canine peripheral blood mononuclear cells infected with *Mycobacterium avium* subsp. *hominissuis*

Among the Th17-related signaling pathways, 'Th17 Activation Pathway' and 'Differential Regulation of Cytokine Production in Macrophages and T Helper Cells by IL17A and IL17F' were commonly activated in canine PBMCs at all times of infection (Figure 4A, B). In particular, the molecules associated with Th17 immune responses (CSF2, IL22, IL17A, and IL17F) were highly expressed in the 'Th17 Activation pathway' after 24 h.p.i. (Table 7). Regarding 'Differential Regulation of Cytokine Production in Macrophages and T Helper Cells by IL17A and IL17F', the molecules (CCL3, CCL4, CSF2, CSF3, IL17A, and IL17F) were activated after 24 h.p.i. (Table 8). The key genes of Th17 pathways including transcription factors (RORC and RORA), chemokine (CCR6), cytokines (IL-17A, IL-17F, and IL-23R) were increased after time of MAH infection (Figure 4C).

The patterns of cytokines observed by gene expression analysis in canine PBMCs showed they were related to the Th1 and Th17 immune responses. The expression of genes related to Th1-related cytokines (TNF-α, IFN-γ, and IL-12p35) and Th17-related cytokines (IL-23 and IL-6) were significantly increased in canine PBMCs after 6 h post infection. The expression of genes related to Th2-related cytokines (IL-4 and IL-13) and Treg-related cytokines (IL-10) were slightly increased at 12 h, while Th17-related cytokines (IL-1β and IL-17) were highly increased (Fold change; 107.05 ± 7.12 and 73.37 ± 2.04) at that time (Figure 5). The quantification of

cytokines (IL-17, IL-1β, IL-6, IL-10, IL-4, IL-12, and IFN-γ) was measured by ELISA from supernatant of canine PBMCs infected with MAH. The results also showed that IL-17 and IL-1β were highly expressed (concentration; 4642.87 ± 604.14 pg/ml and 1566.33 ± 252.73 pg/ml) at 24 hpi (Figure 6).

Inactivation of apoptosis signaling and intracellular replication of *Mycobacterium avium* subsp. *hominissuis* in infected cells

Apoptosis signaling was inhibited in canine PBMCs after 6, 12 and 24 h post infection (z-score = -0.408, -1.043, and -1.633). In particular, the BAX-CYCS-CASP9-CASP3/CASP7 pathways were inactivated after 24 h.p.i. (Figure 7). Regarding the mRNA abundance for genes in this pathway, *caspase 3*, *caspase 8*, *caspase 9*, and *bax* were increased until 12 h.p.i., however, they were down regulated after that time (Figure 8A). The activities of caspase 3/7 in canine monocyte-derived macrophages (MDMs) infected with MAH decreased slightly over the course of infection compared to the uninfected cells (Figure 8B). To determine whether MAH was affected by the apoptosis of macrophages, we measured the activities of caspase 3/7 after induction of apoptosis with H_2O_2. Both MDMs infected with MAH after H_2O_2 treatment and MAH – infected MDMs without H_2O_2 showed lower the activities of caspase3/7 compared to uninfected cells treated with H_2O_2 (Figure 8C). Cell invasion was measured by enumerating intracellular bacteria after amikacin treatment to kill extracellular bacteria. MAH replicated in canine MDMs after

invasion (Figure 8D), where the percentage of intracellular MAH was 26.5±3 % in canine MDMs after 4 h.p.i. After invasion, the number of intracellular MAH significantly increased in canine MDMs ($p < 0.001$) after 24 h post infection (4 h; 26450 ± 3256 CFU/ml, 12 h; 11800 ± 3527 CFU/ml, and 24 h; 17955 ± 1542 CFU/ml).

Discussion

As the global incidence of nontuberculous mycobacterial infection increases, *Mycobacterium avium* complex (MAC) organisms have been increasingly isolated from various hosts (Inderlied, Kemper, & Bermudez, 1993; Martín-Casabona et al., 2004). In particular, *M. avium*, which causes chronic pulmonary disease, has been isolated from several mammals (Huchzermeyer & Michel, 2001). *M. avium* infection has been reported in a wide range of animals, including companion dogs and cats (Campora et al., 2011; Pavlik et al., 2000). Disseminated *M. avium* infection in dogs has been reported, and most case report showed granulomatous inflammation in infected organs (Campora et al., 2011; Ghielmetti & Giger, 2020; Horn et al., 2000; M.-C. Kim et al., 2016; Lam et al., 2012). As the number of cases of *M. avium* infection in dog increases, understanding the mechanisms of *M. avium* infection is necessary to prevent potential mycobacterial infection. In the present study, we analyzed host immune response against MAH infection in canine peripheral blood mononuclear cells by transcriptome analysis.

Transcriptome analysis of canine immune responses to MAH showed that they were related to the activation of the Th1 and Th17 immune responses and the inhibition of apoptosis. The hierarchical clustering analysis showed that these immune responses were clustered depending on the time of infection. At an early time of infection, both Th1 and Th17 immune responses were activated, while signaling pathways expressed at 24 h were associated with the Th17 immune

response. An analysis of signaling pathways also showed that they were related to the inhibition of apoptosis.

T cell immunity regulates pulmonary MAH infection, with Th1 and Th17 responses being particularly essential during MAH infection (Matsuyama et al., 2014). Th1 immune responses play a critical role in mycobactericidal activities early during an infection. Th1 responses are important for the clearance of mycobacteria through the production of cytokines (Patel et al., 2005; Thegerström et al., 2012). IFN-γ inhibits mycobacterial growth by IFN regulatory factors induced by infection (Vila-del Sol et al., 2008). TNF-α plays a key role in increasing host resistance to *Mycobacterium* infection during the Th1 response (Keane et al., 2001). In the present study, commonly expressed signaling pathways showed that Th1 immune response-related molecules (TNF-α, IL-8, IFN-γ, IL-1β, TREM1, and PTGS2) were activated. Furthermore, the observed abundances of mRNA related to T cell responses also indicated Th1 cell-related molecules (TNF-α and IFN-γ) were significantly activated early in an infection.

Th17 cells play a role in antimycobacterial immunity to mycobacterial infections, accelerating the accumulation of Th1 cells (Gopal et al., 2012). IL-23, IL-6 and IL-1β produced by antigen presenting cells induce the Th17 pathway (Shu et al., 2018). Th17 lineage cytokines (IL-17A, IL-17F, and IL-22) and chemokines (CXCL1, CXCL2, CXCL5, and CXCL8) are known to control chronic lung infection caused by mycobacteria (Busman-Sahay, Walrath, Huber, & O'Connor Jr, 2015; Lombard

et al., 2016; Shu et al., 2018). In particular, IL-17 promotes the migration of neutrophils to the inflamed sites for the early clearance of bacteria by inducing the production of the chemokines CXCL1 and CXCL5 (Shen & Chen, 2018). In the present study, the expression of Th17-related mRNA showed that IL-23 and IL-6 were significantly activated early during infection, while IL-1β and IL-17 were highly activated after 6 h post infection. Comparison analysis showed that IL-6, IL-23, IL-17A, IL-17F, RORγT, and IL-22 were commonly activated in Th17-related signaling pathways.

In the Th1-diminished condition, IL-17 from Th17 cells is essential for inducing mature granuloma formation according to the Th17 cell immune response balance (Yoshida et al., 2010). In the present study, CSF2, CSF3, IL-22, IL-17A, IL-17F, CCL3, and CCL4 were significantly activated after 24 h.p.i. in the 'Th17 Activation Pathway' and 'Differential Regulation of Cytokine Production in Macrophages and T Helper Cells by IL17A and IL17F' pathways. Cytokine analysis also showed IL-17 and IL-1β were highly expressed compared to other cytokines at 24 h.p.i. IL-17 is also known to inhibit the apoptosis of *Mycobacterium*-infected macrophages to promote intracellular growth (Cruz, Ludovico, et al., 2015; Vázquez et al., 2012). In these studies, IL-17A was reported to inhibit p53 of the intrinsic apoptotic pathway by increasing BCL2 levels and decreasing BAX expression, CASP 3 activity, and cytochrome c release. Apoptosis is a bactericidal mechanism in infected host cells; however, *Mycobacterium* survives and replicates within macrophages by preventing apoptosis through several mechanisms (M. Chen et al., 2006; O'Sullivan et al., 2007;

Rojas et al., 1998). In particular, *M. avium* was recently reported to inhibit bacterial programmed cell death induced by both the extrinsic pathway though caspase 8 and the intrinsic apoptotic pathway through caspase 3 (Kabara & Coussens, 2012; Sharbati et al., 2011).

In the analysis of signaling pathways, Apoptosis signaling was inhibited at all times of infection. The BAX-CYCS-CASP9-CASP3/CASP7 signaling pathway was particularly inhibited at 24 h. The abundance of *caspase 3*, *caspase8*, *caspase9*, and *bax* after 24 h was also downregulated in the observed gene expression profiles. Furthermore, the activity of caspase 3/7 decreased over time in canine monocyte-derived macrophages infected with MAH. In addition, MAH were internalized into macrophages (26.5%), and the number of intracellular MAH cells were significantly increased during infection over time. These results may indicate that MAH replicates in canine macrophages by preventing apoptosis. However, caspase activity was not significantly down regulated and genes related to apoptosis signaling were significantly increased at the early time of infection, although they were decreased compared to that observed in uninfected cells after 24 h. Therefore, additional studies are needed to elucidate the mechanism of apoptosis inhibition after latent MAH infection.

Although MAH infection in dogs has increased, canine immune responses to MAH have not been studied. In the present study, transcriptome analysis results showed that canine peripheral blood mononuclear cells expressed genes associated with the

activation of the Th1 and Th17 responses and the inhibition of apoptosis in response to MAH infection. In addition, intracellular MAH cells were observed to replicate in canine monocyte-derived macrophages. These results could be related to the case reports of MAH – infected dogs that showed granulomatous inflammation in infected tissues. These results might reveal why *M. avium* infection in dogs has continuously been reported although they are known as be resistant to members of the *Mycobacterium avium* complex. However, additional studies are needed to assess whether MAH inhibits apoptosis and induce the proliferation of Th17 cells during long-term infections. Nevertheless, the results of our present study will help to identify the host responses against *M. avium* in various species and understand the immune response toward *M. avium* in infected dogs.

Table 2. Nucleotide sequences of primers.

Gene	Forward sequence (5'→3')	Reverse sequence (5'→3')	Reference
IL-13	TGATCAATGTCTCCGACTGC	ACAGTGCTTTCAGCATCCTCT	Pujol, Myriam, et al. (2017)
IL-17	GCTCCCCAGAGCAGACTTT	AAGAACCCTAATGAGTTTAGTCAGAAA	
IL-1β	TACCTGTGGTCTTGGGCATC	TCTAGCTGTAGGGTGGGCTT	
IL-4	GCTTACTAGCACTCACCAGCA	TCGTTTCTCGCTGTGAGGATG	
IL-23	GACTCACAGAACGGACAGCA	TCAAATCTGGCTGGCTCTGG	
IFN-γ	GTTGCTGCCTACTTGGGAAC	GGCGTCTGACATGCCTCTA	
IL-5	ACCTGCAAGTATTTCTTGGTGTAA	AAGCCGGTTTGTTCTCAACTT	
IL-6	TGGCTACTGCTTTCCCTACC	TTGAAGTGGCATCATCCTTG	
TNF-α	TCACTTCCTCTGACCCCTCA	AGCCCTGAGCCCTTAATTCT	
TGF-β1	TACATTGACTTCCGCAAGGA	GTTAGCGTGGTAACCCTTGG	
IL-10	GCACCCTACTTGAGGACGAC	AGCTCTCGGAGCATGTGG	
IL-12p35	CAGAGCAACAGATGGAGCAA	TTATTAACTCCATTCAAAAGCAACTG	
GAPDH	GATGGGCGTGAACCATGAGA	TGGTCATGGATGACTTTGGCT	
CSF3	TTCCTGGAGCTGGCATATCG	CAAGAGTGCAGGGCTCCTTT	XM_022423955.1
F3	GCACCAGCCACGAGAAAGGTAT	GCTCCAAGGGCACCTTCTTTA	NM_001024640.1
HBEGF	GACTCTCCCACCGAATCCAC	TGGCTTGGAGGAGAAAGCAG	XM_005617276.3
PTGS2	GAGCACGCCTCGGGAACT	TCGCCGTAGAATCCTGTTCG	NM_001003354.1
SELENOP	CCCAGCAATGTGGAGAAGCCT	GGCTTGAAGAAGAGCAACCAC	NM_001115118.1
SUCNR1	TTTGTTGTGGGAGTCTTTGGGA	GCATGGGAAGGGTGCACAAA	XM_022408748.1
CXCL8	GACTTCCAAGCTGGCTGTTG	GGGCCACTGTCAATCACTCT	NM_001003200.1
RORa	GGCTTCTTTCCCTACTGTTCTT	CAGAATATATCTAAATCACATCTG	Kol, Amir, et al. (2016)
RORc	CTTACAATGCTGACAACCACAC	CATCTTTGACTTCTCCCGCT	
IL17A	CAATGAGGACCCTGAGAGATAC	GACGGAGTTCATGTGGTAGTT	
IL17F	AGTGTGAGGGTTGACATTCG	GTCGCGGGTAATGTTGTAGT	
CCR6	TGTCCTCACTCTCCCATTCT	AGTTGAAGTTGATGGCGTAGAT	
IL23R	CACAGACTACAAGGCGGAAA	TTGTGTATATTCCTGGTCTCAGC	
Condition	**95°C for 3 min, followed by 40 cycles of 95°C for 3 s and 60°C for 30 s**		
OAZ1	CACGGGCTCCAAACACATTA	TCATCGCGGTTCTTATGGAA	Herrmann, Ina, et al. (2018)
IDO1	GCACCGAGCCCATAAAGAGTT	GAGTTGCCTTTCCAACCAGAC	
CXCL11	AGTGTGAAGGGCATGGTTACA	CCTTTGAACATGGGGAAATCTTG	
CD163	GCGGCTTACAGTTTCCTTGAG	AGACACAGAAATTAGCCCAGCA	
CCL22	ACTACATCCGTCACCCTCTG	TGACAGTTAGGAAGACCACGC	
LCN2	AGCTGAAAGATGACCAGAGCTACAA	TACTCCAGGGTAAAGCTGAATGTCG	
CASP3	TTCATTATTCAGGCCTGCCGAGG	TTCTGACAGGCCATGTCATCCTCA	Del Puerto, H. L., et al. (2010)
CASP8	ACAAGGGCATCATCTATGGCTCTGA	CCAGTGAAGTAAGAGGTCAGCTCAT	
CASP9	TCAGTGACGTCTGTGTTCAGGAGA	TTGTTGATGATGAGGCAGTAGCCG	
BAX	TTCCGAGTGGCAGCTGAGATGTTT	TGCTGGCAAAGTAGAAGAGGGCAA	
BCL2	CATGCCAAGAGGGAAACACCAGAA	GTGCTTTGCATTCTTGGATGAGGG	
Condition	**50°C for 2 min and 95°C for 10 min, followed by 40 cycles of 95°C for 15 s and 60°C for 60 s**		

Table 3. Comparison analysis of canonical pathways in *Mycobacterium avium* subsp. *hominissuis*-infected canine peripheral blood mononuclear cells at 0, 6, 12, and 24 h. Canonical pathways are indicated with the z-score from the pathway activation analysis.

Canonical Pathways	0h	6h	12h	24h
PPAR Signaling	1.633	-4.747	-3.651	-2.058
Dendritic Cell Maturation	-1.569	4.529	3.452	1.414
TREM1 Signaling	-1.265	3.71	3.578	2.353
LXR/RXR Activation	1	-1.897	-3.053	-3.742
Th17 Activation Pathway	-0.333	3.71	3.441	2.117
IL-6 Signaling	-0.378	3.781	3.124	2.271
Role of IL-17F in Allergic Inflammatory Airway Diseases	-0.447	3	3.051	2.673
Neuroinflammation Signaling Pathway	0.707	4.906	2.252	1.27
HMGB1 Signaling	1	2.92	3.413	1.718
Phospholipase C Signaling	1.961	2.197	2.694	-1.414
Type I Diabetes Mellitus Signaling	0.447	2.746	2.5	2.5
Interferon Signaling	-	3	2.714	2
Osteoarthritis Pathway	-0.756	4.025	2.449	-0.471
Cardiac Hypertrophy Signaling (Enhanced)	-0.367	3.763	2.251	-1.315
Small Cell Lung Cancer Signaling	0.816	2.121	2.121	2.53
Colorectal Cancer Metastasis Signaling	-0.174	2.219	2.546	-2.458
IL-23 Signaling Pathway	-0.378	1.941	2.138	2.828
B Cell Receptor Signaling	1.89	2.121	2.694	0.507
Synaptogenesis Signaling Pathway	1.622	1.021	0.289	-4.249
MIF-mediated Glucocorticoid Regulation	1.134	2.309	2.714	1

Table 4. Top 20 Canonical pathways in canine peripheral blood mononuclear cells infected with *Mycobacterium avium* subsp. *hominissuis* for 6 h.

Ingenuity Canonical Pathways	-log (*p*-value)	Ratio	z-score
Atherosclerosis Signaling	12.4	0.408	-
Hepatic Fibrosis / Hepatic Stellate Cell Activation	10.9	0.337	-
Agranulocyte Adhesion and Diapedesis	10.5	0.332	-
HMGB1 Signaling	9.62	0.337	2.92
Granulocyte Adhesion and Diapedesis	9.43	0.326	-
LXR/RXR Activation	9.04	0.359	-1.897
Axonal Guidance Signaling	8.69	0.243	-
Hepatic Cholestasis	8.54	0.307	-
Cardiac Hypertrophy Signaling (Enhanced)	7.24	0.232	3.763
Role of Macrophages, Fibroblasts and Endothelial Cells in Rheumatoid Arthritis	7.23	0.257	-
Acute Phase Response Signaling	7.2	0.298	1.852
IL-10 Signaling	7.03	0.397	-
IL-6 Signaling	6.75	0.325	3.781
Role of Hypercytokinemia/hyperchemokinemia in the Pathogenesis of Influenza	6.35	0.465	-
STAT3 Pathway	6.2	0.309	0.756
LPS/IL-1 Mediated Inhibition of RXR Function	6.11	0.266	0.853
G-Protein Coupled Receptor Signaling	5.49	0.246	-
NF-κB Signaling	5.33	0.272	3.063
cAMP-mediated signaling	5.31	0.255	2.023
PPAR Signaling	5.3	0.317	-4.747

Table 5. Top 20 Canonical pathways in canine peripheral blood mononuclear cells infected with *Mycobacterium avium* subsp. *hominissuis* for 12 h.

Ingenuity Canonical Pathways	-log (p-value)	Ratio	z-score
Atherosclerosis Signaling	12.9	0.368	-
Granulocyte Adhesion and Diapedesis	9.3	0.282	-
Role of Macrophages, Fibroblasts and Endothelial Cells in Rheumatoid Arthritis	8.81	0.232	-
Osteoarthritis Pathway	8.78	0.259	2.449
Hepatic Cholestasis	8.21	0.261	-
IL-6 Signaling	7.98	0.302	3.124
IL-10 Signaling	7.94	0.37	-
Axonal Guidance Signaling	7.92	0.201	-
HMGB1 Signaling	7.72	0.271	3.413
Cardiac Hypertrophy Signaling (Enhanced)	7.65	0.198	2.251
Acute Phase Response Signaling	7.4	0.26	1.48
Differential Regulation of Cytokine Production in Macrophages and T Helper Cells by IL-17A and IL-17F	7.35	0.667	-
Role of Pattern Recognition Receptors in Recognition of Bacteria and Viruses	7.25	0.271	2.828
Role of Hypercytokinemia/hyperchemokinemia in the Pathogenesis of Influenza	7.23	0.442	-
Role of Osteoblasts, Osteoclasts and Chondrocytes in Rheumatoid Arthritis	7	0.238	-
Altered T Cell and B Cell Signaling in Rheumatoid Arthritis	6.94	0.322	-
LXR/RXR Activation	6.75	0.281	-3.053
Toll-like Receptor Signaling	6.75	0.338	1.528
Hepatic Fibrosis / Hepatic Stellate Cell Activation	6.71	0.247	-
Differential Regulation of Cytokine Production in Intestinal Epithelial Cells by IL-17A and IL-17F	6.7	0.565	-

Table 6. Top 20 Canonical pathways in canine peripheral blood mononuclear cells infected with *Mycobacterium avium* subsp. *hominissuis* for 24 h.

Ingenuity Canonical Pathways	-log (p-value)	Ratio	z-score
Atherosclerosis Signaling	16.9	0.536	-
Hepatic Fibrosis / Hepatic Stellate Cell Activation	15.5	0.453	-
LXR/RXR Activation	14.9	0.508	-3.742
Axonal Guidance Signaling	12.1	0.327	-
Cardiac Hypertrophy Signaling (Enhanced)	11.6	0.323	-1.315
Osteoarthritis Pathway	10.3	0.382	-0.471
Role of Osteoblasts, Osteoclasts and Chondrocytes in Rheumatoid Arthritis	8.73	0.361	-
Agranulocyte Adhesion and Diapedesis	8.43	0.373	-
Role of Macrophages, Fibroblasts and Endothelial Cells in Rheumatoid Arthritis	8.34	0.329	-
Granulocyte Adhesion and Diapedesis	8.15	0.376	-
Differential Regulation of Cytokine Production in Macrophages and T Helper Cells by IL-17A and IL-17F	8.07	0.833	-
Colorectal Cancer Metastasis Signaling	7.82	0.34	-2.458
LPS/IL-1 Mediated Inhibition of RXR Function	7.78	0.349	0.756
Differential Regulation of Cytokine Production in Intestinal Epithelial Cells by IL-17A and IL-17F	7.68	0.739	-
Regulation of the Epithelial-Mesenchymal Transition Pathway	7.53	0.361	-
Role of Cytokines in Mediating Communication between Immune Cells	7.07	0.519	-
FXR/RXR Activation	6.56	0.38	-
Ovarian Cancer Signaling	6.4	0.373	0.209
Role of Hypercytokinemia/hyperchemokinemia in the Pathogenesis of Influenza	6.23	0.535	-
Human Embryonic Stem Cell Pluripotency	6.11	0.369	-

Table 7. Differentially expressed genes of 'Th17 Activation Pathway' in canine peripheral blood mononuclear cells infected with *Mycobacterium avium* subsp. *hominissuis*.

Symbol	Entrez Gene Name	6h		12h		24h	
		FC	p-value	FC	p-value	FC	p-value
BATF	basic leucine zipper ATF-like transcription factor	2.385	0.033	-	-	-2.167	0.0874
CCL20	C-C motif chemokine ligand 20	2.41	0.0571	-	-	-	-
CSF2	colony stimulating factor 2	-	-	14.046	0.312	235.871	0.355
DEFB110	defensin beta 110	-	-	2.338	0.416	-	-
DEFB114	defensin beta 114	2.44	1	-	-	-2.013	0.536
DEFB118	defensin beta 118	2.274	0.19	-	-	-	-
DEFB124	defensin beta 124	-	-	3.4	0.424	3.021	0.0761
DEFB125	defensin beta 125	2.469	0.00123	-	-	3.226	0.321
DEFB128	defensin beta 128	-	-	2.497	0.111	-	-
IFNG	interferon gamma	4.854	0.238	3.133	0.193	2.638	0.583
IL6	interleukin 6	151.151	0.0123	76.046	0.0879	63.558	0.26
IL10	interleukin 10	-	-	-	-	5.965	0.25
IL21	interleukin 21	-	-	-	-	3.483	0.106
IL22	interleukin 22	-	-	5.035	0.151	125.256	0.196
IL12A	interleukin 12A	-	-	-	-	-7.231	0.346
IL12B	interleukin 12B	3.398	0.0144	3.034	0.00755	5.301	0.148
IL12RB1	interleukin 12 receptor subunit beta 1	2.117	0.0139	-	-	-	-
IL17A	interleukin 17A	64.059	0.00997	31.612	0.065	164.794	0.196

IL17F	interleukin 17F	3.306	0.127	18.132	0.279	50.502	0.0022
IL1B	interleukin 1 beta	10.655	0.211	39.655	0.0194	30.245	0.0152
IL1R1	interleukin 1 receptor type 1	2.498	0.159	-	-	-	-
IL21R	interleukin 21 receptor	2.478	0.0498	-	-	-	-
IL23A	interleukin 23 subunit alpha	-	-	-	-	4.233	0.177
IL23R	interleukin 23 receptor	-	-	-2.148	0.227	-3.806	0.518
IRAK2	interleukin 1 receptor associated kinase 2	6.554	0.0517	3.262	0.102	2.55	0.222
IRAK3	interleukin 1 receptor associated kinase 3	-	-	2.799	0.00694	3.45	0.0178
IRF4	interferon regulatory factor 4	-	-	-	-	2.064	0.00668
NFATC4	nuclear factor of activated T cells 4	-3.305	0.424	11.138	0.127	-8.387	0.22
NFKB1	nuclear factor kappa B subunit 1	2.324	0.106	-	-	2.237	0.0477
NFKB2	nuclear factor kappa B subunit 2	3.807	0.00829	4.007	0.00819	2.637	0.027
PTGER2	prostaglandin E receptor 2	5.519	0.0145	-	-	2.841	0.141
PTGER4	prostaglandin E receptor 4	-	-	-	-	-2.443	0.167
RELA	RELA proto-oncogene, NF-kB subunit	-	-	2.062	0.0146	-	-
RORA	RAR related orphan receptor A	-	-	-	-	-2.115	0.555
RORC	RAR related orphan receptor C	6.997	0.398	2.582	0.577	4.191	0.354
SOCS3	suppressor of cytokine signaling 3	3.562	1	5.803	0.422	-	-

Table 8. Differentially expressed genes of 'Differential Regulation of Cytokine Production in Macrophages and T Helper Cells by IL17A and IL17F' in canine peripheral blood mononuclear cells infected with *Mycobacterium avium* subsp. *hominissuis*.

Symbol	Entrez Gene Name	6h		12h		24h	
		FC	p-value	FC	p-value	FC	p-value
CCL2	C-C motif chemokine ligand 2	-	-	-	-	6.555	0.0171
CCL3	C-C motif chemokine ligand 3	24.603	0.186	14.776	0.166	76.672	0.0894
CCL4	C-C motif chemokine ligand 4	17.036	0.0929	12.157	0.164	39.417	0.0952
CCL5	C-C motif chemokine ligand 5	-	-	2.095	0.0512	2.657	0.0425
CSF2	colony stimulating factor 2	-	-	14.046	0.312	235.871	0.355
CSF3	colony stimulating factor 3	296.498	0.00161	42.335	0.0175	2712.837	0.352
IL6	interleukin 6	151.151	0.0123	76.046	0.0879	63.558	0.26
IL9	interleukin 9	-4.908	0.423	-	-	-	-
IL10	interleukin 10	-	-	-	-	5.965	0.25
IL13	interleukin 13	3.523	1	10.015	0.171	3.486	0.471
IL12A	interleukin 12A	-	-	-	-	-7.231	0.346
IL12B	interleukin 12B	3.398	0.0144	3.034	0.00755	5.301	0.148
IL17A	interleukin 17A	64.059	0.00997	31.612	0.065	164.794	0.196
IL17F	interleukin 17F	3.306	0.127	18.132	0.279	50.502	0.0022
IL1B	interleukin 1 beta	10.655	0.211	39.655	0.0194	30.245	0.0152
TNF	tumor necrosis factor	13.068	0.0771	7.568	0.00275	8.211	0.107

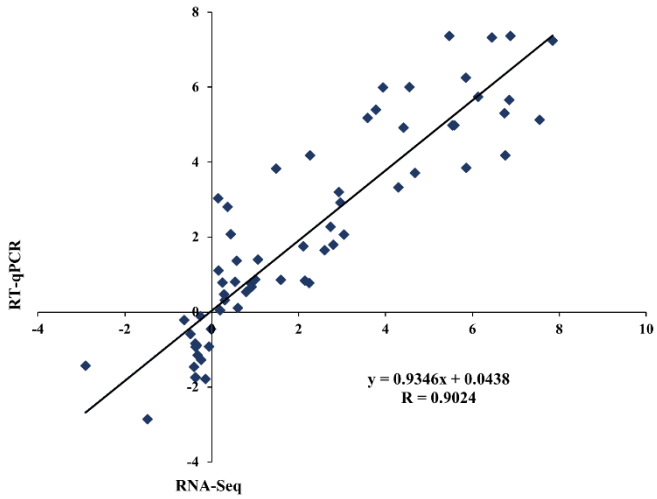

Figure 2. Validation of gene expression by RNA-Seq and quantitative real-time PCR. The relative expression level was compared to that observed in the control cells to determine the fold change in expression for each gene.

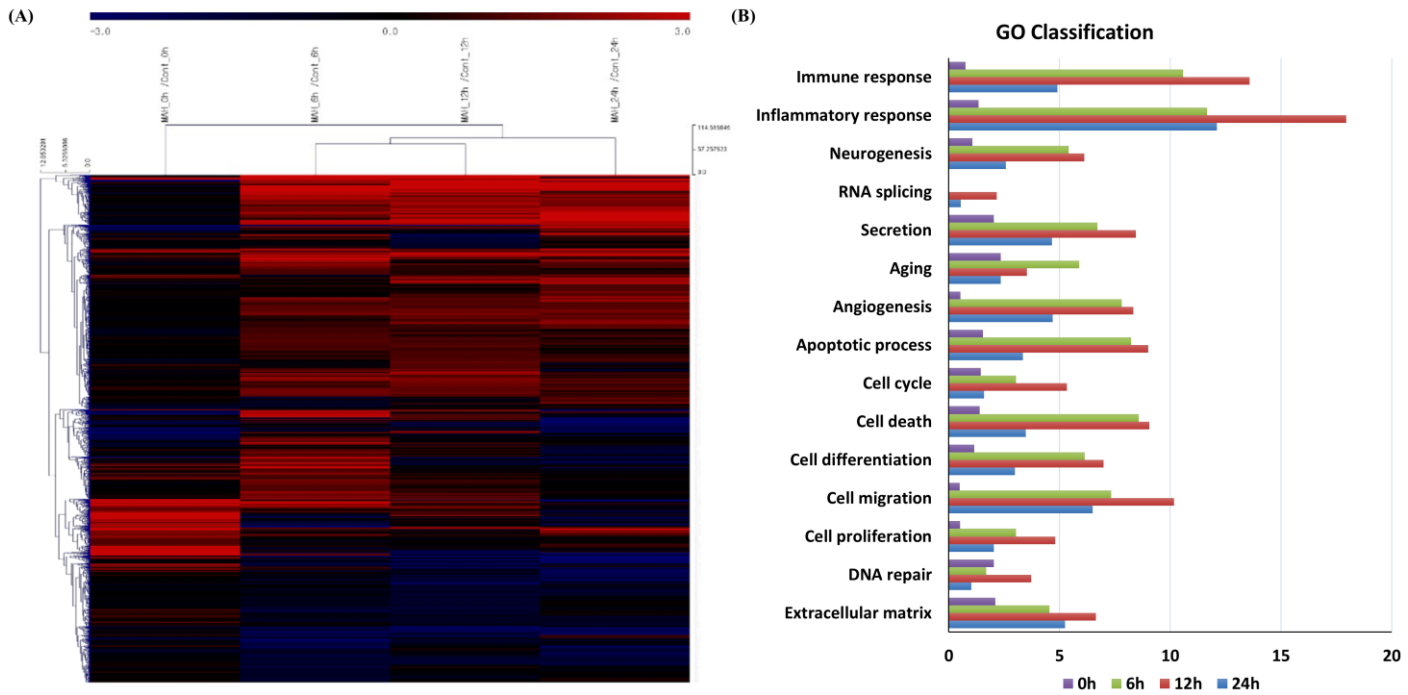

Figure 3. Gene expression analysis of canine peripheral blood mononuclear cells infected with *Mycobacterium avium* subsp. *hominissuis* at 0, 6, 12, and 24 h post infection. (A) Clustering analysis and (B) GO analysis of DEGs in MAH infected-canine PBMCs ($|Fold\ \ change| \geq 2.0$, normalized data (log2)=4, p-value< 0.05).

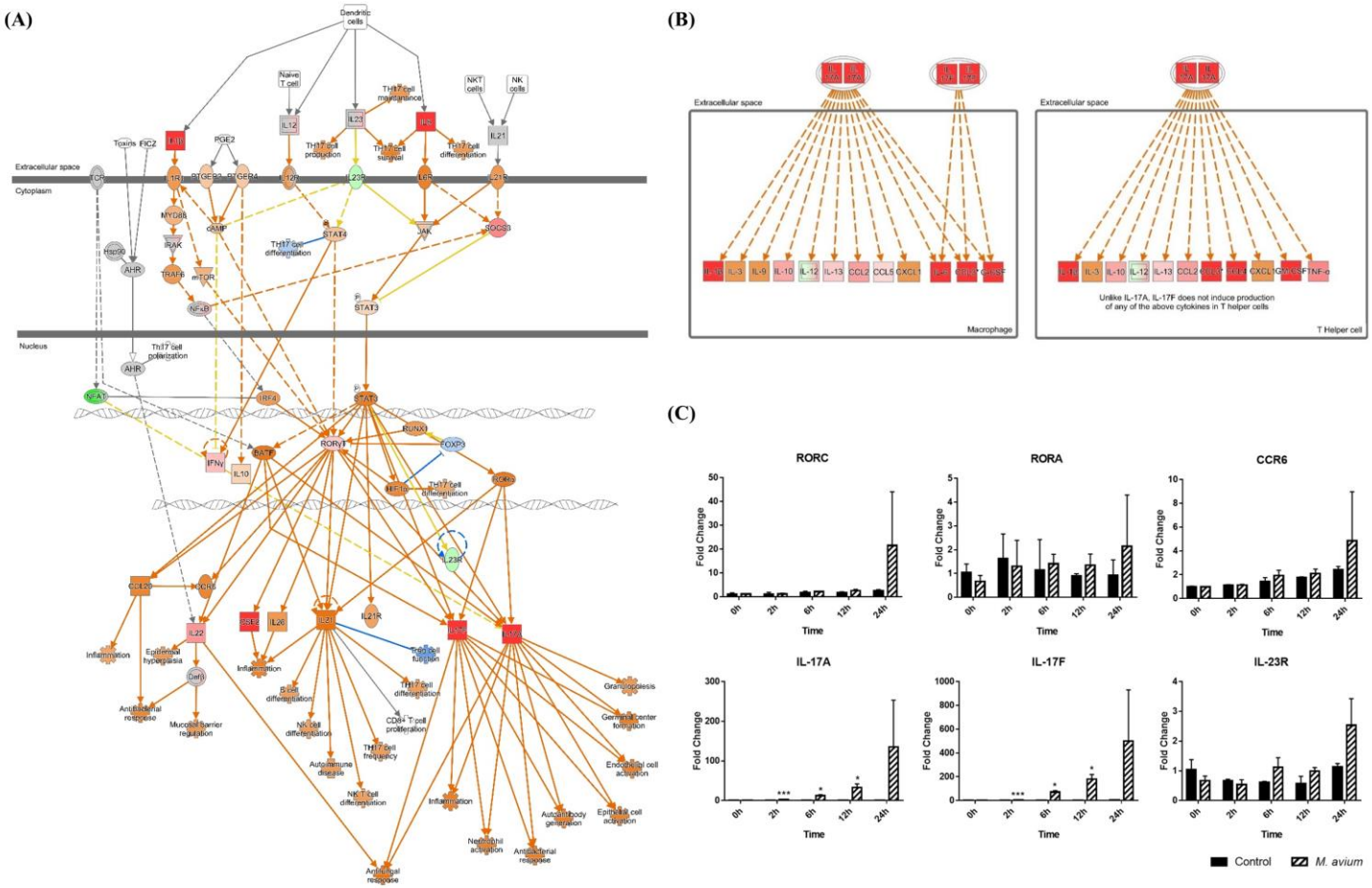
(A)
Dendritic cells
Naive T cell
Th17 cell maintenance
NKT cells
NK cells
IL12
IL23
IL6
IL21
Toxins
FICZ
PGE2
IL1
Extracellular space
Cytoplasm
TCR
IL1R
PGE2R
PGE2R4
IL12R
IL23R
IL6R
IL21R
MYD88
cAMP
JAK
SOCS3
Hsp90
AHR
IRAK
TRAF6
mTOR
NF-kB
STAT4
STAT3
Th17 cell differentiation
Th17 cell proliferation
Th17 cell expansion
Th17 cell differentiation
Nucleus
Th17 cell polarization
AHR
NFAT
IRF4
STAT3
RUNX1
FOXP3
RORγT
BATF
IFNγ
IL10
EGR2
IRF10
Th17 cell differentiation
IL23R
CCR20
HDCR
IL22
CSF2
IL26
IL21
IL21R
IL17A
IL17F
Inflammation
Epithelial hyperplasia
Defβ
Antimicrobial response
Mucosal barrier regulation
Inflammation
B cell differentiation
NK cell differentiation
CD8+ T cell proliferation
Th17 cell frequency
Autoimmune disease
NK T cell differentiation
Th17 cell differentiation
Th17 cell function
Granulopoiesis
Germinal center formation
Endothelial cell activation
Inflammation
Autoantibody generation
Epithelial cell activation
Neutrophil activation
Antimicrobial response
Anti-fungal response
(B)
Extracellular space
IL-1
IL-3
IL-9
IL-10
IL-12
IL-13
CCL2
CCL5
CXCL1
TNF
GM-CSF
Macrophage
Extracellular space
IL-1
IL-3
IL-10
IL-12
IL-13
CCL20
CXCL1
GM-CSF
NF-κ
Unlike IL-17A, IL-17F does not induce production of any of the above cytokines in T helper cells
T Helper cell
(C)
RORC
RORA
CCR6
IL-17A
IL-17F
IL-23R
Fold Change
Time
0h
2h
6h
12h
24h
Control
M. avium

Figure 4. Activation of Th17 pathways in canine peripheral blood mononuclear cells infected with *Mycobacterium avium* subsp. *hominissuis*. (A) Ingenuity pathway analysis of 'Th17 Activation Pathway' at 24 hpi and (B) 'Differential Regulation of Cytokine Production in Macrophages and T Helper Cells by IL17A and IL17F' at 24 hpi. Individual nodes represent proteins with relationships represented by edges. The genes shown in red indicate upregulation, green indicates downregulation, orange indicates predicted activation, and an uncolored node indicates that the genes were not differentially expressed in this pathway. (C) Gene expression levels of Th17 pathways during MAH infection. RORC, RORA, IL-17A, IL-17F, IL-23R, and CCR6 were indicated by an mRNA fold-change in canine PBMCs infected with MAH. mRNA expression in uninfected cells at 0 h was considered 1 as a reference for fold-change in expression. Each bar represents the mean ± SD of nine independent experiments. $*p < 0.05$, $**p < 0.01$, and $***p < 0.001$.

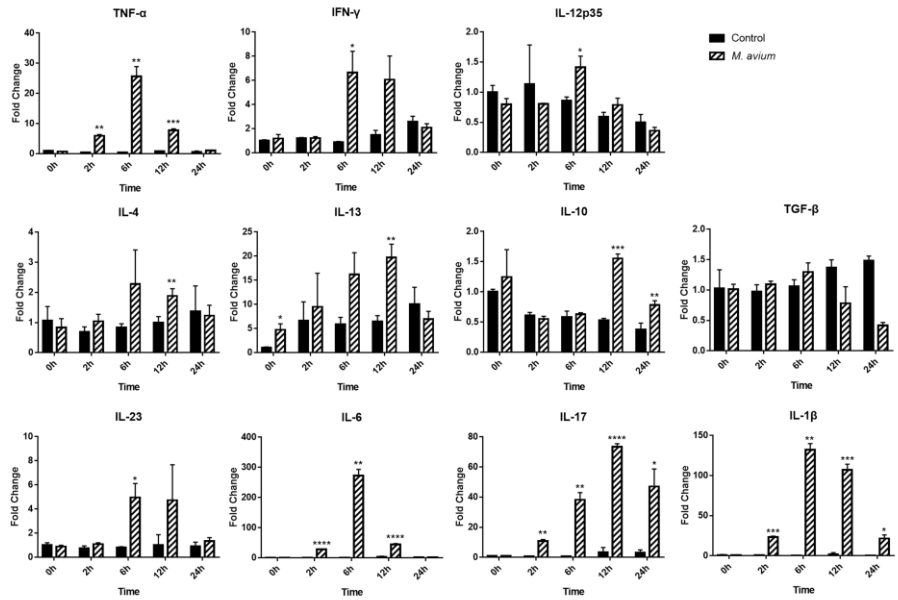

Figure 5. Different cytokine mRNA expression in *Mycobacterium avium* subsp. *hominissuis*-infected canine peripheral blood mononuclear cells. Quantification of the cytokines IL-12p35, IFN-γ, and TNF-α (Th1-type), IL-4 and IL-13 (Th2-type), IL-1β, IL-6, IL-17, and IL-23 (Th17-type), and IL-10 and TGF-ß (T regulatory-type), as indicated by an mRNA fold-change in canine PBMCs infected with MAH. Cytokine mRNA expression in uninfected cells at 0 h was considered 1 as a reference for fold-change in expression. Each bar represents the mean ± SD of nine independent experiments. *$p < 0.05$, **$p < 0.01$, ***$p < 0.001$, and ****$p < 0.0001$.

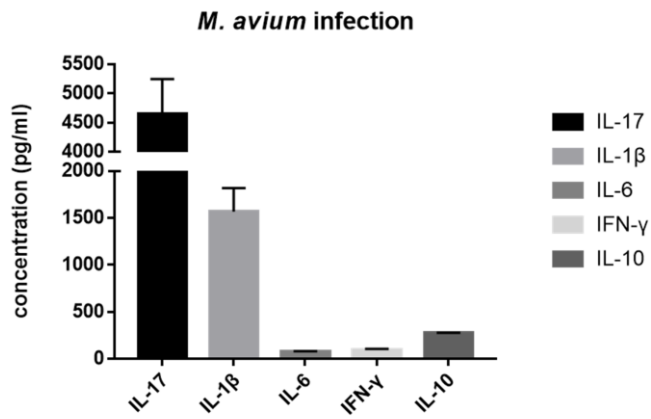

Figure 6. Cytokine expression in canine peripheral blood mononuclear cells infected with *Mycobacterium avium* subsp. *hominissuis* at 24 hpi. Supernatants were analyzed for IL-17, IL-1β, IL-6, IFN-γ, IL-10, IL-4, and IL-12 by ELISA. IL-4 and IL-12 were not detected. Each bar represents the mean ± SD of independent experiments (n = 6).

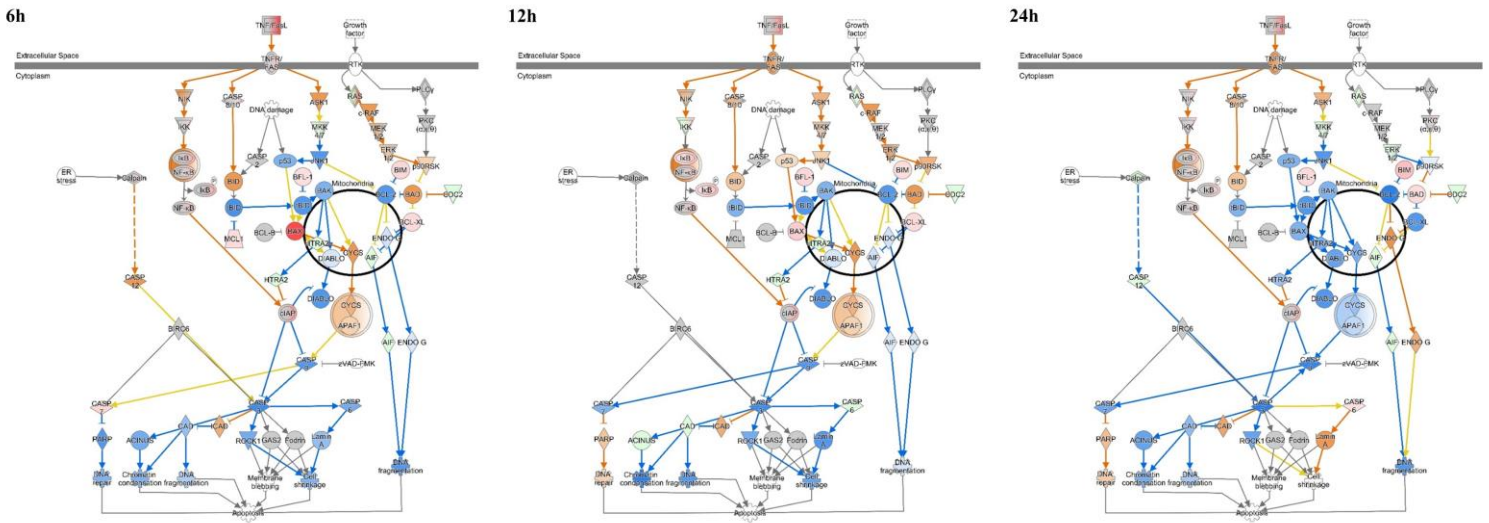

Figure 7. Ingenuity pathway analysis of 'Apoptosis Signaling' in *Mycobacterium avium* subsp. *hominissuis*-infected canine peripheral blood mononuclear cells for 6, 12, and 24 h. Individual nodes represent proteins with relationships represented by edges. The genes shown in red indicate upregulation, green indicates downregulation, orange indicates predicted activation, blue indicates predicted inhibition, and an uncolored node indicates that the genes were not differentially expressed in this pathway.

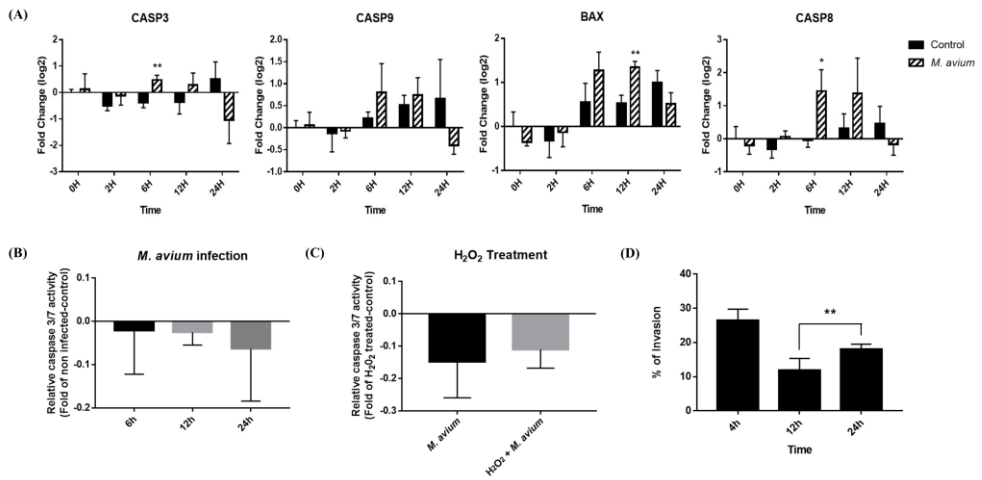

Figure 8. Analysis of apoptosis signaling in *Mycobacterium avium* subsp. *hominissuis* infection. (A) Expression profiling of apoptosis-related genes in MAH-infected canine PBMCs. Quantification of mRNA related to apoptosis, as represented by an mRNA fold-change in canine PBMCs infected with MAH. The mRNA expression in noninfected cells at 0 h was considered 1 as a reference for the fold-change in expression. (B) Caspase 3/7 activity in canine monocyte-derived macrophages infected with MAH. The fold-change was calculated between the cells infected with and without MAH. (C) Caspase 3/7 activity in MAH-infected MDMs with or without apoptosis induction. The fold-change was calculated between the MAH-infected cells treated with or without 100μm H_2O_2 and the apoptosis-induced cells. (D) The intracellular survival and replication ability of MAH in canine monocyte-derived macrophages. Graph showing the percentage of intracellular MAH cells in MDMs and after treatment with amikacin. Each column represents the mean $\pm$ SD of nine independent experiments. *p <0.05, **p <0.01.

Chapter II

Mycobacterium intracellulare induces a Th17 immune response via M1-like macrophage polarization in dogs

Abstract

Mycobacterium avium complex (MAC) is one of the most prevalent pathogenic nontuberculous mycobacteria that cause chronic pulmonary disease. The prevalence of MAC infections has been rising globally in a wide range of hosts, including companion animals. MAC infection has also been reported in dogs; however, little is known about interaction between MAC and the host, especially in immune responses. Therefore, needs to develop an in vitro model have been raised to investigate the interaction after MAC infection. Based on the current situation, an in vitro canine model was developed using co-culture systems of canine T helper cells and autologous monocyte-derived macrophages (MDMs) and applied to analyze the host immune response driven by *M. intracellulare* in this study. Transcriptome analysis revealed that canine MDMs differentiated into M1-like macrophages during *M. intracellulare* infection and the macrophages secreted molecules that induced Th1/Th17 cell polarization. Furthermore, canine lymphocytes co-cultured with *M. intracellulare*-infected macrophages induced the adaptive Th17 responses after 5 days. Taken together, our results indicate that *M. intracellulare* elicits a Th17 response through macrophage activation in this system. Those findings might help the understanding of the canine immune response to MAC infection and diminishing the potential zoonotic risk in One Health aspect.

Keywords: *Mycobacterium intracellulare*, Monocyte-derived macrophages, Th17 cells, Dog, Transcriptome analysis

Introduction

Nontuberculous mycobacteria (NTM) are opportunistic bacteria that are highly abundant in environment niches such as soil and water sources. *Mycobacterium avium* complex (MAC) is one of the most prevalent pathogenic NTM that causes chronic pulmonary diseases in humans and other mammals. In dogs, MAC infection can cause mycobacterial granulomas in various organs, including the spleen, liver, lung, bone marrow, and various lymph nodes (M.-C. Kim et al., 2016; Malik et al., 2013). Dogs with mycobacteriosis caused by MAC usually have poor prognoses due to the difficulty of diagnosis and nonspecific clinical signs. Although diagnosed, most affected dogs die or are euthanized regardless of any treatment after the progress of the infection. A recent study reported that domestic dogs are more susceptible to MAC infection because of their restricted genetic pool (Ghielmetti & Giger, 2020). Furthermore, there is a potential zoonotic risk of transmission from infected companion dogs to their owners, especially in immunocompromised people, although interspecies transmission of MAC is still remaining to be clear. Some reports have shown that MAC members can be transmitted from dogs to humans (van Ingen, Boeree, et al., 2009). In addition, NTM infection mostly occurs by exposure to environmental sources because of the ubiquitous nature. Our previous study showed that MAC accounted for most of NTM isolated from soil that collected in animal shelter and parks (Park et al., 2020). Therefore, it is important to understand the pathogenicity of MAC in dogs not only for treatment and diagnosis but also to prevent potential zoonotic transmission between humans and dogs.

Macrophages are considered to be a primary reservoir for intracellular mycobacterial growth and to be important antigen-presenting cells (Cambier et al., 2014). Macrophage plasticity is key for mycobacterial control, and macrophages polarize to the classical (M1) or alternative (M2) phenotypes in response to bacterial infection (Refai et al., 2018). M1 macrophages release high levels of proinflammatory cytokines that have enhanced microbicidal activity, while M2 macrophages produce anti-inflammatory cytokines and cause persistent infection (Murray et al., 2014; Thiriot et al., 2020). Macrophages have been reported to exhibit transformation from the M1 to the M2 phenotype over the course of mycobacterial infection (Lugo-Villarino et al., 2011; Refai et al., 2018). However, recent studies have shown that *Mycobacterium*-infected macrophages polarize to a unique macrophage population that is clearly distinguishable from the M1 and M2 macrophage subsets (Tomioka et al., 2012). In particular, *M. intracellulare*-infected macrophages represent a novel polarized population that downregulates Th1/Th2 cell production while driving Th17 polarization (Tatano et al., 2014).

In mycobacterial infection, CD4+ T cells are the most dominant in the immune response (Appelberg et al., 2000). The Th1/Th17 balance is thought to be important for protection against mycobacteria (Matsuyama et al., 2014; Wang et al., 2012). The Th1 immune response is essential for controlling mycobacterial infection. Th17 cells participate in the antimycobacterial response by accelerating the accumulation of Th1 cells at an early stage (Gopal et al., 2012; Ouyang et al., 2008). However, the Th17 response has pathological effects during MAC infection under Th1-diminished

conditions. Th17 development induces excessive neutrophilic pulmonary inflammation by reducing Th1 responses and can increase susceptibility to systemic MAC infection (Matsuyama et al., 2014). Inflammation and neutrophil recruitment driven by Th17 cells play a pivotal role in granuloma formation and mycobacterial disease development (Cardona & Cardona, 2019; Torrado & Cooper, 2010).

As mycobacteriosis caused by MAC in dogs has been consistently increased, canine immune response should be revealed to understand the pathogenesis in MAC-infected dogs. As the first step, an in vitro canine model was developed to investigate the immune response to *M. intracellulare* infection. Transcriptome analysis in canine monocyte-derived macrophages was carried out to identify activated macrophages driven by the bacterial infection. In addition, the T cell response was investigated using *M. intracellulare*-infected autologous macrophages. These results will help further our understanding of the pathogenesis of *M. intracellulare*-related crosstalk between macrophages and T helper cells. Furthermore, this study helps to establish a basis for research on MAC infections, which occur in a wide range of hosts, as well as for understanding the mechanism of *M. intracellulare* infection in dogs.

Materials and Methods

Ethics statement

This study was conducted in accordance with the regulations of the Seoul National University Institutional Biosafety Committee (protocol: SNUIBC-R190906-1). Blood samples were obtained in accordance with the Guide for the Care and Use of Laboratory Animals and the Animal Welfare Act, and protocols were approved by the Institutional Animal Care and Use Committee (IACUC) at GENIA (IACUC number; ORIENT-IACUC-20003).

Bacterial strains and cultivation

Mycobacterium intracellulare ATCC13950 was kindly provided by Prof. MK Shin from the College of Medicine, Gyeongsang National University, Republic of Korea. *M. intracellulare* was cultured on Middlebrook 7H10 agar (BD Biosciences, CA, USA) containing 0.1% casitone (BD Biosciences) and Middlebrook 7H9 broth supplemented with 0.04% casitone after 7 days. The infection amount was standardized by using the cells at an optical density of 0.244 at 660 nm (4.9×10^7 CFU/ml). The optical density was measured after vigorous vortexing for 30 s to remove clumps.

Blood cell isolation

Blood samples from 10 healthy beagle dogs were obtained from the animal facility of the 2nd Research Center, GENIA (Eumseong-gun, Chungchengbuk-do, Korea). Professional veterinarians collected whole blood from unanesthetized dogs after clinical, biochemical, and haematological evaluation. The one-year-old male beagle dogs were routinely vaccinated against Bordetella, rabies, distemper, canine adenovirus type 2, parvovirus, parainfluenza, and leptospirosis. Whole blood was diluted 1:1 in RPMI 1640 medium (Gibco, NY, USA) containing 20% inactivated fetal bovine serum (FBS; Gibco). Peripheral blood mononuclear cells (PBMCs) were collected via density gradient centrifugation with Leucoseptube (Greiner Bio-One, Kremsmünster, Austria) containing 1.077 g/ml Ficoll-Paque PLUS (GE Healthcare, Uppsala, Sweden). The PBMCs were suspended in DPBS containing 5% FBS, 1% penicillin/streptomycin, and heparin (2,000 U/mL) and centrifuged at 400 × g for 15 min. The cells were filtered with a 100 μm cell strainer (Falcon, Corning, Durham, USA) after washing with DPBS and centrifuged at 300 × g for 10 min. After repeating the wash step twice, the PBMCs were resuspended in RPMI 1640 medium containing 20% FBS and 1% penicillin/streptomycin for each individual.

Generation of canine monocyte-derived macrophages

Monocytes were isolated positively by using anti-CD14 magnetic microbeads (Miltenyi Biotec Inc., Bergisch Gladbach, Germany). The isolated monocytes were

confirmed by flow cytometry (FACS Canto II, BD Biosciences, San Diego, CA, USA). The purity was above 99% using the anti-CD14 antibody (TÜK4; Bio-Rad) (Figure 9). The monocyte was cultured with RPMI 1640 medium containing 10% heat-inactivated FBS, 1% penicillin/streptomycin and 50 ng/ml recombinant human M-CSF (Peprotech Inc., Rocky Hill, HJ, USA) every 2 days (Hartley et al., 2017; Wheat et al., 2019). The monocyte was differentiated to the macrophage for 5 days, and the morphology was inspected.

Co-culture of canine lymphocytes and autologous monocyte-derived macrophages infected with *Mycobacterium intracellulare*

The canine MDMs were seeded at a density of 1×10^6 cells/well into 6-well plates containing RPMI 1640 medium supplemented with 10% FBS. The MDM was infected with *M. intracellulare* at a multiplicity of infection (MOI) of 1 for 24 h because it is sufficient time for processing the antigen. The MDM as a control was stimulated with 1 μg/ml of lipopolysaccharide (LPS; Sigma-Aldrich, St Louis, MO, USA) or was treated with DPBS. After 24 h of infection, the MDMs were washed and co-cultured with monocyte-depleted PBMCs at a responder cells:stimulators (MDMs) ratio of 10:1. The MDMs and monocyte-depleted PBMCs were co-cultured for 0 – 144 h to characterize the *M. intracellulare*–specific response and the effect of MDM–derived cytokines on T cells. The co-cultured cells at 5 days were confirmed as $CD3^+$ T lymphocytes by flow cytometry.

RNA expression, library preparation, and sequencing

Total RNA was isolated from canine MDMs after *M. intracellulare* infection for 0, 6, 24, and 72 h using an RNeasy Mini Kit (Qiagen, Hilden, Germany). Noninfected MDMs were used as a negative control. The RNA quality was identified by an Agilent 2100 bioanalyzer using an RNA 6000 Nano Chip (Agilent Technologies, Amstelveen, The Netherlands), and RNA was quantified on an ND-2000 spectrophotometer (Thermo Inc., Waltham, MA, USA). The RNA library was constructed with a QuantSeq 3' mRNA-Seq Library Prep Kit (Lexogen, Inc., Vienna, Austria) according to the manufacturer's instructions. In brief, the 5' end of an Illumina-compatible sequence containing an oligo-dT primer was hybridized to the total RNA. After reverse transcription, the RNA template was degraded to synthesize the second strand using an Illumina-compatible linker sequence containing a random primer. To remove all reaction components, the double-stranded library was purified by magnetic beads. The library was amplified with complete adapter sequences and purified from PCR components. High-throughput sequencing was performed with single-end 75-bp sequencing using a NextSeq 500 (Illumina Inc., CA, USA). The RNA-Seq data were deposited into the NCBI Gene Expression Omnibus (GEO) database under accession number GSE158425.

RNA-sequencing read alignment and data analysis

QuantSeq 3' mRNA-Seq reads were mapped to canFam 3 using Bowtie2

(Langmead & Salzberg, 2012). Both the genome assembly sequence and the representative transcript sequences generated Bowtie2 indices. After aligning the transcriptome, transcripts were assembled to identify differentially expressed genes. DEGs were identified based on counts from unique and multiple alignments determined by Bedtools (Quinlan & Hall, 2010). The read counts were processed based on the quantile normalization method using EdgeR within the R package with Bioconductor (Gentleman et al., 2004). The DEGs were analyzed by Ingenuity Pathway Analysis (IPA; Qiagen Inc., https://www.qiagenbioinformatics.com/products/ingenuitypathway-analysis) (Krämer et al., 2013). Each group was subjected to core and comparative analyzes, and signalling pathways were predicted by the molecule activity predictor in IPA.

Quantification of gene expression

Total RNA was extracted from both canine MDMs infected with *M. intracellulare* for 0 – 72 h and lymphocytes co-cultured with *M. intracellulare*-infected MDMs for 0 – 144 h using an RNeasy Mini Kit (Qiagen, Hilden, Germany). Noninfected MDMs and lymphocytes were used as controls. Gene expression was quantified by RT-qPCR to identify the activation of macrophages and T lymphocytes. In addition, RT-qPCR was performed with randomly selected genes to validate the RNA-Seq data (Figure 10). cDNA was synthesized using a High-Capacity cDNA Reverse Transcription Kit (Applied Biosystems, Foster City, CA, USA), and RT-qPCR was

performed with Real-Time qPCR 2X Master Mix (SYBR Green, Elpisbiotech, Daejeon, Republic of Korea) on a Rotor-Gene Q real-time PCR cycler (Qiagen, Hilden, Germany). cDNA was amplified using the canine primers shown in Table 9. The amplification conditions were as follows: 95 ℃ for 3 min and 45 cycles of 95 ℃ for 3 s and 30 s at 60 ℃. A melting curve was constructed for the detection of nonspecific product formation, and the gene expression levels were determined via the $2^{-\Delta\Delta Ct}$ method using glyceraldehyde-3-phosphate dehydrogenase (GAPDH) as the reference gene. The fold change was determined based on the relative gene expression level compared to the control.

Quantification of cytokines

Lymphocytes were co-cultured at 1×10^7 cells/well with *M. intracellulare*-infected MDMs in 6-well plates for 0 – 144 h. The cytokine concentrations in the supernatants were determined by ELISA. Canine IL-17A, IL-1β, IL-12, and IL-4 were detected by DuoSet® (R&D Systems, Minneapolis, MN, USA) and IFN-γ, IL-6, IL-10, and TNF-α were detected by Quantikine® ELISA kits (R&D Systems) according to the manufacturer's instructions.

Intracellular cytokine staining assay

Lymphocytes were co-cultured with *M. intracellulare*-infected MDMs to analyze

T helper cell polarization. After 5 days of incubation, the cells were incubated with 2 μg/ml brefeldin A (Sigma) for 4 h. The cells were then resuspended in PBS containing 2% FBS (FACS buffer) and stained with FITC-anti-CD3 (clone CA17.2A12) and RPE-anti-CD4 (clone YKIX302.9) (both from Bio-Rad Laboratories; Hercules, CA, USA) for 20 min at RT in the dark. After surface staining, the cells were washed once with FACS buffer and incubated in BD fixation/permeabilization solution (BD Biosciences, San Diego, CA, USA) for 30 min at 4°C. For intracellular cytokine staining, the cells were washed twice with BD Perm/Wash buffer (BD Biosciences) and stained with eFluor 450-anti-IL-17A (clone eBio17B7; eBioscience, San Diego, CA, USA) and Alexa Flour 647-anti-IFN-γ (clone CC302; Bio-Rad) for 30 min at 4°C. Following intracellular cytokine staining, the cells were washed twice with BD Perm/Wash buffer and resuspended in FACS buffer. Single-stained samples for each antibody were used to compensate for the fluorescence spillover. Cells were analyzed using FlowJo v10 software (BD Biosciences).

Intracellular survival and replication

The bacterial invasion assay was conducted as previously described with slight modification (Bermudez & Young, 1994; Sangari et al., 2000). MDMs were infected for 2 h with *M. intracellulare* at an MOI of 1. Cells were washed with DPBS after centrifugation at 400 × g for 5 min. Extracellular bacteria were eliminated by

treatment with amikacin at a concentration of 200 μg/ml for 2 h. Following incubation, the cells were lysed with 1% Triton X-100 (Sigma-Aldrich, MO, USA). The viable intracellular bacteria were enumerated by serial dilution and plating onto Middlebrook 7H10 agar containing 0.1% casitone after vigorous vortexing for 30 s.

Statistical analysis

Statistical significance was analyzed by an unpaired t-test with Welch's correction using GraphPad Prism version 7.00 (Windows, GraphPad Software, La Jolla California USA, www.graphpad.com) for comparisons between the *M. intracellulare*-infected and non-infected groups. Significant differences were determined at $p < 0.05$. Fold change is represented by the mean ratio of gene expression in *M. intracellulare*-infected cells/noninfected cells.

Data availability

Raw files and normalized datasets are available from the Gene Expression Omnibus (GEO) https://www.ncbi.nlm.nih.gov/geo/query/acc.cgi?acc=GSE158425 under the accession number GSE158425.

Results

Transcriptome analysis of canine monocyte-derived macrophages against *Mycobacterium intracellulare* infection

To identify the canine immune response against *M. intracellulare*, canine MDMs were analyzed through RNA-Seq after infection with *M. intracellulare* for 0, 6, 24, and 72 h. Sixteen cDNA libraries from noninfected and *M. intracellulare*-infected cells were sequenced. A total of 1,542 differentially expressed genes (DEGs) were significantly expressed in the *M. intracellulare* infection group compared to the uninfected group. Transcriptional profiles were analyzed by Ingenuity Pathway Analysis (IPA) using the significant DEGs ($|fold\ \ change| \geq 1.5$). A comparison analysis was performed using canonical pathways that were expressed at each time point (6h, 24h, 72h). Table 10 shows the pathway commonly expressed during *M. intracellulare* infection. The top 20 pathways were related to macrophage activation and induction of T helper cell responses. The activated pathways (Role of IL-17F in Allergic Inflammatory Airway Diseases, IL-6 Signaling, TREM1 Signaling, HMGB1 Signaling, Th17 Activation Pathway, Role of Pattern Recognition Receptors in Recognition of Bacteria and Viruses, CD28 Signaling in T Helper Cells, CD40 Signaling, IL-23 Signaling Pathway, Dendritic Cell Maturation) were involved in M1 macrophage activation. In contrast, inactivated pathways (LXR/RXR Activation, PPARα/RXRα Activation, PPAR Signaling) were related to M2 macrophage differentiation. The activation states were predicted by particular

genes expressed in those pathways. Among the genes, the upregulated genes (*CCL3*, *CCL4*, *CCL5*, *IL6*, *IL1B*, *ICAM1*, *CSF2, TREM1*, *CD40*) were related to M1 macrophage activation, and the downregulated gene *CD36* was related to M2 macrophages (Table 11).

The pathways were also involved in the induction of the T cell response. The activated pathways TREM1 Signaling, HMGB1 Signaling and Dendritic Cell Maturation were associated with the Th1 response, and other activated pathways (Role of Th17F in Allergic Inflammatory Airway Diseases, IL-6 Signaling, Th17 Activation Pathways and IL-23 Signaling Pathway) were also related to the Th17 response. In addition, the inactivated pathways (LXR/RXR Activation, PPARα/RXRα Activation, PPAR Signaling) were involved in the inhibition of the Th17 response. Of the molecules expressed in these pathways, Th1/Th17 cell response-related molecules (CCL3, CCL4, CCL5, CCL7, IL1B, IL6, CSF2, CXCL8, ICAM1, S100A8, PTGS2, CD40, CD80) were commonly upregulated during *M. intracellulare* infection. However, IL15, which is known to be related to the Th1 cell response, was inactivated (Table 12).

Canine macrophages differentiate into M1-like macrophages after *Mycobacterium intracellulare* infection

After identifying the commonly expressed pathways, at 6 h, 24 h, and 72 h, each pathway was analyzed in relation to macrophage activation. Pathways were trimmed

based on significance $[-log(p-value) \geq 1.3]$. The activation status was predicted by the z-score. Figure 11A shows that most M1 macrophage-associated pathways were activated, whereas Figure 11B shows that M2 macrophage-associated pathways were negatively regulated or inactivated. The grey boxes in Table 13 indicate pathways that were continuously activated or inactivated throughout *M. intracellulare* infection. However, some pathways were not consistent with the M1 activation states. In particular, apoptosis-related pathways (Apoptosis Signaling, Myc Mediated Apoptosis Signaling, Induction of Apoptosis by HIV1, Production of Nitric Oxide and Reactive Oxygen Species in Macrophages) were negatively regulated over time. The Apoptosis Signaling pathway was predicted to be inactivated throughout the infection.

Because of this discrepancy with the characteristics of classical M1 macrophages, macrophage activation-related genes were quantified by RT-qPCR during 72 h of infection. The expression levels of M1 macrophage markers (*IL-23*, *IL-1β*, *IL-6*, *TNF-α*, *IDO1*) were significantly upregulated in *M. intracellulare*-infected MDMs compared to noninfected MDMs (Figure 12A). In contrast, M2 macrophage markers did not show any significant changes during *M. intracellulare* infection (Figure 12B). An invasion assay also showed that *M. intracellulare* replicated in canine MDMs after infection. The amount of intracellular *M. intracellulare* increased after 5 days of infection (Figure 13). These results indicate that apoptosis signaling was inactivated despite the M1 markers being upregulated during the infection.

Mycobacterium intracellulare-infected canine macrophages produce molecules to induce the T helper cell response

Analysis of pathways commonly activated during infection showed that macrophages induce Th1 and Th17 responses upon *M. intracellulare* infection. Most of the molecules upregulated in that pathway were also associated with both Th1 and Th17 responses, although some molecules involved in the Th1 response were downregulated. To specifically identify the expression of genes that induce Th1/Th17 cell responses, the activation states of the Th1 Pathway and Th17 Activation Pathway were analyzed. The Th1 Pathway was activated at only 6 and 72 h (z-score;6h=2.333,24h=-0.333,72h=1.069) by upregulated genes (CD40, CD80, ICAM1, IL-6, NF-κB) (Figure 14A). On the other hand, the Th17 Activation Pathway was activated throughout *M. intracellulare* infection (z-score;6h=2.236,24h=1.633,72h=2.333) because Th17-associated molecules (CSF2, IL-1B, IL-6) were upregulated (Figure 14B). These results were also confirmed by analysis of the expression of particular genes by RT-qPCR. Gene expression profiling revealed that the expression of the IL-23, IL-1β, and IL-6 genes, which induce Th17 cell polarization, was significantly increased compared to that in the control group. Among Th1-related genes (IFN-γ, TNF-α, IL-12), only TNF-α showed significantly increased expression. Th2 (IL-4, IL-13) and Treg (IL-10, TGF-β)-related genes did not show significantly increased expression in canine MDMs infected with *M. intracellulare* (Figure 12).

Th17 cell response in canine lymphocytes co-cultured with MDMs after *Mycobacterium intracellulare* infection

To investigate the T cell response to *M. intracellulare* infection, lymphocytes were co-cultured for 6 days with autologous MDMs, which were infected with *M. intracellulare* for 24 h. T cells were mainly enriched after five days of co-culture, and the proportion of $CD4^+$ T cells was higher than that of $CD8^+$ T cells among the co-cultured cells, similar to the result for PBMCs (Figure 15). Gene expression profiling of lymphocytes showed that Th17-related genes (*IL-1β*, *IL-17*) were significantly upregulated compared to the control (Figure 16). In particular, the gene expression of IL-17 was highest among cytokines associated with subsets of $CD4^+$ helper T cells. Other cytokines associated with Th1 (*IFN-γ*, *IL-12*), Th2 (*IL-4*, *IL-13*), and Tregs (*IL-10*, *TGF-β*) were not significantly upregulated except for *TNF-α*. However, *TNF-α* was significantly expressed only at 12 h, and the expression level was also very low $(fold\ \ change = 1.007 \pm 0.117)$. To confirm the production of cytokines, supernatants of lymphocytes were analyzed by ELISA (Figure 17). All cytokines related to subsets of $CD4^+$ helper T cells were produced after *M. intracellulare* infection, with the exception of Th2 cells. Th17-related cytokines (IL-17A, IL-1β, IL-6) exhibited higher expression levels than other cytokines produced in Th1 cells (TNF-α, IFN-γ) and Tregs (IL-10). To identify the IL-17A and IFN-γ-secreting $CD4^+$ T cells, lymphocytes were analyzed by flow cytometry after incubation for 5 days with noninfected MDMs, *M. intracellulare*-infected MDMs, and LPS-infected MDMs (Figure 18). The production of IFN-γ from $CD4^+$ T cells

was confirmed by LPS-stimulated lymphocytes (Figure 19). The percentage of IL-17A-producing $CD4^+$ T cells were higher than those of IFN-γ-producing $CD4^+$ T cells. Thus, *M. intracellulare* activated macrophages to M1-like phenotype and *M. intracellulare*-infected macrophages polarized $CD4^+$ T cells to Th17 cells.

Discussion

Mycobacterium avium complex has been highlighted as an emerging opportunistic intracellular pathogen that is ubiquitous in the environment, often leading to high rates of host-pathogen contact. In the case of dogs, it has been reported that domestic dogs are more susceptible to mycobacteriosis caused by MAC (Ghielmetti & Giger, 2020). Therefore, it is important to investigate the MAC infection in dogs not only for treatment and diagnosis but also to prevent potential zoonotic risk. However, the susceptibility and pathogenicity of MAC in dogs have been remained to be revealed because of the difficulty to evaluate the canine immune response in vitro. Therefore, we investigated the canine immune response against *M. intracellulare* infection by co-culture systems of canine T helper cells and MDMs. Our study showed that susceptibility and inflammatory responses to *M. intracellulare* in dogs were regulated by Th17 cells driven by M1-like macrophage activation.

Transcriptome analysis showed that MDMs were activated to the M1-like macrophage state and secreted cytokines to induce Th1/Th17 cell responses to *M. intracellulare* infection. Top 20 canonical pathways showed that M1 macrophage-related pathways were activated, while M2 macrophage-related pathways were negatively modulated. These pathways were modulated by commonly expressed molecules at 6, 24, and 72 h. Among the molecules, chemokines (*CCL3*, *CCL4*, *CCL5*) and cytokines (*IL6*, *IL1B*) are known to induce M1 macrophage polarization in response to mycobacterial infection. *Mycobacterium*-infected macrophages

secrete these proinflammatory mediators that play a key role in leukocyte recruitment (Saha, Prasanna, Chandrasekar, & Nandi, 2010). These molecules induce protective immune responses upon M1 polarization (Roy et al., 2018). *ICAM1* is an adhesion molecule whose expression is increased by proinflammatory cytokines in an NF-κB-dependent manner (Hubbard & Giardina, 2000). *ICAM1* has been reported to regulate macrophage activation by inhibiting M2 polarization (M. Yang, Liu, Piao, Shao, & Du, 2015). Proinflammatory cytokines also induce *CSF2*, which activates the expression of cytokines and chemokines to enhance macrophage differentiation to the M1 state (Shinohara, Yano, Bucana, & Fidler, 2000; Ushach & Zlotnik, 2016). *TREM1* increases *IL-1β* production through M1 macrophages as a key player in protective innate immunity during MAC infection (Ariel et al., 2020; F.-C. Yang, Chiu, Chen, Mak, & Chen, 2019). *CD40* is a representative marker of M1 macrophages involved in antibody isotype switching and vascular inflammation (Zirlik et al., 2007). Conversely, the M2 macrophage marker *CD36* was downregulated during *M. intracellulare* infection. *CD36* regulates the nuclear receptor *PPARγ* as a class B scavenger receptor for the endocytosis of triacylglycerol-rich lipoprotein particles (Chawla, 2010). *PPARγ* enhances the M2 macrophage response, and lipid modification and repair are fundamental properties of M2 macrophage function (Noël, Raes, Ghassabeh, De Baetselier, & Beschin, 2004).

After identifying the pattern of the immune response by the top 20 canonical pathways, the significantly expressed pathways were analyzed in relation to

macrophage activation. The activation states of these pathways showed that most M1 activation-related pathways were activated and they are known to be involved in proinflammatory and protective immune responses against bacterial invasion. On the other hand, M2 activation pathways were negatively modulated and these pathways are related to modulating the nuclear receptor known to enhance M2 activation (Chawla, 2010; Noël et al., 2004). However, some of the identified pathways were not consistent with the M1 activation state. Especially, apoptosis-related pathways were negatively regulated during the infection. Nevertheless, these states might help explain the reported properties of MAC after macrophage invasion. MAC members are known to replicate within macrophages by preventing apoptotic cell death induced by extrinsic or intrinsic apoptotic pathways (Early et al., 2011; Kabara & Coussens, 2012; S. Kim et al., 2021). Our results also showed that the amount of *M. intracellulare* was increased after 6 days of invasion. Therefore, these results differ from the classic M1 phenotype known to have a bactericidal function but are consistent with the MAC characteristics after macrophage invasion. Gene expression profiling of macrophage polarization markers also showed that only M1 macrophage-related genes were significantly expressed. These results reveal that canine MDMs differentiate into M1-like macrophages during *M. intracellulare* infection, although the activation states of pathways involved in macrophage polarization are distinct from the classic M1 and M2 macrophage phenotypes (Murray et al., 2014; Thiriot et al., 2020). However, recent studies have reported that macrophages polarize into a unique macrophage population during mycobacterial

infection (Tomioka et al., 2012). In particular, Tatano et al. reported that *M. intracellulare* induces a novel type of macrophage population that downregulates the Th1/Th2 cell response, while driving Th17 polarization (Tatano et al., 2014).

Our results also indicated that the canine MDMs secreted molecules to induce Th17 polarization in response to *M. intracellulare* infection. The top 20 canonical pathways showed that the activated pathways were related to the Th1/Th17 responses. Among the upregulated molecules of that pathways, chemokines (*CCL3*, *CCL4*, *CCL5*, *CCL7*) and cytokines (*IL-1B*, *IL-6*, *CSF2*), were responsible for mediation of the innate immune response in Th1 and Th17 cells during mycobacterial infection (Domingo-Gonzalez, Prince, Cooper, & Khader, 2017; Lyadova & Panteleev, 2015; Y.-L. Zhang, Han, Kim, Lee, & Rhee, 2017). However, most of the upregulated molecules were associated with inducing pathogenic Th17 cells during mycobacterial infection. In particular, *CCL3*, *CCL4*, and *CCL5* were reported as pathogenic Th17- signature markers during mycobacterial infection (Y. Lee et al., 2012; Ramesh et al., 2014). *CSF2* (*GM-CSF*) is also known to contribute to the pathogenicity of Th17 cells (Shiomi, Usui, & Mimori, 2016). The chemokine *CXCL8* and the adhesion molecule *ICAM1* are directly associated with the Th17 response, which induces the maturation and activation of neutrophils during mycobacterial infection (Y. Li et al., 2018; Lyadova & Panteleev, 2015; Tosi et al., 1992). In addition, the alarmin *S100A8*, known to contribute to neutrophil accumulation during chronic mycobacterial infection, stimulates *IL-6* to promote Th17 differentiation (D.-G. Lee, Woo, Kwok, Cho, & Park, 2013; Scott et al., 2020).

Moreover, *PTGS2* (*COX-2*), which is involved in *PGE2* production after mycobacterial infection, causes a dysfunctional immune response that favors the survival and replication of mycobacteria by inducing the development of Th17 cells (Liu et al., 2020; Martínez-Colón & Moore, 2018). In addition, negatively modulated pathways (LXR/RXR Activation, PPARα/RXRα Activation, PPAR Signaling) were also related to the induction of the Th17 cell response. Nuclear receptor peroxisome proliferator-activated receptors, which primarily regulate these pathways, are known to be major negative regulators of Th17 differentiation (Chang et al., 2019; L. Klotz et al., 2009). These results were also confirmed by both of the 'Th1 Pathway' and 'Th17 Activation Pathway'. Only the Th17 Activation Pathway was activated throughout the infection. In addition, gene expression profiling showed that the genes *IL-23, IL-1β*, and *IL-6*, which induce Th17 cell polarization, were significantly upregulated during *M. intracellulare* infection. In contrast, only *TNF-α* was significantly expressed among molecules related to Th1 cell polarization.

To identify the Th17 cell response against *M. intracellulare* infection, gene expression was quantified in canine lymphocytes. The result showed that Th17-related genes were significantly upregulated in lymphocytes, similar to the finding in macrophages. Moreover, ELISA indicated that IL-17A, IL-1β, and IL-6 were produced at higher levels than other cytokines. Furthermore, IL-17A-expressing $CD4^+$ T cells were higher expressed in comparison to IFN-γ after *M. intracellulare* infection. The results showed that canine MDMs infected with *M. intracellulare* provide an environment that may favor Th17 responses. Our results were similar to

those of studies that showed the production of IL-17 after infection with the *Mycobacterium avium* complex. A study by Kannan et al. showed that *M. avium* infection induced strong induction of IL-17-producing T cells in mice (Kannan, Haug, Steigedal, & Flo, 2020). In particular, a study by Matsuyama et al. reported that the Th17 response was shown to have pathological effects by increasing the susceptibility to systemic *M. avium* infection under Th1-diminished conditions (Matsuyama et al., 2014). Th17 cell development is also known to lead to excessive neutrophilic pulmonary inflammation, which plays a pivotal role in granuloma formation and mycobacterial disease development (Cardona & Cardona, 2019; Torrado & Cooper, 2010). These results will help explain why most reported cases in dogs showed granulomatous inflammation after mycobacterial disease progression induced by MAC members (Barandiaran et al., 2017; Campora et al., 2011; Etienne et al., 2013; Ghielmetti & Giger, 2020; Haist et al., 2008).

Due to the increase of mycobacterial diseases caused by MAC members in dogs, the need to elucidate the canine immune response has been increased. In this study, the host immune response to *M. intracellulare* was investigated using in vitro canine model with autologous macrophages and lymphocytes. Our results suggested that *M. intracellulare* induces M1-like macrophage polarization that provides a cytokine milieu favoring Th17 response in dogs. This study might open the new horizon in the understanding of MAC infection, especially immune response in dogs and help to control the potential public health risk of zoonosis between dogs and humans.

Table 9. Nucleotide sequences of the primers used in this study.

Gene	Forward sequence (5'→3')	Reverse sequence (5'→3')	Reference or Accession number
IL-13	TGATCAATGTCTCCGACTGC	ACAGTGCTTTCAGCATCCTCT	Pujol, Myriam, et al. (2017)
IL-17A	GCTCCCCAGAGCAGACTTT	AAGAACCCTAATGAGTTTAGTCAGAAA	
IL-1β	TACCTGTGGTCTTGGGCATC	TCTAGCTGTAGGGTGGGCTT	
IL-4	GCTTACTAGCACTCACCAGCA	TCGTTTCTCGCTGTGAGGATG	
IL-23	GACTCACAGAACGGACAGCA	TCAAATCTGGCTGGCTCTGG	
IFN-γ	GTTGCTGCCTACTTGGGAAC	GGCGTCTGACATGCCTCTA	
IL-5	ACCTGCAAGTATTTCTTGGTGTAA	AAGCCGGTTTGTTCTCAACTT	
IL-6	TGGCTACTGCTTTCCCTACC	TTGAAGTGGCATCATCCTTG	
TNF-α	TCACTTCCTCTGACCCCTCA	AGCCCTGAGCCCTTAATTCT	
TGF-β1	TACATTGACTTCCGCAAGGA	GTTAGCGTGGTAACCCTTGG	
IL-10	GCACCCTACTTGAGGACGAC	AGCTCTCGGAGCATGTGG	
IL-12	CAGAGCAACAGATGGAGCAA	TTATTAACTCCATTCAAAAGCAACTG	
IDO1	GCACCGAGCCCATAAAGAGTT	GAGTTGCCTTTCCAACCAGAC	Herrmann, Ina, et al. (2018)
CXCL11	AGTGTGAAGGGCATGGTTACA	CCTTTGAACATGGGGAAATCTTG	
CD163	GCGGCTTACAGTTTCCTTGAG	AGACACAGAAATTAGCCCAGCA	
CCL22	ACTACATCCGTCACCCTCTG	TGACAGTTAGGAAGACCACGC	
LCN2	AGCTGAAAGATGACCAGAGCTACAA	TACTCCAGGGTAAAGCTGAATGTCG	
GAPDH	GATGGGCGTGAACCATGAGA	TGGTCATGGATGACTTTGGCT	
ALDH1A2	TCCAGCAAGATCGAGATGCC	CAAGAACTGCCCTGTCTCGT	NM_001287089.2
CCL3	CAAGCAGATTCCACGCAAGT	ATAATACCGGGCTTGGAGCA	NM_001005251.2
CCL4	ACTGCCTGCTGCTTCTCTTA	GCTCGCTGGGATTAGCACA	NM_001005250.1
CCL5	TACATTTCCGGCCGACTACC	ACAAAGACGACTGCTGGCAT	NM_001003010.2
CD36	TGGACCCAGAACTCCTGTCT	ATGCTTGCTGTTGCTGTGTG	NM_001177734.3
CD40	CACGATTGGTCCCCGAAGA	TCTCTCCTGGTGGGCACATA	NM_001002982.1
CD80	TGCTTTGTCCTAGCCACACT	AGGCAATCCCCTTTCCAACT	NM_001003147.1
CSF2	GAATCTCCCTGTGCAACCCA	AAAGGCAGTGACTTGTGAGGT	NM_001003245.1
EMR1	ATGACAGAAGCAGGGCATCA	CTCGTTCACATCAACTGCCAT	NM_001038668.1
F3	GCACCAGCCACGAGAAAGGTAT	GCTCCAAGGGCACCTTCTTTA	NM_001024640.1
GJC1	GCAGACTTCCTTGCCCTCAT	AGGGGGAGCAGATGGTGTAT	NM_001020812.2
IL1RN	CGAAATGGCAGTGTCCCGTT	ACGGGCACCACATCTAACTT	NM_001003096.3
MITF	TGGATTGGGGCCACCTAAAAC	CTTGGTGGGGTTTTCGAGGT	NM_001003337.1
NR4A1	GCCCTGTATCCAAGCCCAAT	TAGTAGTCGGAACCGCTGGA	NM_001003227.1
PI3	ATCCGGTCAAAGCCAAAGGT	ATGGCGCACTGGATCAGAAT	NM_001290099.2
PTGS2	GAGCACGCCTCGGGAACT	TCGCCGTAGAATCCTGTTCG	NM_001003354.1
S100A8	TATCCTCTGTCAACTCTGTTTCGG	TATGGCACTCTCCAGTTCCG	NM_001146144.1

Table 10. Top 20 canonical pathways of *Mycobacterium intracellulare*-infected canine MDMs as determined by comparison analysis of IPA. The canonical pathways are indicated by the z-scores determined from the pathway activation analysis.

Canonical Pathways	6 h	24 h	72 h
Role of IL-17F in Allergic Inflammatory Airway Diseases	3	2.714	2.333
IL-6 Signaling	2.84	1.807	2.668
TREM1 Signaling	3.578	2.828	0.688
HMGB1 Signaling	2.524	2	2.183
LXR/RXR Activation	-1.789	-2.673	-2.183
Th17 Activation Pathway	2.236	1.633	2.333
Hepatic Fibrosis Signaling Pathway	3.087	0.169	2.412
FAT10 Cancer Signaling Pathway	2.449	0.816	2.236
PPARα/RXRα Activation	-1.897	-1.265	-2.309
Renin-Angiotensin Signaling	2.121	1.667	1.667
Cholecystokinin/Gastrin-mediated Signaling	2.53	1.667	1.155
Role of Pattern Recognition Receptors in Recognition of Bacteria and Viruses	2.887	1.732	0.535
PPAR Signaling	-1.155	-2.333	-1.604
CD28 Signaling in T Helper Cells	1.633	1.633	1.667
MIF-mediated Glucocorticoid Regulation	2.236	1.342	1.342
CD40 Signaling	2	1.134	1.633
Osteoarthritis Pathway	2.357	1.414	0.943
Cardiac Hypertrophy Signaling (Enhanced)	1.512	1.633	1.567
IL-23 Signaling Pathway	2	0.447	2.236
Dendritic Cell Maturation	3.838	0	0.816

Table 11. The list of genes that were commonly expressed in the canonical pathways of 6, 24, and 72 h.

Gene	Description	Fold Change		
		6h	24h	72h
ABCB1	ATP-Binding Cassette Sub-Family B Member 1	6.46	2.10	0.94
ACKR3	Atypical Chemokine Receptor 3	8.74	6.54	5.01
CCL3	C-C Motif Chemokine Ligand 3	9.34	5.74	3.01
CCL4	C-C Motif Chemokine Ligand 4	10.40	6.14	4.51
CCL5	C-C Motif Chemokine Ligand 5	5.78	7.95	4.60
CCL7	C-C Motif Chemokine Ligand 7	3.61	3.43	6.47
CD40	CD40 Molecule	6.76	1.40	1.09
CD80	CD80 Molecule	11.38	2.01	5.08
CDC42	Cell Division Cycle 42	1.23	1.87	1.73
CREM	CAMP Responsive Element Modulator	2.99	4.36	0.82
CSF2	Colony Stimulating Factor 2	8.56	5.54	3.11
CXCL8	C-X-C Motif Chemokine Ligand 8	6.65	5.61	7.79
ICAM1	Intercellular Adhesion Molecule 1	4.99	1.24	0.73
IL1B	Interleukin 1 Beta	11.32	6.88	3.40
IL1RN	Interleukin 1 Receptor Antagonist	7.06	4.51	1.47
IL6	Interleukin 6	11.64	2.79	5.40
NFKB1	Nuclear Factor Kappa B Subunit 1	3.34	0.73	1.33
PTGS2	Prostaglandin-Endoperoxide Synthase 2	15.08	6.01	3.74
S100A8	S100 Calcium Binding Protein A8	1.76	7.74	9.39
TREM1	Triggering Receptor Expressed On Myeloid Cells 1	6.08	2.48	3.38
CD36	CD36 Molecule	-1.31	-4.53	-8.44
CYBB	Cytochrome B-245 Beta Chain	-0.60	-6.33	-4.69
IL15	Interleukin 15	-5.83	-5.19	-4.35
NR3C1	Nuclear Receptor Subfamily 3 Group C Member 1	-1.29	-0.91	-4.81
TIMP1	TIMP Metallopeptidase Inhibitor 1	-1.78	-5.00	-4.68
TNFSF13	TNF Superfamily Member 13	-1.10	-1.04	-2.85

Table 12. Canonical pathways related to macrophage activation in canine MDMs infected with *Mycobacterium intracellulare*.

	Ingenuity Canonical Pathways	6h			24h			72h		
		-log (p-value)	Ratio	z-score	-log (p-value)	Ratio	z-score	-log (p-value)	Ratio	z-score
M1	Dendritic Cell Maturation	10.1	0.120	3.838	9.19	0.109	0	11	0.130	0.816
	TREM1 Signaling	16	0.263	3.578	14.3	0.237	2.828	14.1	0.250	0.688
	Neuroinflammation Signaling Pathway	15.6	0.114	3.43	18.5	0.121	-0.169	20	0.137	0.316
	Role of IL-17F in Allergic Inflammatory Airway Diseases	6.68	0.214	3	10.8	0.286	2.714	7.48	0.238	2.333
	Role of Pattern Recognition Receptors in Recognition of Bacteria and Viruses	14.5	0.162	2.887	13.4	0.149	1.732	15.5	0.175	0.535
	IL-6 Signaling	7.12	0.120	2.84	7.63	0.120	1.807	8.25	0.136	2.668
	HMGB1 Signaling	14.7	0.158	2.524	10	0.121	2	12	0.145	2.183
	Th1 Pathway	4.91	0.098	2.333	5.3	0.098	-0.333	7.58	0.131	1.069
	Crosstalk between Dendritic Cells and Natural Killer Cells	10.1	0.178	2.324	6.73	0.133	0	11.6	0.200	-0.243
	MIF-mediated Glucocorticoid Regulation	3.02	0.139	2.236	3.2	0.139	1.342	2.85	0.139	1.342
	Th17 Activation Pathway	1.31	0.054	2.236	2.01	0.065	1.633	3.49	0.097	2.333
	CD40 Signaling	2.58	0.092	2	4.42	0.123	1.134	3.1	0.108	1.633
	IL-23 Signaling Pathway	1.84	0.091	2	2.79	0.114	0.447	2.46	0.114	2.236
	Acute Phase Response Signaling	5.72	0.088	1.941	4.86	0.077	1.155	8	0.110	1
	Chemokine Signaling	4.91	0.119	1.897	8.04	0.155	0.832	5.39	0.131	0.905
	CD28 Signaling in T Helper Cells	1.74	0.056	1.633	1.94	0.056	1.633	3.15	0.080	1.667
	LPS-stimulated MAPK Signaling	2.08	0.073	1.633	2.95	0.085	0.378	4.68	0.122	0.632
	NF-κB Signaling	7.95	0.106	1.606	7.03	0.095	2.183	6.64	0.101	0.471

	IL-8 Signaling	6.35	0.088	1.604	11.6	0.118	1.091	13.3	0.137	1.043
	IL-15 Signaling	3.7	0.107	1.414	6.65	0.147	0.905	7.74	0.173	1.387
	Toll-like Receptor Signaling	6.14	0.143	1.414	3.89	0.104	0.816	5.77	0.143	0
	JAK/Stat Signaling	1.55	0.063	1.342	3.77	0.100	1.414	3.99	0.113	1.667
	MIF Regulation of Innate Immunity	2.58	0.111	1.342	1.94	0.089	1	1.69	0.089	1
	p53 Signaling	1.73	0.061	1.342	5.46	0.112	0.905	5.51	0.122	-0.632
	Production of Nitric Oxide and Reactive Oxygen Species in Macrophages	8.88	0.108	1.342	5.16	0.077	-1.604	8.95	0.113	-0.218
	Fcγ Receptor-mediated Phagocytosis in Macrophages and Monocytes	4.25	0.100	1.265	2.46	0.070	1.134	6.23	0.130	1.387
	GM-CSF Signaling	1.74	0.070	1	4.14	0.113	1.134	5.24	0.141	0.707
	LPS/IL-1 Mediated Inhibition of RXR Function	6.25	0.083	1	3.75	0.061	-0.447	6.95	0.092	1
	Induction of Apoptosis by HIV1	4.35	0.131	0.707	2.92	0.098	0.816	5.86	0.164	-0.632
	Integrin Signaling	2.18	0.051	0.632	2.47	0.051	0.302	2.33	0.056	0
	TNFR1 Signaling	6	0.180	0.333	3.38	0.120	2.449	3.82	0.140	-1.134
	CCR5 Signaling in Macrophages	1.71	0.061	0	2.48	0.071	0	4.7	0.111	0.707
	Natural Killer Cell Signaling	3.36	0.064	0.277	3.74	0.064	0.832	4.63	0.079	1
	Death Receptor Signaling	8.08	0.154	0	4.94	0.110	0	6.71	0.143	-1.387
	Myc Mediated Apoptosis Signaling	6.97	0.196	0	5.21	0.157	0.707	4.66	0.157	-1.414
	Nitric Oxide Signaling in the Cardiovascular System	3.17	0.080	0	4.15	0.089	-1	3.52	0.089	1.667
	IL-15 Production	1.81	0.058	-0.378	2.58	0.066	0	2.12	0.066	1.414
	Apoptosis Signaling	6.71	0.131	-0.832	7.16	0.131	-0.832	8.92	0.162	-1
M2	PPARα/RXRα Activation	2.02	0.051	-1.897	2.28	0.051	-1.265	2.66	0.062	-2.309
	Wnt/β-catenin Signaling	1.89	0.052	-1.89	2.13	0.052	-1.134	2.1	0.058	-0.447
	LXR/RXR Activation	12.4	0.164	-1.789	6.65	0.109	-2.673	8.94	0.141	-2.183
	PPAR Signaling	5.63	0.115	-1.155	3.69	0.087	-2.333	6.85	0.135	-1.604

CD27 Signaling in Lymphocytes	1.58	0.076	-1	1.7	0.076	1	2.11	0.094	1.342
PD-1, PD-L1 cancer immunotherapy pathway	3.31	0.084	-0.707	2.92	0.075	1.134	4.38	0.103	-0.632
VEGF Signaling	2.13	0.067	-0.378	4.39	0.095	0	5.2	0.114	0.905
PI3K/AKT Signaling	3.85	0.072	-0.302	4.24	0.072	0.905	6.6	0.100	0.535
cAMP-mediated signaling	1.55	0.043	0.333	1.4	0.039	1	1.68	0.047	-1
mTOR Signaling	7.33	0.093	0.378	2.44	0.051	-0.816	7.38	0.097	1.155
VEGF Family Ligand-Receptor Interactions	1.36	0.056	0.447	2.71	0.078	-0.378	2.91	0.089	1.414
CXCR4 Signaling	1.46	0.046	1.633	2.62	0.057	0	3.6	0.074	0.302
PI3K Signaling in B Lymphocytes	1.46	0.049	1.89	1.65	0.049	1.134	2.7	0.070	0.632
STAT3 Pathway	3.77	0.081	1.897	6.33	0.103	0	7.69	0.125	0.277
Th2 Pathway	4.43	0.088	2.121	6.33	0.103	-0.905	8.51	0.132	0.535
TGF-β Signaling	1.77	0.063	2.236	3.23	0.083	0.816	4.08	0.104	0.707

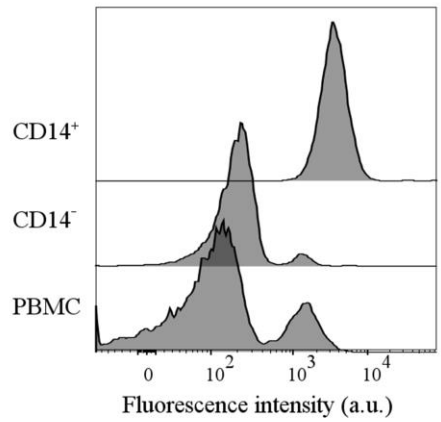

Figure 9. The purity of isolated monocytes. The proportion of $CD14^+$ cells in positively isolated $CD14^+$ cells (upper), CD14 negative fraction (middle), and PBMCs (lower) by flow cytometry.

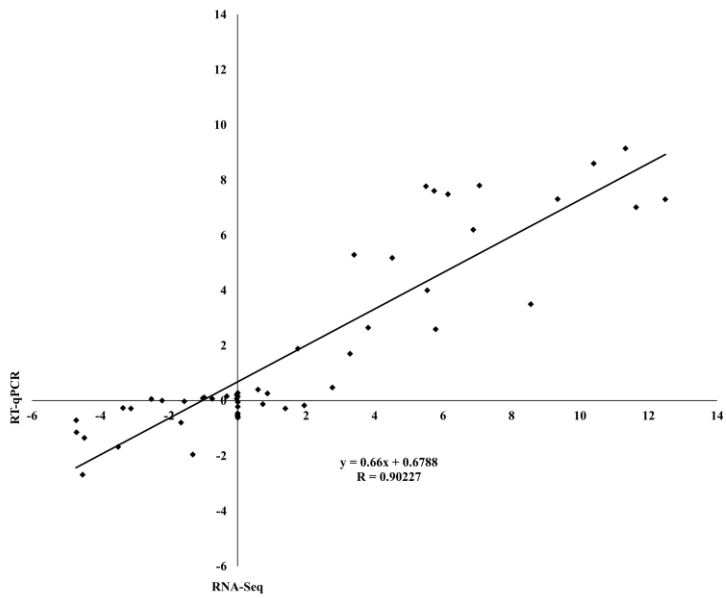

Figure 10. Validation of gene expression by RNA-Seq and quantitative real-time PCR. The relative expression levels were compared to those observed in the control cells to determine the fold changes in expression for each gene.

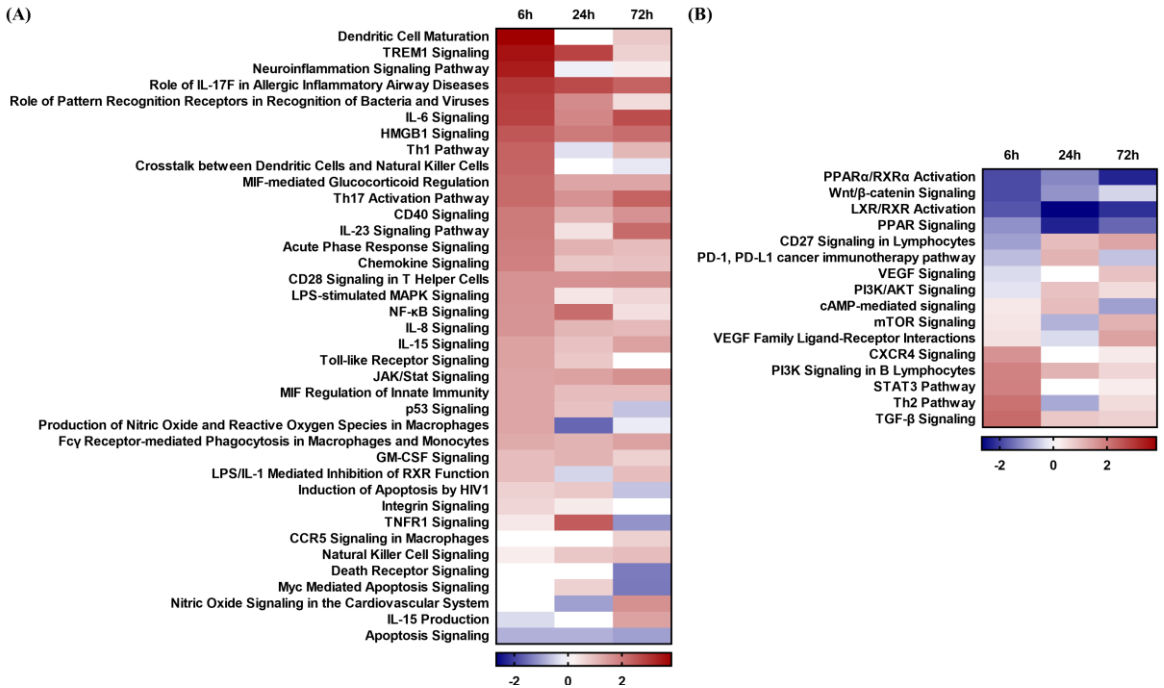

Figure 11. Heatmap of the canonical pathways related to macrophage activation in canine MDMs infected with *Mycobacterium intracellulare*. The heatmap displays the canonical pathways related to (A) M1 macrophage and (B) M2 macrophage polarization. The color gradient reflects the predicted directions based on the z-scores, where blue represents inhibition and red represents activation.

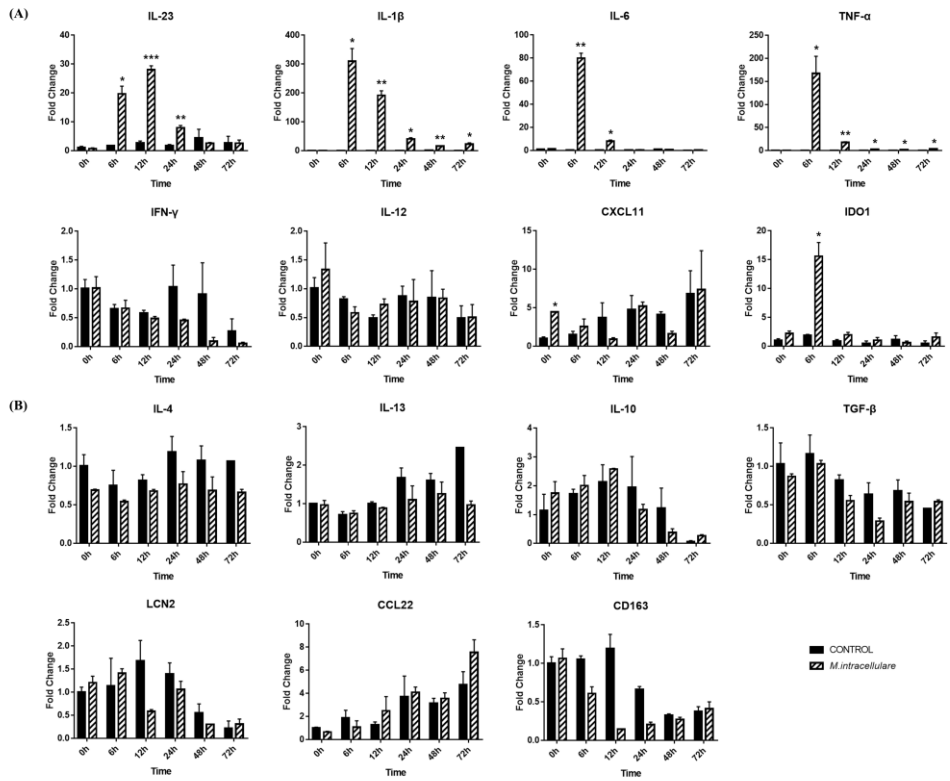

Figure 12. Gene expression analysis of canine MDMs infected with *Mycobacterium intracellulare*. The expression levels of genes related to (A) M1 and (B) M2 macrophages are presented as fold-changes in mRNA expression. mRNA expression was analyzed chronologically after canine MDMs were infected with *M. intracellulare* for 0 – 72 h. The mRNA expression in noninfected cells at 0 h was given a value of 1 as a reference for fold-change in expression. Each bar represents the mean ± SEM from three independent experiments in individual dogs. **p* <0.05, ***p* <0.01, and ****p* <0.001.

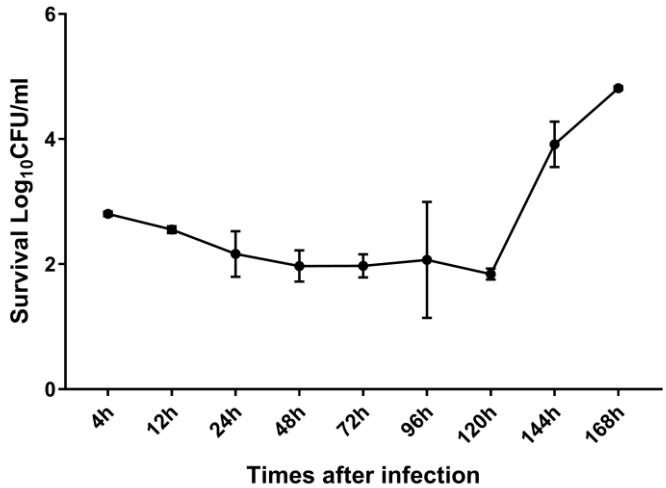

Figure 13. Intracellular survival and replication of *Mycobacterium intracellulare* in canine monocyte-derived macrophages. Intracellular survival of *M. intracellulare* was examined in canine MDMs for 7 days. Data are shown as mean ± SEM of three independent experiments.

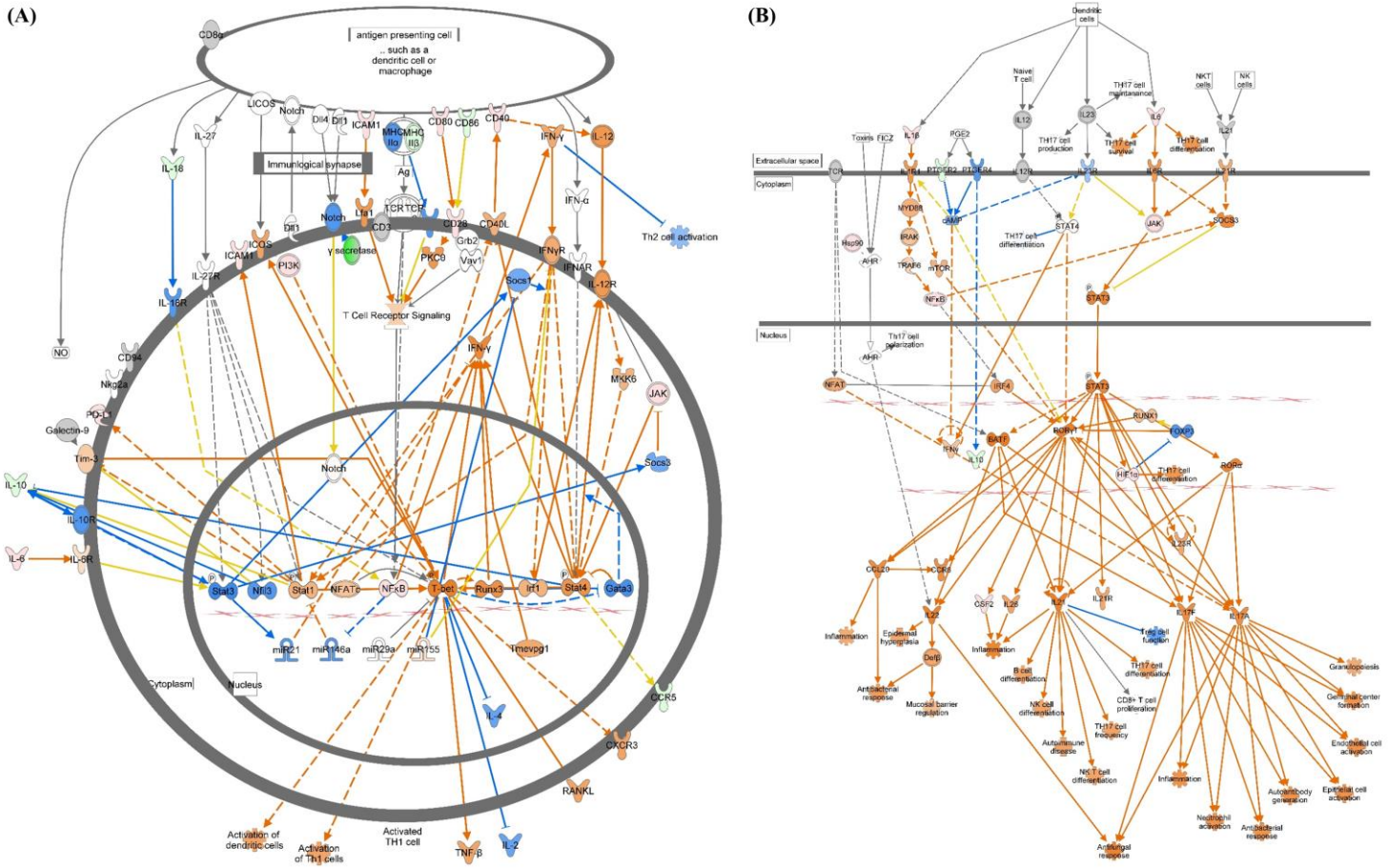
(A)
antigen presenting cell
.. such as a dendritic cell or macrophage
Immunological synapse
T Cell Receptor Signaling
Th2 cell activation
Cytoplasm
Nucleus
Activation of dendritic cells
Activation of Th1 cells
Activated TH1 cell
(B)
Dendritic cells
Naive T cell
TH17 cell maintenance
NKT cells
NK cells
TH17 cell production
TH17 cell survival
TH17 cell differentiation
Extracellular space
Cytoplasm
Nucleus
Th17 cell differentiation
Th17 cell polarization
Inflammation
Epidermal hyperplasia
Antibacterial response
Mucosal barrier regulation
B cell differentiation
NK cell differentiation
CD8+ T cell proliferation
Autoimmune disease
NKT cell differentiation
Granulopoiesis
Germinal center formation
Endothelial cell activation
Autoantibody generation
Epithelial cell activation
Neutrophil activation
Antifungal response

Figure 14. Ingenuity pathway analysis of the T helper cell response in *Mycobacterium intracellulare*-infected canine MDMs. (A) The Th1 Pathway and (B) Th17 Activation Pathway were expressed at 72 h post infection. The individual nodes represent proteins with relationships represented by edges. The red and green colors indicate up- and downregulation based on the expression values, respectively. The activation states by z-scores are shown as follows: orange indicates activation, blue indicates inactivation, and uncolored nodes indicate genes that were not differentially expressed in this pathway.

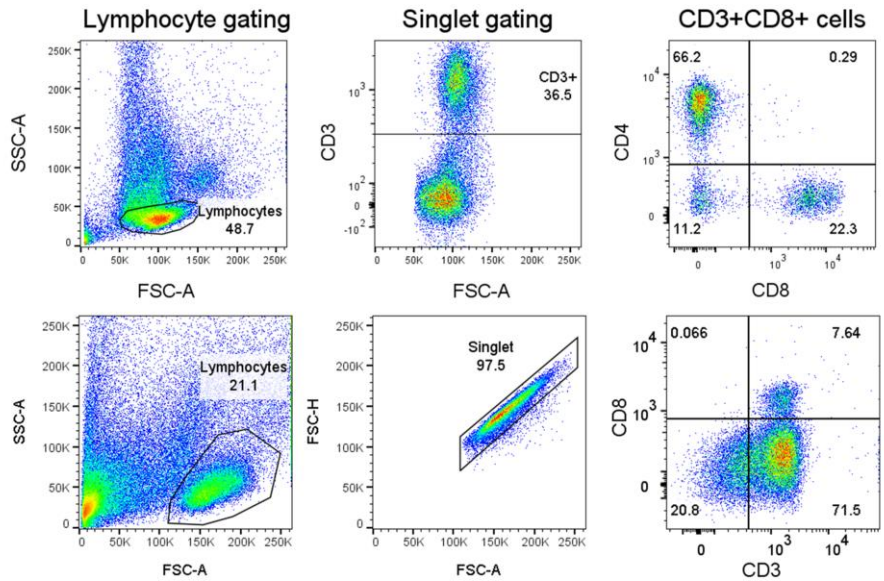

Figure 15. Phenotyping PBMCs and co-cultured cells. The proportion of $CD4^+$ T cells and $CD8^+$ T cells in PBMCs (upper) and the lymphocytes co-cultured with *M. intracellulare*-infected MDMs for six days (lower) by flow cytometry.

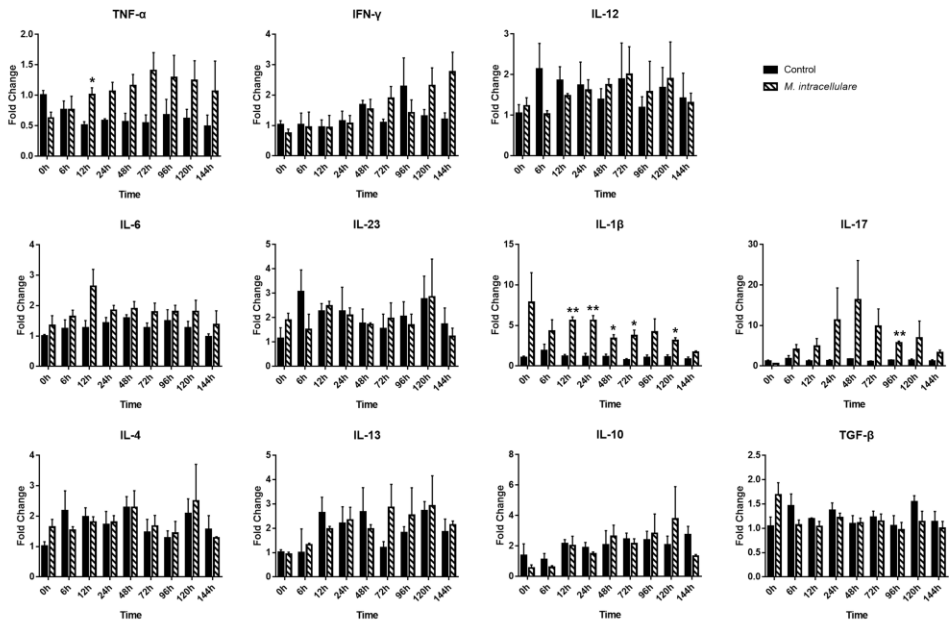

Figure 16. Differential cytokine mRNA expression in monocyte-depleted PBMCs co-cultured with *Mycobacterium intracellulare*-infected canine MDMs. The cytokines TNF-α, IFN-γ, and IL-12 (Th1); IL-4 and IL-13 (Th2); IL-6, IL-23, IL-1β, and IL-17 (Th17); and IL-10 and TGF-β (Treg) were quantified based on their fold changes in mRNA expression in canine monocyte-depleted PBMCs co-cultured with *M. intracellulare*-infected MDMs. The mRNA expression in non-infected cells at 0 h was given a value of 1 as a reference for fold change in expression. Each bar represents the mean ± SEM from three independent experiments in individual dogs. **p* <0.05, ***p* <0.01.

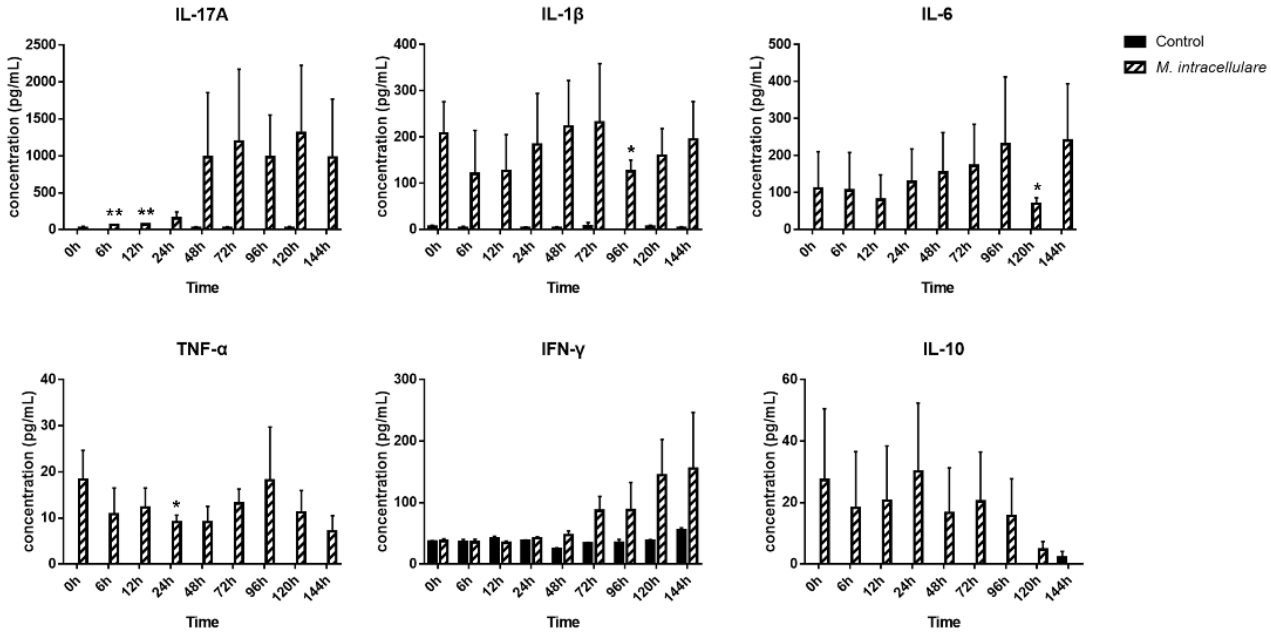

Figure 17. Cytokine expression in canine monocyte-depleted PBMCs co-cultured with canine MDMs after *Mycobacterium intracellulare* infection. The supernatant concentrations of IL-17A, IL-1β, IL-6, TNF-α, IL-12, IFN-γ, IL-10, and IL-4 were determined by ELISA. IL-4 and IL-12 were not detected. Cytokine expression in noninfected cells at each time point was used as a control. Each bar represents the mean ± SEM from three independent experiments in individual dogs. **p* <0.05, ***p* <0.01.

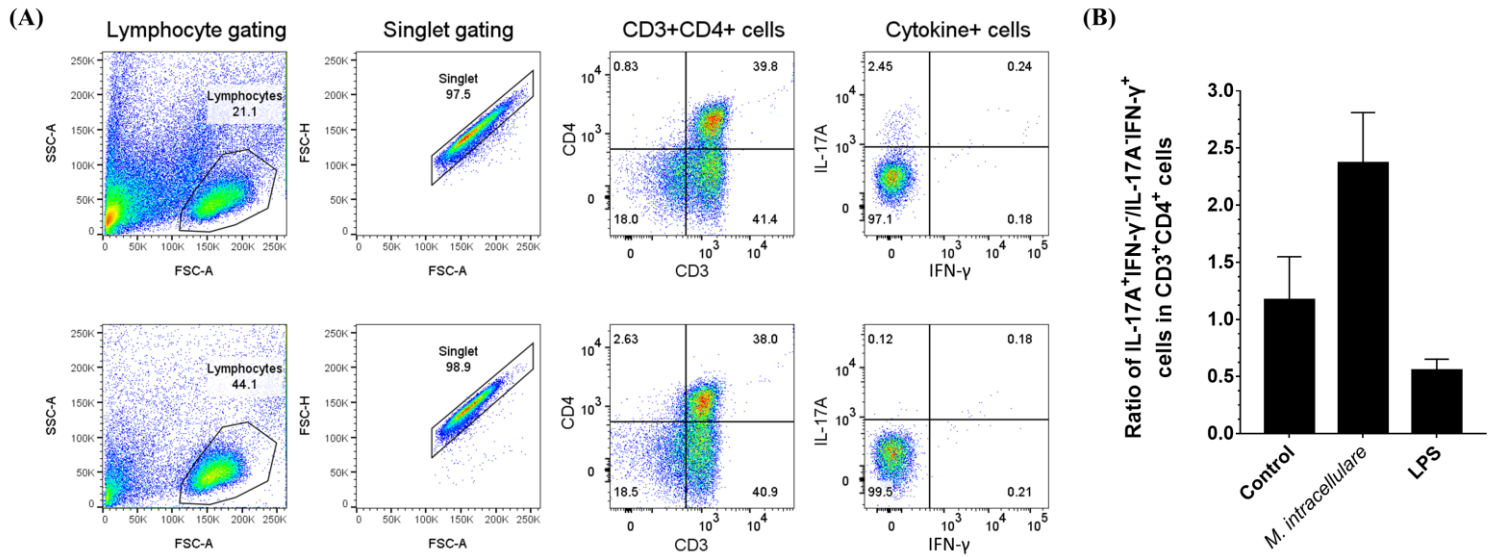

Figure 18. IL-17A-and IFN-γ-producing cells among canine CD4$^+$ T cells in response to *Mycobacterium intracellulare*. (A) Example of the flow cytometry gating strategy of IL-17A- or IFN-γ- producing canine CD4$^+$ T cells co-cultured with *M. intracellulare*-infected MDMs for 5 days (upper row) or noninfected MDMs (lower row). (B) Bar graph presenting the ratio of the proportion of IL-17A- to IFN-γ- producing CD4$^+$ T cells. Monocyte-depleted PBMCs were co-cultured with noninfected (control), *M. intracellulare*-infected, or LPS-stimulated MDMs. More than 30,000 CD4$^+$ T cells were analyzed. Each bar presents the mean ± SEM from five individuals.

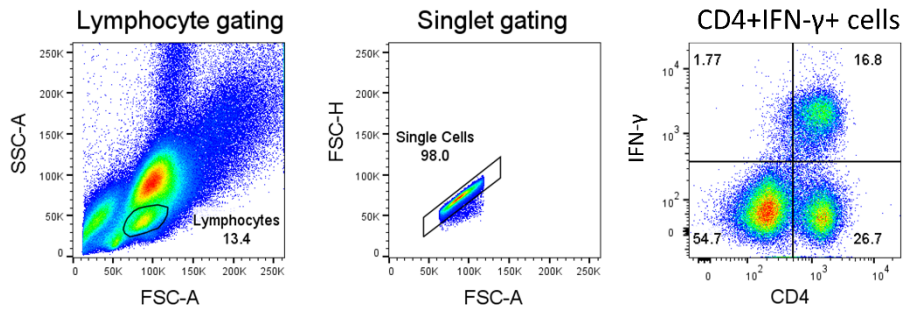

Figure 19. IFN-γ producing CD4$^+$ T cells from lymphocytes stimulated with LPS.

Lymphocytes were stimulated with 1ug/ml of LPS overnight. IFN-γ production in canine CD4$^+$ cells were confirmed by intracellular cytokine staining.

Chapter III

Whole genome analysis of *Mycobacterium intracellulare* isolates from environment reveals genetic diversity and the evolution of virulence

Abstract

Nontuberculous mycobacteria (NTM) are ubiquitous bacteria that are widely distributed in natural environments. *Mycobacterium intracellulare* is an opportunistic pathogen that causes pulmonary NTM infection in a wide range of hosts. In a previous study, the distribution and antibiotic resistance profiles of NTM isolated from Korea were analyzed. *M. intracellulare* was the most distributed among NTM, and most isolates were multidrug-resistant strains. In this study, multidrug resistant *M. intracellulare* isolates were analyzed by single-molecule sequencing to delineate the diversity of environmental strains with respect to phylogeny and pathogenesis. Whole genome sequencing and *de novo* assembly were performed for six *M. intracellulare* isolates and the type strain ATCC13950. To identify the host immune response induced by *M. intracellulare* isolates, the bacterial burden and cytokine expression were investigated in murine alveolar macrophages. Although some isolates were identified as *M. intracellulare* by sequencing of the housekeeping genes *rpoB*, *hsp65*, and *16S rRNA*, complete sequence phylogeny suggested that they should be reclassified as *M. intracellulare*-related strains such as *M. chimaera* and *M. paraintracellulare*. *M. intracellulare* isolates and the type strain had virulence factors involved in the type VII secretion system (esx-1 to esx-5) and transporters (mce4, mce5, mce7, mce9). However, *mce2* genes were identified only in isolate B1-4. Antimicrobial resistance gene prevalence was not consistent with the drug susceptibility test results of a previous study. Differences in the burden of *M.*

intracellulare and cytokine expression in macrophages were associated with genetic relevance. Whole genome sequencing of *M. inracellulare* isolates not only provides important insights into virulence factors and pathogenesis, but also helps to construct databases of complete sequences for *M. intracellulare* and related strains.

K**eywords:** *Mycobacterium intracellulare*, Whole genome sequencing, Virulence factors, Phylogeny, Pan genome

Introduction

Nontuberculous mycobacteria (NTM) are opportunistic pathogens that are highly abundant in environmental niches such as soil and water (Falkinham, 2015). The *Mycobacterium avium* complex (MAC) is the causative agent of most pulmonary NTM infections worldwide (Griffith et al., 2007; Kasperbauer & Daley, 2008; Stout et al., 2016; van Ingen et al., 2017). As the representative species of the MAC, *Mycobacterium avium* and *Mycobacterium intracellulare* are clinically important mycobacterial species (Diel et al., 2018). *M. intracellulare* is frequently isolated from environmental sources and clinical specimens in Korea (Y.-S. Kwon, Koh, & Daley, 2019; Park et al., 2020).

It is difficult to differentiate *M. intracellulare* subspecies from related strains with conventional methods because they are genetically related closely (Pranada et al., 2017; Van Ingen et al., 2012). This has caused taxonomic controversies in *M. intracellulare* and related strains (van Ingen et al., 2018). Some strains were identified as *M. intracellulare* initially by conventional methods, but the strains were reclassified recently as *M. intracellulare*-related strains such as *M. indicus pranii*, *M. yongonense*, *M. paraintracellulare*, and *M. chimaera* by sequence-based typing (S.-Y. Kim et al., 2015; S.-Y. Kim et al., 2017). Moreover, lipid profiling by MALDI-TOF MS and mycolic acid analysis by HPLC reclassified one *M. intracellulare* strain as *M. chimaera* (Epperson et al., 2018; Pranada et al., 2017; Tortoli et al., 2004). Several bacterial strains remain to be validated, although sequence-based typing

analyses and MALDI-TOF MS are quick and effective methods for distinguishing *M. intracellulare* strains.

Recent complete genome sequencing of *M. intracellulare* clinical strains revealed some discrepant cases in previously classified species (Tateishi et al., 2021). Whole genome sequencing has identified genetic differences between species and strains as well as differences in virulence and pathogenesis. Comparative genome analysis of MAC have provided insight into the genomic characteristics of pathogenic mycobacteria. However, the genome sequencing of MAC was predominantly performed in *M. avium* (Bannantine et al., 2020; J. Lim et al., 2021; Uchiya et al., 2017). The genomic characteristics of *M. intracellulare* still need to be elucidated.

This study presents the complete genomes of *M. intracellulare* ATCC13950, four multidrug-resistant *M. intracellulare*, and two *M. intracellulare*-like isolates from the environment in Korea. The comparative genome analysis delineates the difference between the type strain and the environmental isolates with respect to virulence factors. The complete genome phylogeny suggested the reclassification of *M. intracellulare* isolates as *M. intracellulare*-related strains. This study would help to understand the pathological and genetic distinctions between *M. intracellulare* and isolates from the environment.

Materials and Methods

Bacterial strain and culture conditions

Six *M. intracellulare* isolates were previously isolated from soils in parks, where companion animals are allowed to roam free (off-leash). These isolates were identified as *M. intracellulare* through *rpoB*, *hsp65*, and *16S rRNA* gene analysis in a previous study (Park et al., 2020). *M. intracellulare* ATCC13950 was used as a reference strain. Seven *M. intracellulare* strains were cultured on Middlebrook 7H10 agar (BD Biosciences, CA, USA) containing 0.1% casitone (BD Biosciences) and subcultured in Middlebrook 7H9 broth supplemented with 0.04 % casitone for 7 days.

DNA extraction and genome sequencing

Genomic DNA was extracted from the *M. intracellulare* isolates using the cetyl-trimethyl-ammonium bromide-sodium chloride (CTAB)-lysozyme method (Larsen, Biermann, Tandberg, Hsu, & Jacobs Jr, 2007). Genome sequencing of seven *M. intracellulare* strains was performed on a PacBio Sequel single-molecule real-time (SMRT) sequencing instrument (Pacific Biosciences, Menlo Park, CA). The library was constructed with a SMRTbell™ Template Prep Kit 1.0 following the manufacturer's instructions (Pacific Biosciences). The constructed library was validated by an Agilent 2100 Bioanalyzer. *De novo* assembly was conducted using SMRT Link v8.0, Flye v 2.7.1, and CANU v 1.5 (Kolmogorov, Yuan, Lin, & Pevzner,

2019; Koren et al., 2017; Lin et al., 2016). The resulting contigs were circulated using Circlator 1.4.0 (Hunt et al., 2015). The genome was annotated through prokka v 1.14.6 (Seemann, 2014).

Pangenome analysis and Functional analyses

The Bacterial Pangenome Analysis (BPGA) Tool was used for pangenome analysis (Chaudhari, Gupta, & Dutta, 2016). Gene sets were obtained from the Roary (v 3.13.0) analysis were aligned using MAFFT (Page et al., 2015). Functional analysis was performed based on the Basic Local Alignment Search Tool (BLAST) algorithm. Circular comparisons of *M. intracellulare* isolates were generated by BRIG (BLAST Ring Image Generator) version 0.95 according to the user manual and showed the genomic similarity between the *M. intracellulare* ATCC13950 and the six isolates (Alikhan, Petty, Zakour, & Beatson, 2011). USEARCH was used to run the BLAST (Edgar, 2010). The genomes were classified functional by the Clusters of Orthologous Group (COG) with 50% identity (Galperin, Makarova, Wolf, & Koonin, 2015). Virulence factors (VFs) were analyzed by three databases: Virulence Factors of Pathogenic Bacteria (VFDB) (L. Chen et al., 2005), Victors (Sayers et al., 2019) and PATRIC (Wattam et al., 2017). Antimicrobial resistance (AMR) genes were annotated with the databases from ARG-ANNOT (Gupta et al., 2014), Lahey/NCBI and CARD (Jia et al., 2016). Both VF and AMR were analyzed based on an identity cutoff of 0.7. COG classification and VF analysis were visualized using GraphPad

Prism software (v7.0) (Windows, GraphPad Software, La Jolla California USA, www.graphpad.com). The protein–protein interaction (PPI) network was constructed using the STRING database (https://string-db.org/). These data were visualized with Cytoscape 3.9.0.

Phylogenetic analysis

A phylogenetic tree was constructed using 15 complete sequences in the *Mycobacterium avium* complex. Eight reference genomes were downloaded from NCBI GenBank (GCA_000014985.1, GCA_009741445.1, GCA_000007865.1, GCA_000829075.1, GCA_002285715.1, GCA_002219285.1, GCA_000222105.4, GCA_010723675.1). Fifteen genomes were analyzed in the MAUVE alignment tool with the neighbor-joining method based upon overall nucleotide similarities between the MAC strains (Darling, Mau, Blattner, & Perna, 2004).

Growth curves

M. intracellulare ATCC13950 and six isolates were grown in 7H9 medium until they reached stationary phase. Each sample was measured at an optical density of 600 nm using a spectrophotometer (GeneQuant Pro RNA/DNA Calculator, Amersham Pharmacia Biotech, Cambridge, UK) at 24 h intervals for 40 days.

Cell culture and infection

Murine alveolar macrophage cell line AMJ2-C11 were obtained from American Type Culture Collection (ATCC, Manassas, VA) and cultured in RPMI1640 supplemented with 10% FBS. AMJ2-C11 were infected with *M. intracellulare* ATCC13950, S1-36A, S1-32, S2-11, S2-8, N6-8, and B1-4 at a multiplicity of infection (MOI) of 1.

Intracellular survival and replication

AMJ2-C11 were infected with 6 isolates and type strain of *M. intracellulare* at an MOI of 1. After 4h of infection, the cells were washed with DPBS and incubated for 4, 120, and 168 h. The viable intracellular bacteria were extracted with treatment of 0.1% Triton X-100 (Sigma-Aldrich, MO, USA) after cells were washed. Bacteria were vigorously vortexed and agitated for 30 s to lyse cells. Bacteria were serially diluted and then plated onto 7H10 agar plate to enumerate viable bacteria.

Quantification of cytokines

Cytokine concentrations were measured by an ELISA kit (eBioscience Co, Invitrogen, San Diego, CA). Murine IL-1β (BMS6017), IFN-γ (BMS606), TNF-α (BMS607), TGF-β (BMS608), IL-12 (BMS616), IL-13 (BMS6015), IL-4 (BMS613), IL-6 (KMC0061), IL-23 (BMS6017), and IL-10 (88-7105-22) were detected in the

supernatants of AMJ2-C11 at 24 h post 7 *M. intracellulare* strains. Cytokine concentrations were determined with corresponding detection horseradish peroxidase (HRP)-conjugated antibodies. Optical absorbance was read at 450 nm and analyzed.

Cell staining

At hours 4 – 168 of infection, AMJ2-C11 were washed and fixed with 4% formaldehyde solution for 4 hours at room temperature. To visualize acid-fast *M. intracellulare* within cells and analyze their intracellular reproduction, the cells stained by the Ziehl-Neelsen method. Intracellular mycobacteria were counted under a microscope, and their mean number per macrophages was determined. The cells stained by the Ziehl-Neelsen methods were further counterstained with 1% methylene blue.

Statistical analysis

All experiments were repeated at least three times. Data were presented as mean ± standard deviation (SD). Statistical analysis was performed with GraphPad (GraphPad Software, La Jolla, CA) using an unpaired t-test with Welch's correction, and statistically significant differences are indicated as * $p < 0.05$.

Ethics statement

This study was conducted in accordance with the regulations of the Seoul National University Institutional Biosafety Committee (protocol: SNUIBC-R190906-1).

Data deposition

This whole genome sequencing project has been deposited at GenBank under BioProject PRJNA733007. The complete genome sequences of seven *M. intracellulare* strains determined in this study have been deposited in the GenBank database under accession nos. CP076382, CP076381, CP076380, CP076379, CP076378, JAHKNE000000000, and JAHKND000000000.

Results

Overview of genomic features

Six environmental isolates were selected to investigate the interrelationship with type strains ATCC13950. All isolates were confirmed to be *M. intracellulare* based on housekeeping genes sequencing of the *16S rRNA*, *rpoB*, and *hsp65* genes in a previous study (Park et al., 2020). *De novo* assembly of the long PacBio reads with an average genome coverage of 143x resulted in single scaffolds (one contig for each of the five genomes; MI13950, S1-36A, S1-32, S2-8, S2-11) representing the complete *M. intracellulare* genomes (average 5,552,877 bp; Table 13). Even though B1-4 and N6-8 were not a single contig, the reads were assembled into high quality, near complete genomes (approx. 90% complete) supported by high N50 values and few scaffolds. The average GC content was calculated to be 67.96%.

Comparative genome analysis of *M. intracellulare* isolates

The genomes of the six *M. intracellulare* isolates was assessed using BLAST Ring Image Generator (BRIG) on the basis of similarity against *M. intracellulare* ATCC13950. The BRIG comparative analysis displayed multiple variations in the six *M. intracellulare* isolates when compared to the *M. intracellulare* ATCC13950 genome (Figure 20A). The frequency of accessory genes was determined from the

pangenome analyses by Roary (Figure 20B). The accessory genome is composed of shell genes that are present in at least 15% but less than <95% of the strains (n=2,714 genes) and could be genes that are present in less than 15% of strains (n=4,371 genes representing 45.34% of the pangenome). In particular, strain B1-4 had the highest number of accessory genes and unique genes (Figure 21A). Out of a total of 2,711 unique genes, 1,900 genes belonged to B1-4 of 7 strains.

Functional annotation

Functional clustering of the pangenome was performed with COG based on protein sequence similarity (Figure 21B). Apart from the proteins of unknown function or general function only, the main functional categories of all the strains were information storage and processing, cellular processes and signaling, and metabolism; the core genes were more relevant for metabolism activity, such as lipid transport and metabolism, amino acid transport and metabolism, and energy production and conversion. However, the core (2,465 genes), accessory (1,439 genes), and unique genes (2,612 genes) were mainly annotated as unknown function in the poorly characterized category.

Virulence factors and antimicrobial resistance genes of *M. intracellulare* isolates

The virulence factors of *M. intracellulare* isolates and the type strain were analyzed using three databases (VFDB, Victors, PATRIC). The virulence factors of the core genome from 7 *M. intracellulare* strains were classified by COG (Figure 22A). The virulence factors within core genes were more relevant for metabolism and unknown function, such as lipid transport and metabolism and unknown function. In particular, most virulence factors were classified as unknown function (42.14%, 185 genes).

To explore the interactions among core virulence factors of unclassified function, a protein-protein interaction (PPI) network was constructed based on functional association by STRING. The PPI network was composed of 148 nodes and 446 edges (Figure 23). The average node degree was 6.03, and the average local clustering coefficient was 0.449. One network showed the strongest degree of significance (PPI enrichment, $p < 1.0e-16$). The network revealed six important functional categories principally involved in the effector delivery system, exoenzyme, immune modulation, nutritional/metabolic factor, regulation, and stress survival based on VFDB. These six functional categories were not fully separated but rather formed an interconnected network regulating each other.

Of these virulence factors, the genes with 100% identity were most commonly associated with the ESX systems and a mammalian cell entry (mce) gene family (Table 14). Of the ESX systems, genes related to the five type VII secretion systems (T7SS; ESX-1 to ESX-5) showed 100% similarity. Among the core genomic virulence factors, mce4, mce5, mce7, and mce9 showed 100% similarity, and mce1,

mce3 and mce8 showed high similarity (average 92.8% identity). Twenty virulence factors were detected from the accessory genes within six *M. intracellulare* strains and the type strain ATCC13950 (Figure 22B). Of these, 10 virulence factors were only identified in the B1-4 strain. In particular, factors in the mce2 family (mce2A, mce2B, mce2C, mce2D, mce2E, mce2F, mce2R) were mainly identified in B1-4.

To identify the presence of antimicrobial resistance genes, the genomes of *M. intracellulare* isolates and the type strain were submitted to three databases: ARG-ANNOT, Lahey/NCBI and CARD. No accessory genes were identified with the three databases. Of the core genes, seven clusters (715, 1649, 1971, 4055, 4829, 5559, 6942) were identified as antimicrobial resistance genes (Table 15).

Genome sequence-based phylogenetic analysis of the *Mycobacterium avium* complex including six *M. intracellulare* isolates

The phylogenetic tree was constructed using the genomes newly sequenced in this study (*M. intracellulare* S1-36A, S1-32, S2-11, S2-8, N6-8, B1-4, ATCC13950) and those that were already available at high depth (*M. colombiense* CECT3035, *M. avium* 104, *M. avium* subsp. *hominissuis* TH135, *M. avium* subsp. *paratuberculosis* K-10, *M. avium* subsp. *avium* DSM44156, *M. timonense* JCM30726, *M. marseillense* FLAC0026, *M. chimaera* DSM44623) (Figure 24). Five *M. intracellulare* isolates (S1-36A, S2-8, S1-32, S2-11, N6-8) were clustered together

in a branch with *M. intracellulare* ATCC13950; however, B1-4 was more closely related to *M. chimaera* DSM44623 than to *M. intracellulare* ATCC13950.

Growth rate of *M. intracellulare* isolates and the type strain

The optical density (OD) of *M. intracellulare* isolates and the type strain were measured over a 38-day incubation period. There were clear differences in growth of the *M. intracellulare* isolates and *M. intracellulare* ATCC13950 (Figure 25). The growth rates were separated into three different groups: one group included 3 *M. intracellulare* strains (ATCC13950, S2-11, S1-32) that reached log phase within two weeks. The other two strains (S1-36A, S2-8) reached OD saturation within three weeks. N6-8 and B1-4 showed different kinetic trends and increased over four weeks. This finding supported the results of our phylogenetic study, suggesting that the two isolates might be *M. intracellulare*-related strains rather than the *M. intracellulare* type strain.

The differential burden of mycobacteria in murine alveolar macrophages infected with *M. intracellulare* isolates

Murine alveolar macrophages were infected with each of the seven *M. intracellulare* strains at a MOI of 1. CFU was enumerated at 4 h, 3 h, and 5 days

after infection (Figure 26). The percentage of survival *M. intracellulare* within macrophages indicated that B1-4 was higher than other isolates after 4 hours. All strains were replicated within macrophages until 5 days. Only N6-8 and S2-11 increased after 7 days after infection.

Differential expression of cytokines in murine alveolar macrophages by infection of *M. intracellulare* isolates

To identify the production of cytokines induced by each isolate of *M. intracellulare*, murine alveolar macrophages were infected with seven isolates of *M. intracellulare* for 24 h. The supernatant of macrophages was analyzed by ELISA (Figure 27). Compared to uninfected controls, three cytokines (TNF-α, IL-6, TGF-β) were induced by infected macrophages while other cytokines (IL-1β, IFN-γ, IL-12, IL-4, IL-23, IL-10, IL-13) were not detected. Both TNF-α and IL-6 were significantly produced by all *M. intracellulare* strains-infected macrophages. Macrophages infected with *M. intracellulare* ATCC13950 and S1-36A were significantly produced TGF-β. B1-4 induced a higher expression level of TGF-β compared to other isolates although it was not significant. Of all isolates, only N6-8 and S2-11 induced low expression levels of cytokines compared to other isolates.

Death of macrophages with increased *M. intracellulare* loads

Analysis of mycobacterial loads in alveolar macrophages throughout 48 – 120 hours of infection demonstrated that the macrophages each basically contained a single isolate following infection (Figure 28A). In the macrophages infected with environmental isolates of *M. intracellulare*, a considerable number of macrophages had increased mycobacterial loads. In parallel, the number of viable macrophages was dramatically reduced (Figure 28B, Figure 29), probably due to necrotic cell death, which had been indicated by the typical morphology of some cells in this population at 72 hours following infection (Figure 30). These cells normally contained a large number of ingested *M. intracellulare*. In contrast, macrophages infected with *M. intracellulare* ATCC13950 showed an increase in the number of viable macrophages as the *M. intracellulare* load decreased (Figure 28). *M. intracellulare* ATCC13950-infected macrophages were not observed any morphological signs of cell death (Figure 30). The morphological differences of macrophages differentiation between environmental isolates and type strain were observed after 48 hours in infection (Figure 29). *M. intracellulare* ATCC13950-infected macrophages predominantly appeared as spindeloid macrophages with an elongated cell body and cytoplasmic extensions on the apical ends of the cell bodies similar to M2 macrophages morphology (Figure 30). Macrophages infected with the isolates S1-36A, S1-32, and S2-8 also presented spindeloid and numerous multinucleated giant cells with abundant cytoplasmic projections on the cellular surface. On the contrary, macrophages infected with N6-8 and S2-11 appeared as

enlarged amoeboid cell shape with roundish cell bodies observed in M1 macrophages. Macrophages infected with B1-4 presented a small and roundish morphology at 48 hours following infection, and spindeloid cells were also observed 72 hours after infection.

Discussion

Mycobacterium avium complex (MAC) is the most common cause of nontuberculous mycobacteria-related pulmonary disease (Y.-S. Kwon & Koh, 2016). *Mycobacterium intracellulare* is a representative opportunistic pathogen of the MAC, which includes *Mycobacterium avium* (Diel et al., 2018). The MAC infection occurs mainly from environment rather than through person-to-person transmission (Shin et al., 2020). *M. intracellulare* was predominantly isolated within NTM species in urban areas in Korea. The isolates showed broad spectrum of antibiotic resistance even to the aminoglycosides and macrolides (Park et al., 2020).

To understand the molecular mechanisms of phylogenetics and pathogenesis in *M. intracellulare*, the whole genomes were sequenced using single-molecule real-time sequencing. This study presented the complete genomes of 5 multidrug-resistant *M. intracellulare* isolates (S1-36A, S1-32, S2-11, S2-8, B1-4) and 1 *M. intracellulare* isolate (N6-8), including the type strain *M. intracellulare* ATCC13950. The *M. intracellulare* isolates were previously identified as *M. intracellulare* based on the housekeeping genes *hsp65*, *rpoB*, and *16S rRNA* (Park et al., 2020). The four *M. intracellulare* strains and the type strain were assembled in single complete genomes. The B1-4 and N6-8 were assembled into high quality completed genome; however, they were not constructed in a single contig. Genome size of 5 isolates (S1-36A, S1-32, S2-11, S2-8, N6-8) was approximately 5.4 Mbp, which is similar to that of the type strain *M. intracellulare* ATCC13950. Genome size of the B1-4 was 6.4 Mbp,

which is larger than the other isolates.

Pangenome analysis showed that most of the core genome of *M. intracellulare* isolates and the type strain were classified into unknown function group by COG. Of virulence factors classified as unknown function, the VF genes were mainly related to ESX systems and a mammalian cell entry (mce) gene family. Type VII secretion systems (T7SSs) are critical for the secretion of effector proteins in mycobacteria (Rivera-Calzada, Famelis, Llorca, & Geibel, 2021). The core genes of seven *M. intracellulare* strains showed 100% identity with each mycobacterial T7SS substrate related to the five ESXs (esx-1 to esx-5; Table 14). The numbers of encoded ESX systems differ between mycobacterial strains (Newton-Foot, Warren, Sampson, Van Helden, & van Pittius, 2016; Rivera-Calzada et al., 2021). ESX-1 is involved in intracellular survival and phagosomal rupture (Augenstreich et al., 2017; Beckwith et al., 2020; Simeone et al., 2012). ESX-2 and ESX-4 have been regarded as nonessential (Cole et al., 2001; Singh et al., 2015); however, ESX-4 was recently reported to be essential for intracellular growth in phagocytes (Girard-Misguich et al., 2018; Laencina et al., 2018). ESX-3 has a pivotal role in metal ion acquisition under iron-limiting conditions (Serafini, Boldrin, Palù, & Manganelli, 2009; Tufariello et al., 2016) and inhibits the cellular immune system (Mittal et al., 2018; Portal-Celhay et al., 2016). ESX-5 is involved in nutrient uptake and is predominantly identified in slow-growing species including most pathogenic species (Abdallah et al., 2008; Ates et al., 2015).

Mce family proteins play a vital role in the cell wall invasion and persistence of mycobacteria in macrophages (F. Zhang & Xie, 2011). The genes belonging to the Mce5, Mce7, and Mce9 operons are absent in *M. tuberculosis* but are present in most NTM species, while Mce4 is highly conserved in *M. tuberculosis* and NTM species (Fedrizzi et al., 2017). In this study, the mce4, mce5, mce7, and mce9 genes exhibited 100% identity all *M. intracellulare* isolates and the type strain. However, the mce2 family genes (mce2A, mce2B, mce2C, mce2D, mce2E, mce2F, mce2R) were identified only in B1-4 (Figure 22B). The expression of the mce2 operon is regulated by Mce2R, which is needed for mycobacterial growth and may play a role in the dormancy of mycobacteria (de la Paz Santangelo et al., 2009; Marjanovic, Miyata, Goodridge, Kendall, & Riley, 2010; F. Zhang & Xie, 2011). The Mce2E suppressed the innate immune response and promoted epithelial cells proliferation (Qiang et al., 2019).

Antimicrobial resistance (AMR) genes were detected in the 7 clusters (715, 1649, 1971, 4055, 4829, 5559, 6942) of the core genome based on an identity cutoff of 0.7 in three databases (ATG-ANNOT, Lahey/NCBI, CARD). The EfpA efflux pump from the MFS family of transporters confers increased tolerance to a wide variety of anti-TB drugs, both first-line (rifampicin, isoniazid) and second-line drugs (moxifloxacin, amikacin) (G. Li, Zhang, Guo, Jiang, et al., 2015; G. Li, Zhang, Guo, Wei, et al., 2015; Rai & Mehra, 2021). The *efpA* gene is highly conserved across pathogenic and nonpathogenic mycobacteria (Machado et al., 2012; Rai & Mehra, 2021). MurA, UDP-N-acetylglucosamine enolpyrubyl transferase, catalyzes the

initial step of peptidoglycan biosynthesis (Lovering, Safadi, & Strynadka, 2012; Liming Xu et al., 2014). The *MurA* gene is an essential gene for mycobacterial growth (Sassetti, Boyd, & Rubin, 2003). Translation elongation factor Tu (Ef-Tu) is a conserved protein that plays a pivotal role in protein biosynthesis and mycobacterial evasion of the host immune system (Harvey, Jarocki, Charles, & Djordjevic, 2019; Monahan, Betts, Banerjee, & Butcher, 2001; Sajid et al., 2011). AviRb encodes rRNA methyltransferases within 23S rRNA and mediates resistance to the oligosaccharide antibiotics avilamycin (Treede et al., 2003). MtrA contributes to susceptibility to first-line antimycobacterial drugs, including rifampin and isoniazid and controls cell division and cell wall metabolism (Gorla et al., 2018). MfpA, a pentapeptide-repeat protein in mycobacteria, protects gyrase from fluoroquinolone antibiotics by acting as a mimic of the transported (T) DNA segment (L. Feng et al., 2021). RbpA, an RNA polymerase-binding protein, is involved in resistance to the first-line anti-tuberculosis drug rifampin (Dey, Verma, & Chatterji, 2010, 2011). The antimicrobial resistance genes were not consistent with the phenotypic drug susceptibility test in a previous study (Park et al., 2020). The antibiotic resistance patterns of *M. intracellulare* isolates were diverse by strain (Table 16). Most *M. intracellulare* isolates exhibited multidrug resistance to streptomycin, amikacin, azithromycin, ethambutol, isoniazid, and imipenem, except N6-8. N6-8 was susceptible to all tested drugs; however, seven AMR genes were detected in common. In addition, a previous study showed that mutations in the 16S rRNA (*rrs*) and 23S rRNA (*rrl*) genes, which are involved in resistance to

aminoglycoside antibiotics (Sreevatsan et al., 1996), and the erythromycin ribosome methylase (*erm*) gene, which is related to macrolide resistance (Nash, Andini, Zhang, Brown-Elliott, & Wallace Jr, 2006), were not associated with resistance in these isolates. This result revealed that antimicrobial resistance genes might be dependent on intrinsic mechanisms without any genetic changes and some resistance phenotypes could not be ascribed to a causative mutation.

The pangenome analysis showed that the proportion of noncore genes to core genes was comparatively high in B1-4, and the phylogenetic analysis revealed that only B1-4 was clustered with *M. chimaera* (NZCP019221.1), while other strains were clustered together in a branch with *M. intracellulare* type strain ATCC13950. To determine its similarity to *M. intracellulare*-related strains, B1-4 was reconstructed by reference assembly with all available MAC sequences in NCBI databases (data not shown). The results indicated that B1-4 was similar to both M. *chimaera* (NZ_CP019221.1) and *M. paraintracellulare* (NZ_016948.1). These data can also support the previous report that B1-4 clustered with other *M. chimaera* isolates (B1-7-2) in a phylogeny analysis based on the *rpoB* gene (Park et al., 2020). Additionally, N6-8 was classified with *M. paraintracellulare* (NZ_AP024251.1) by reference assembly although the strain was clustered with *M. intracellulare* ATCC13950 in the phylogenetic analysis with the complete sequences. N6-8 was deposited as *M. paraintracellulare* in the NCBI database (JAHKND000000000). These results have a limitation in that the number of completed sequences of *M. intracellulare* and closely related strains was not sufficient to perform a full comparative analysis. The

taxonomy of *M. intracellulare* at the species or subspecies level has become controversial (Pranada et al., 2017; Van Ingen et al., 2012). Strains classified as *M. intracellulare* by conventional methods with sequence-based typing have been recently reclassified as *M. intracellulare*-related strains, including *M. indicus pranii*, *M. yongonense*, *M. paraintracellulare*, and *M. chimaera* (S.-Y. Kim et al., 2015; S.-Y. Kim et al., 2017). The complete genome sequencing of *M. intracellulare* clinical strains suggested that the classification of previously isolated species should be reconsidered (Tateishi et al., 2021). However, the complete sequences of *M. intracellulare* and related strains still need to be constructed for comparison to other strains of MAC (Bannantine et al., 2020; J. Lim et al., 2021; Uchiya et al., 2017). Despite these limitations, the growth rates also showed differences between the two strains (B1-4, N6-8) and *M. intracellulare* isolates. B1-4 and N6-8 showed a different kinetic trend in comparison with other strains. Four isolates and the ATCC13950 strain reached log phase within 2 weeks, whereas B1-4 and N6-8 growth continued over four weeks.

To identify the host immune response induced by *M. intracellulare* isolates, the bacterial burden and cytokine expression were investigated in murine alveolar macrophages infected with *M. intracellulare* isolates for 7 days. The differential burden of mycobacteria and cytokine expression were associated with genetic relatedness. Only two isolates (N6-8, S2-11) genetically distant from *M. intracellulare* ATCC13950 exhibited a dramatic increase in alveolar macrophages at 7 days after infection. Three cytokines (TNF-α, IL-6, TGF-β) expressed in infected

alveolar macrophages also represented lower levels compared to other isolates. However, B1-4 showed a kinetic trend of bacterial burden similar to that of *M. intracellulare* ATCC13950, but was not clustered with ATCC13950 in the phylogeny. In addition, the expression level of TGF-β in macrophages infected with B1-4 was higher than that of other strains, which was similar to that of *M. intracellulare* ATCC13950. Furthermore, spindeloid cells identified in *M. intracellulare* ATCC13950-infected macrophages were also observed in B1-4-infected macrophages 72 hours after infection. However, the number of infected and viable cells was not associated with genetic similarities and differences. In contrast to the environmental isolates, macrophages infected with *M. intracellulare* ATCC13950 proliferated 120 hours after infection, and no morphological signs of necrosis/apoptosis were observed during infection. Additionally, the infected macrophages differentiated into spindeloid macrophages with an elongated cell body observed in the M2 macrophage morphology (McWhorter, Wang, Nguyen, Chung, & Liu, 2013; Vereyken et al., 2011; Verreck, de Boer, Langenberg, van der Zanden, & Ottenhoff, 2006; Waldo et al., 2008). As previously reported, these results are considered to be related to the induction of chronic inflammation and might reveal differences in clinical and environmental isolates (Le et al., 2020; Parisi et al., 2018).

This study presented complete sequences of environmental isolates of *M. intracellulare* through whole genome sequencing and investigated the host immune response induced by isolates in alveolar macrophages. Comparative genomic approaches have led to a reconsideration of the classification of some *M.*

intracellulare strains. Pangenome analysis provided genetic information that can be used to elucidate the virulence and pathogenesis of *M. intracellulare*. However, the population size of *M. intracellulare* and related strains in this study was limited. Nevertheless, the results clarify the genetic similarity and diversity of *M. intracellulare* isolates, which will enable a better understanding of the evolution of *M. intracellulare* in environment.

Table 13. Summary table for the high quality draft assemblies obtained.

Strain	# contigs	N50 (bp)	GC(%)	#ORF	Length (bp)
MI13950	1	5,402,454	68.1	5,084	5,402,454
S1-36A	1	5,384,204	68.06	5,076	5,384,204
S1-32	1	5,405,657	68.16	5,093	5,405,657
S2-11	1	5,431,761	68.04	5,105	5,431,761
S2-8	1	5,421,348	68.04	5,096	5,421,348
N6-8	2	5,483,504	68.1	5,155	5,493,639
B1-4	8	6,331,077	67.24	5,980	6,331,077

Table 14. Virulence factors of protein–protein interaction networks with 100% identity.

VFDB classification		Gene Symbol	Identity	Align length	E-value	Bit score
Effector delivery system	ESX-1	espR	100	132	4.3E-70	261.2
	ESX-2	eccE2	100	540	0	1076.6
	ESX-2	PPE4	100	487	7.8E-282	966.5
	ESX-2	PPE69	100	390	7.1E-222	766.9
	ESX-2	espG2	100	276	2E-154	542.3
	ESX-2	esxD	100	104	2E-54	208.8
	ESX-2	PE36	100	101	2.7E-48	188.3
	ESX-2	esxC	100	95	3E-49	191.4
	ESX-3	eccD3	100	480	3.9E-262	901
	ESX-3	eccE3	100	345	7.5E-199	690.3
	ESX-3	PE5	100	102	1.1E-49	193
	ESX-3	esxG	100	97	1.4E-46	182.6
	ESX-3	esxH	100	96	2.5E-51	198.4
	ESX-4	esxT	100	98	2.1E-50	195.3
	ESX-5	eccB5	100	505	3.1E-294	1007.7
	ESX-5	eccD5	100	503	2.7E-282	968
	ESX-5	eccE5	100	399	2.9E-231	798.1
	ESX-5	cyp143	100	387	3.9E-228	787.7
	ESX-5	MIP_03872	100	300	2.8E-170	595.1
	ESX-5	PE18	100	99	2.9E-47	184.9
	ESX-5	esxM	100	98	1.1E-51	199.5
	ESX-5	esxN	100	94	6.6E-49	190.3
Immune modulation	19-kD protein	lpqH	100	163	2.1E-87	318.9
	GPL locus	pks	100	3674	0	7278.3
	GPL locus	mps2	100	2552	0	5049.2
	GPL locus	mmpL4a	100	964	0	1873.2
	GPL locus	pe	100	375	1.7E-220	762.3
	GPL locus	OCO_32120	100	112	1.5E-60	229.2

	GPL locus	mbtH	100	76	6.3E-42	166.8
	Lipoprotein	lprG	100	235	1.2E-128	456.4
	Mce4	mce4C	100	354	6.3E-201	697.2
	Mce4	mce4B	100	351	2.1E-196	682.2
Nutritional/Metabolic factor	Heme uptake	OCQ_49970	100	183	1.7E-101	365.9
	Magnesium transport	mgtC	100	238	4.9E-133	471.1
	Mycobactin	mbtE	100	2191	0	4348.9
	Mycobactin	mbtF	100	1479	0	2902.1
	Mycobactin	mbtB	100	1167	0	2308.1
	Mycobactin	mbtI	100	450	1.8E-253	872.1
	Mycobactin	mbtC	100	439	2.3E-253	871.7
	Nitrate reductase	narI	100	244	1.6E-142	502.7
	Pantothenate synthesis	panC	100	312	5.6E-177	617.5
	Trehalose-recycling ABC transporter	lpqY	100	470	2.6E-271	931.4
	Trehalose-recycling ABC transporter	sap	100	228	1.3E-119	426.4
Regulation	PhoP/R	phoR	100	480	2E-271	931.8
	WhiB3	whiB3	100	100	9.2E-57	216.5
Stress survival	KatG	katG	100	746	0	1536.2
Unclassified	Mce5	mce5F	100	419	6.2E-240	827
	Mce5	mce5E	100	413	4.1E-236	814.3
	Mce5	mce5D	100	379	6.9E-214	740.3
	Mce5	mce5B	100	351	1.7E-198	689.1
	Mce7	mce7F	100	579	0	1173.3
	Mce7	eccD2	100	476	8.5E-270	926.4
	Mce7	mce7D	100	475	3E-275	944.5
	Mce7	mce7C	100	372	6.6E-209	723.8
	Mce9	mce9A	100	523	0	1059.7
	Mce9	mce9B	100	359	4.7E-204	707.6
	Mce9	mce9C	100	348	3.7E-198	688
	Heparin-binding hemagglutinin	hbhA	100	205	6.8E-107	384
		Rv1211	100	55	1.3E-26	110.9
	Mycolic acid trans-cyclopropane synthetase	cmaA2	100	308	1.8E-183	639

Table 15. Antimicrobial resistance genes from the core genes of seven *Mycobacterium intracellulare* isolates.

Cluster	Query info	Identity	Align length	Mismatch	Gap	Query start	Query end	Target start	Target end
715	putative MFS-type transporter EfpA	88.6	535	56	1	1	535	1	530
1649	UDP-N-acetylglucosamine 1-carboxyvinyltransferase	97.1	416	12	0	1	416	1	416
1971	Elongation factor Tu	81.4	397	73	1	1	396	1	397
4055	23S rRNA (uridine(2479)-2'-O)-methyltransferase	79	257	54	0	6	262	1	257
4829	DNA-binding response regulator MtrA	99.6	228	1	0	1	228	1	228
5559	Pentapeptide repeat protein MfpA	78	182	40	0	3	184	2	183
6942	RNA polymerase-binding protein RbpA	91.9	111	9	0	1	111	1	111

Table 16. Antibiotic resistance pattern of *Mycobacterium intracellulare* isolates in a previous study (Adapted from Park et al. 2020).

Strain No.	Resistant pattern
S1-36A	RIF, STR, AMK, AZI, ETH, INZ, IMP
S2-11	STR, AMK, AZI, ETH, INZ, MXF, IMP
S2-8	RIF, STR, AMK, AZI, INZ, IMP
S1-32	STR, AMK, AZI, ETH, INZ, IMP
B1-4	ETH, INZ, IMP
N6-8	Susceptible to all tested drugs

STR: streptomycin, AMK: amikacin, AZI: azithromycin, RIF: rifampin, ETH: ethambutol, MXF: moxifloxacin, INZ: isoniazid, IMP: imipenem

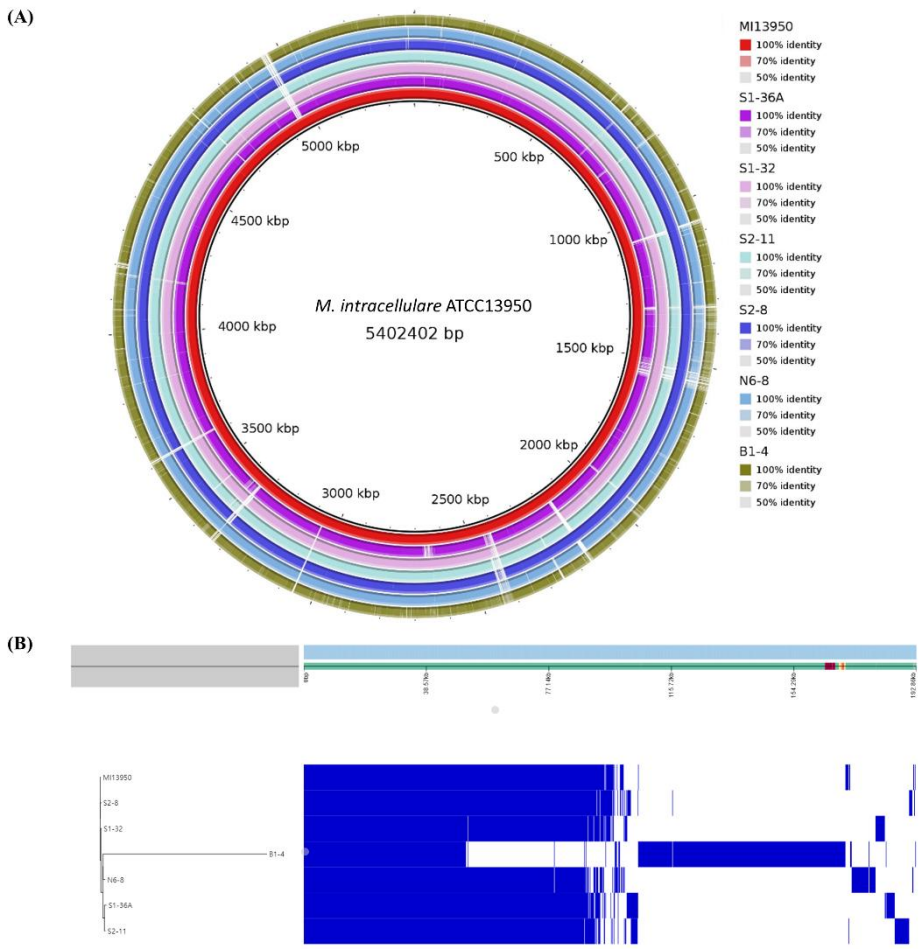

Figure 20. Pangenome analysis of six *Mycobacterium intracellulare* isolates, with ATCC13950 used as a reference. (A) Similarities between the reference genome *M. intracellulare* ATCC13950 (inner circle) and six *M. intracellulare* isolates are presented as concentric rings (the outer concentric rings) through BRIG. (B) Gene presence-absence matrix of *M. intracellulare* isolates. The corresponding phylogenetic tree is presented on the left and strains listed on the tree correspond to each row of the matrix. Each column represents an orthologous gene family. At the right of each panel is a compressed gene cluster matrix where blue blocks indicate the presence of the gene in that cluster and white indicates its absence.

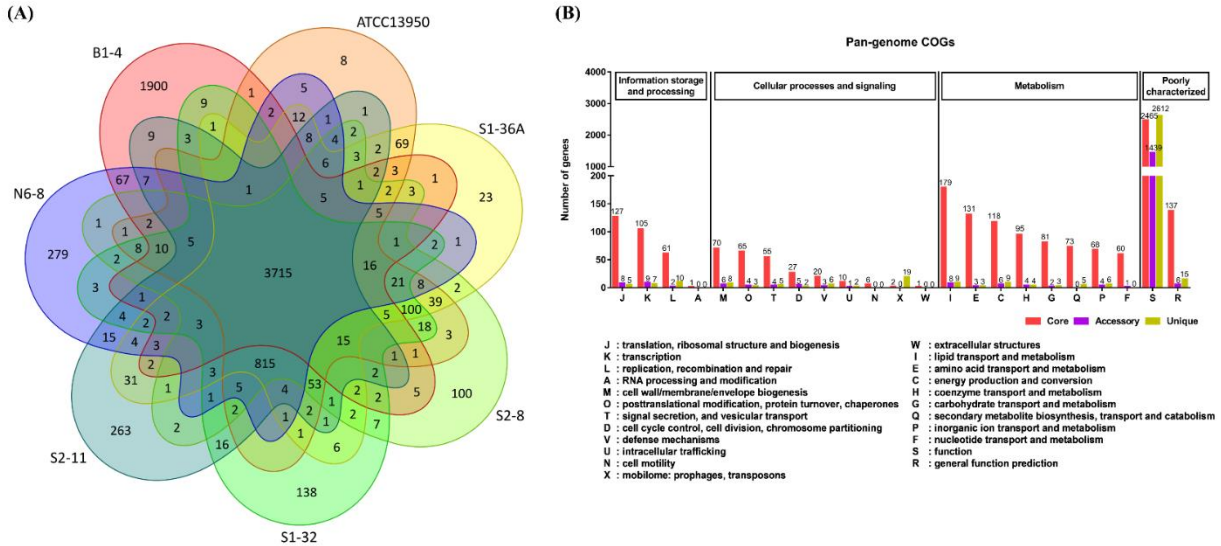

Figure 21. Comparison of the pangenome of seven *Mycobacterium intracellulare* strains. (A) Venn diagram of the seven *M. intracellulare* genomes. (B) Characterization of the gene sets of seven *M. intracellulare* strains showing diverse functions. The distribution of COG categories across the core, accessory and unique genomes. Dissimilar gene sets are expressed in different colors, with red representing the core genes, purple representing the accessory genes, and green representing the unique genes. The height of each column represents the number of genes from each functional category.

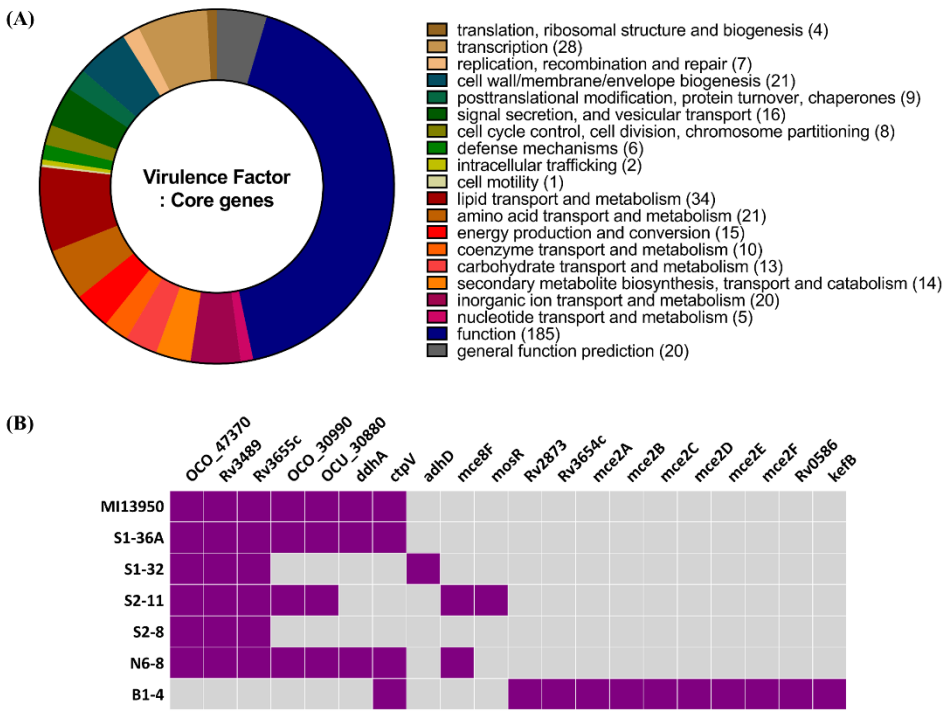

Figure 22. Virulence factors of the seven *Mycobacterium intracellulare* isolates. (A) The proportion of COG categories within the virulence factors from the core genome of seven *M. intracellulare* genomes. (B) Presence of virulence factors among the accessory genes within the seven *M. intracellulare* strains. Purple indicates the presence of the gene, and gray indicates its absence.

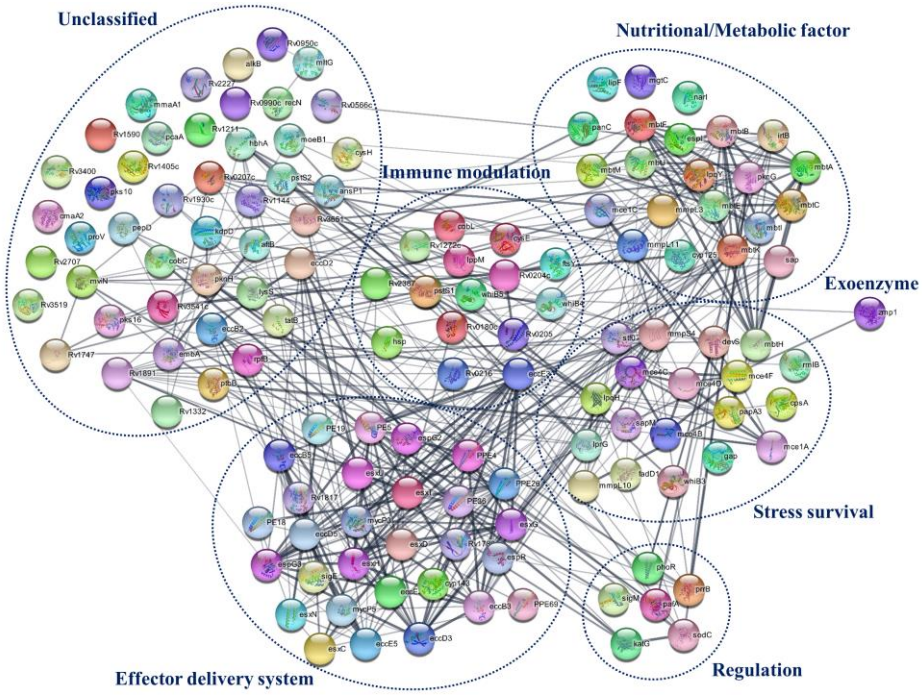

Figure 23. Protein–protein interaction network of the virulence factors identified as unclassified function by COG classification. Functional connections among the virulence factors of the unclassified function group with a high confidence threshold parameter, according to the STRING protein–protein interaction database. The thickness of the gray lines represents the strength of the data supporting a protein–protein interaction. The blue dotted circles define clusters of proteins as classified by VFDB.

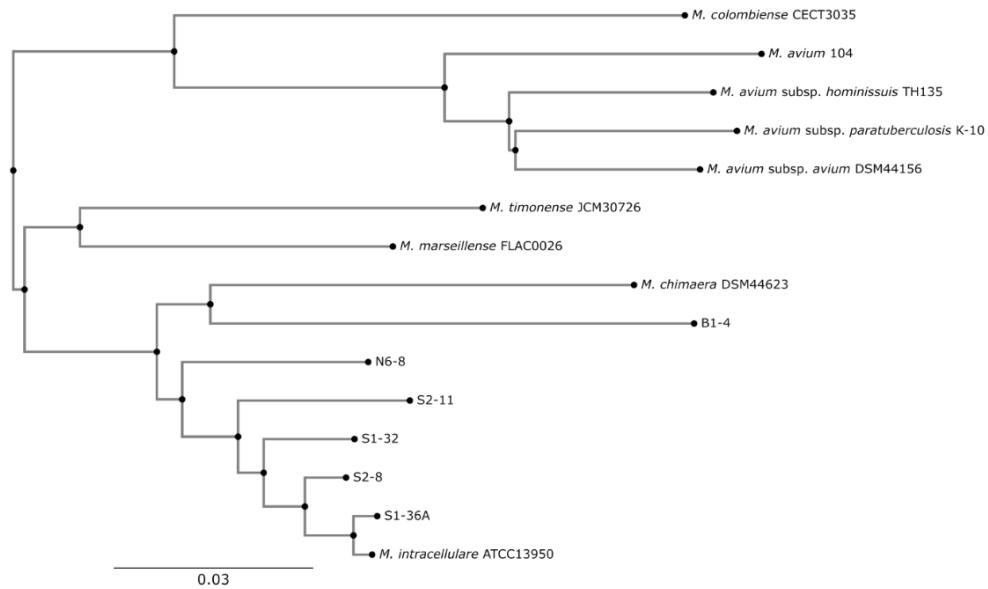

Figure 24. Phylogenetic tree based on whole genome sequence alignment of 15 *Mycobacterium avium* complex. Whole genome phylogeny of the *Mycobacterium avium* complex reconstructed using the newly sequenced genomes and the genomes that were already available. The tree was built using the concatenated alignments of the 15 fully conserved genes within the genus with the neighbor-joining method by Mauve Genome Alignment. The scale length was equal to 0.03 nucleotide substitutions per site.

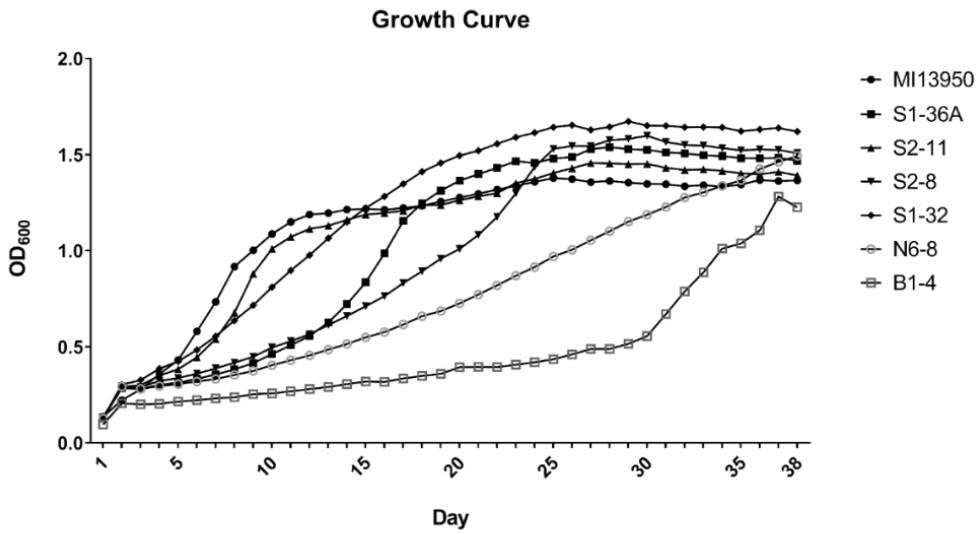

Figure 25. Growth rate of seven *Mycobacterium intracellulare* strains. Bacteria were incubated in 7H9 broth, and the OD_{600} was measured at 24-hour intervals for 38 days.

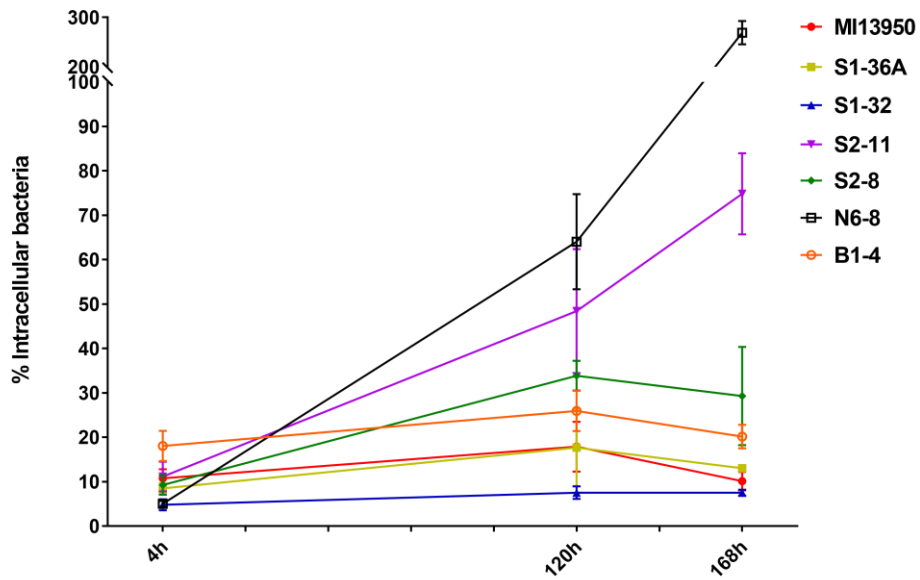

Time	MI13950	S1-36A	S1-32	S2-11	S2-8	N6-8	B1-4
4h	10.75 ± 2.06	8.52 ± 1.12	4.83 ± 1.25	11.15 ± 3.33	9.26 ± 2.19	5.02 ± 0.66	18.06 ± 3.40
120h	17.89 ± 5.60	17.69 ± 8.86	7.54 ± 1.41	48.41 ± 13.95	33.87 ± 3.34	64.04 ± 10.71	25.94 ± 4.52
168h	10.13 ± 2.07	13.03 ± 0.21	7.53 ± 0.65	74.84 ± 9.13	29.3 ± 11.06	269.12 ± 23.59	20.15 ± 2.63

Figure 26. The differential burden of mycobacteria in murine alveolar macrophages infected with *Mycobacterium intracellulare* isolates. The percentage of intracellular *M. intracellulare* was measured in murine alveolar macrophages for 7 days. The values obtained at 0 h after infection was set as 100%. Data are shown as mean ± SD of three independent experiments.

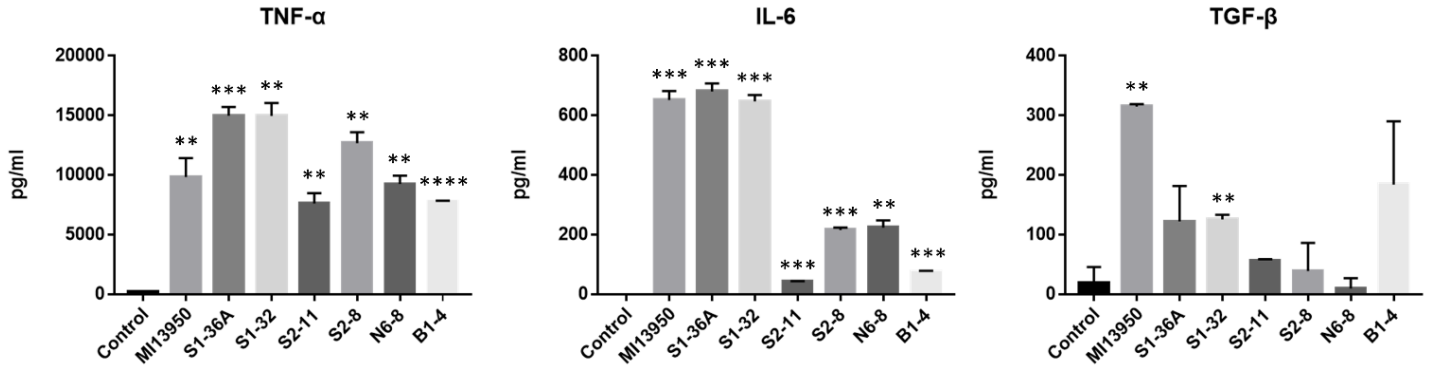

Figure 27. *Mycobacterium intracellulare* isolates induces differential cytokine expression in murine alveolar macrophages. The supernantant concentrations of TNF-α, IL-6, IL-1β, TGF-β, IFN-γ, IL-12, IL-4, IL-23, IL-10, and IL-13 were determined by ELISA. Only TNF-α, IL-6, and TGF-β were detected in murine alveolar macrophages after seven *M. intracellulare* (ATCC13950, S1-36A, S1-32, S2-11, S2-8, N6-8, B1-4) infection for 24 hours. Cytokine expression in noninfected cells (Control) was used as a control. Each bar represents the mean ±SD from three independent experiments. ** p <0.01, *** p <0.005, **** p <0.001

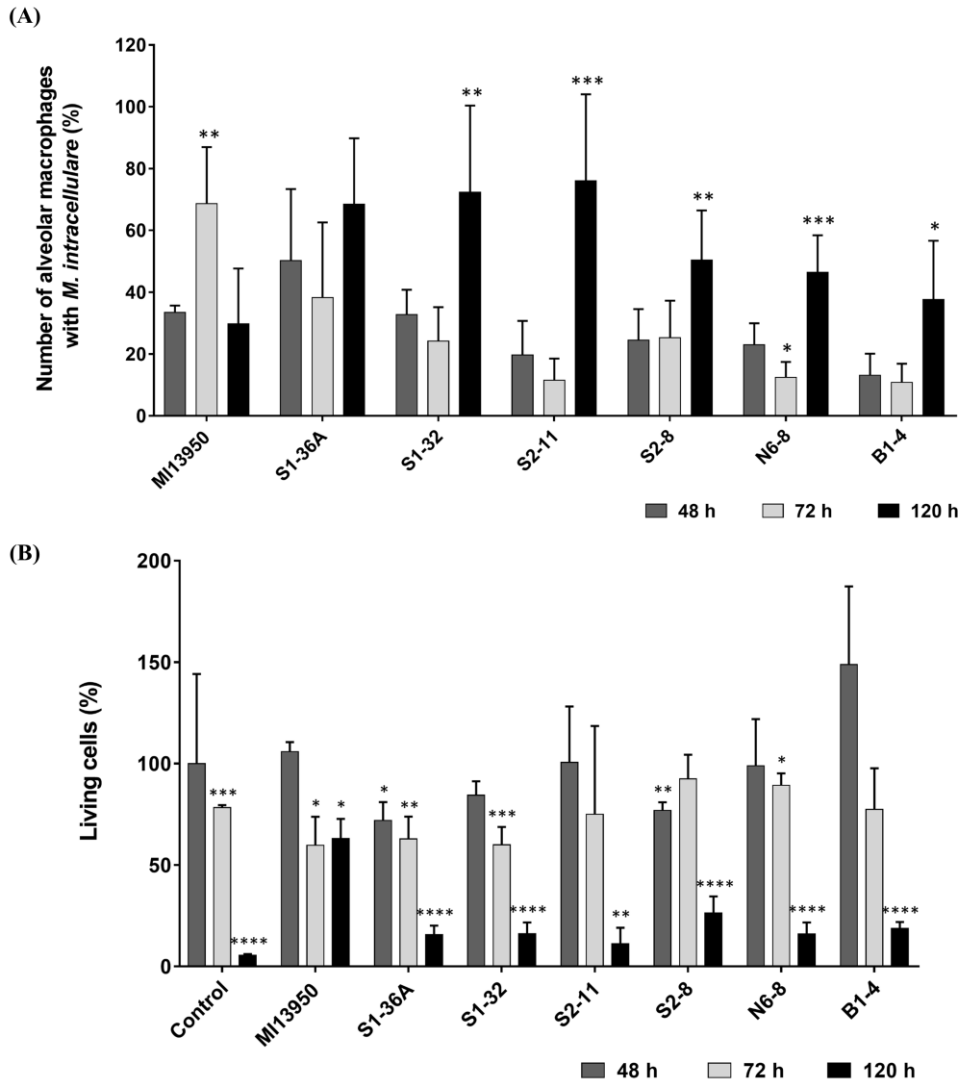

Figure 28. The number of alveolar macrophage after *Mycobacterium intracellulare* isolates infection for 5 days. (A) The number of alveolar macrophages with *M. intracellulare* isolates expressed as a percentage of the total number of infected macrophages stained by the Ziehl-Neelsen (ZN) methods. (B) The number of alive macrophages with or without *M. intracellulare* isolates. Cell

viability estimated with methylene blue dye. Data are expressed as the means ± SD from three independent experiments. *p <0.05, **p <0.01, ***p <0.005, ****p <0.001 for the comparison of the number of macrophages with or without macrophages for the following time points: (a) Day2 versus day 3 and day5 and (b) 4 h versus day 2, day 3, and day5.

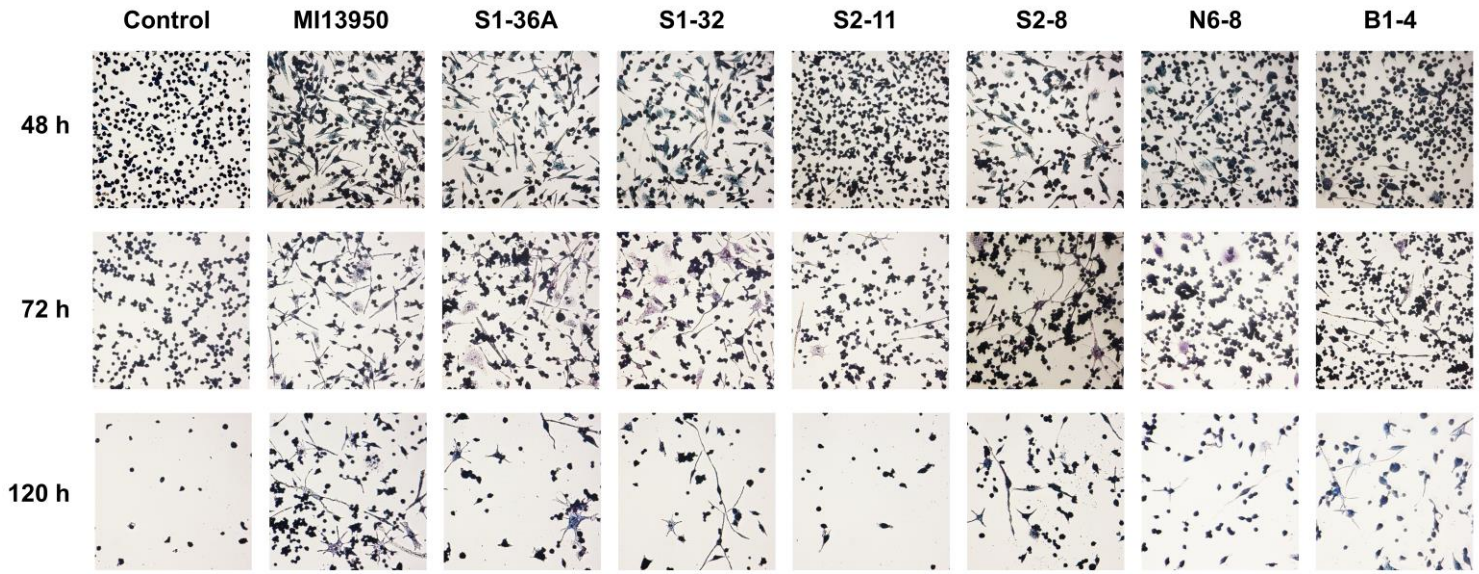

Figure 29. Mouse alveolar macrophages infected with seven *Mycobacterium intracellulare* strains for 5 days. Uninfected macrophages (Control) were included as a negative control. Ziehl Neelsen staining. Original magnification, x200.

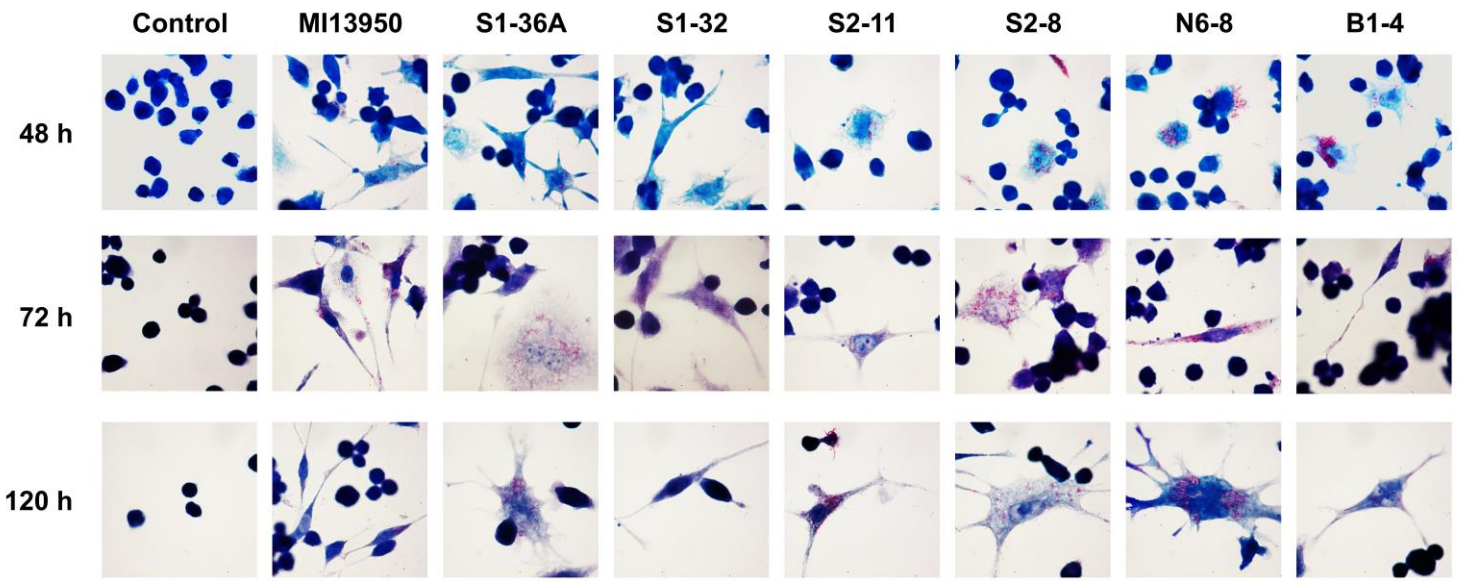

Figure 30. Representative microphotographs of mouse alveolar macrophages infected with seven *Mycobacterium intracellulare* strains. Uninfected macrophages (Control) were included as a negative control. Ziehl Neelsen staining. Original magnification, x1000.

General Discussion

Mycobacterium avium complex is one of the most prevalent pathogenic nontuberculous mycobacteria that cause chronic pulmonary disease in humans (Stout et al., 2016). MAC is an opportunistic bacterium that is highly abundant in environmental niches such as soil and water sources and has a wide range of host susceptibilities, including dogs and cats (Campora et al., 2011; Falkinham, 2015; Madarame et al., 2017; Thorel, Huchzermeyer, & Michel, 2001). Canine mycobacteriosis caused by MAC has been reported sporadically; however, most of the reported cases have poor prognoses due to difficulties in diagnosis and nonspecific clinical signs (Ghielmetti & Giger, 2020; M.-C. Kim et al., 2016). However, the host immune response to MAC infection in dogs has not been examined. In this study, the cellular immune response to MAC infection was investigated in canine peripheral blood mononuclear cells.

MAC consists of two main species: *M. intracellulare* and *M. avium* (Runyon, 1965). *M. avium* subsp. *hominissuis* is the most common etiological agent in canine mycobacteriosis (Ghielmetti & Giger, 2020; Marianelli et al., 2020). The host immune response to MAH infection in dogs was investigated by transcriptome analysis. Th1 and Th17 response-related pathways were activated by the upregulation of TNF-α, IL-8, IFN-γ, IL-1β, TREM1, PTGS2, IL-6, IL-23, CSF2, CSF3, CCL3, CCL4, IL-17A, IL-17F, RORγT, and IL-22. Gene expression profiling also showed that *IL-1β*, *IL-17A*, *IL-17F*, *TNF-α*, *IFN-γ*, *IL-23*, and *IL-6* were

significantly expressed. Of these cytokines, IL-17 and IL-1β were highly produced at 24 hpi. In addition, apoptosis-related pathways were inhibited by downregulation of the BAX-CYCS-CASP9-CASP3/CASP7 pathway. Caspase 3/7 activity was slightly decreased and the abundance of *caspase 3*, *caspase8*, *caspase9*, and *bax* was decreased in canine monocyte-derived macrophages after MAH infection. Furthermore, 26.5% of MAH was internalized by canine macrophages and the number of intracellular MAH was increased with the duration of infection. This result revealed that MAH replicated in canine macrophages by preventing apoptosis and induced Th1 and Th17 responses after infection.

M. avium and *M. intracellulare* are major causative agents of MAC pulmonary disease worldwide (Ichikawa et al., 2015). In humans, *M. avium* and *M. intracellulare* exhibit significantly different pathogenicity and biology (Koh et al., 2012). Patients with *M. intracellulare*-induced lung disease exhibited a more severe presentation and had a worse prognosis than patients with *M. avium*-induced lung disease in terms of disease progression and treatment response (Koh et al., 2012). Additionally, a study with a mouse model suggested that *M. intracellulare* was more virulent than *M. avium* (Tomioka, Saito, Sato, & Dawson, 1993). Furthermore, *M. intracellulare* is more frequently isolated from patients or environmental sources than *M. avium* (Y.-S. Kwon et al., 2019; Park et al., 2020; Z. Zhang et al., 2015). In Korea, *M. intracellulare* is the most common NTM species in animal shelters and parks (Park et al., 2020). In this study, the host immune response to *M. intracellulare* infection was investigated in canine macrophages and lymphocytes.

Transcriptome analysis showed that MDMs were activated to the M1 phenotype and secreted cytokines to induce Th1/Th17 cell responses to *M. intracellulare* infection. The pathways related to M1 macrophages were activated by the upregulation of the following molecules: CCL3, CCL4, CCL5, IL-6, IL-1β, ICAM1, CSF2, TREM1, and CD40. Th1-and Th17-related pathways were activated by the upregulation of certain molecules (CCL3, CCL4, CCL5, CCL7, CSF2, CXCL8, ICAM, S100A8, IL-6, PTGS2, IL-1B, IL-6, CSF2). Gene expression profiling of canine macrophages showed that *IL-23*, *IL-1β*, *IL-6*, and *TNF-α*, which are associated with M1 macrophage activation and the Th1/Th17 response, were significantly upregulated. To identify the T cell immune response, canine lymphocytes were cocultured with *M. intracellulare*-infected macrophages. The results revealed that Th17 cells predominantly responded to *M. intracellulare* infection. *IL-1β* and *IL-17* were only significantly expressed in canine lymphocytes. IL-17A, IL-1β, and IL-6 were produced at higher levels than other cytokines. IL-17A was more highly expressed in $CD4^+$ T cells than IFN-γ after *M. intracellulare* infection. These results showed that canine MDMs infected with *M. intracellulare* provide an environment that may favor Th17 responses.

This study revealed that Th1 and Th17 responses were induced by *M. avium* subsp. *hominissuis* and *M. intracellulare* in dogs. In particular, Th17 cells predominantly responded to *M. intracellulare* infection after the diminished Th1 cell response. However, the number of internalized *M. intracellulare* in canine macrophages was lower than that of *M. avium* subsp. *hominissuis*. The number of intracellular MAH

increased within 24 hours, whereas *M. intracellulare* increased after 5 days. However, both strains suppressed apoptosis signaling during infection.

In human, only *M. avium* subsp. *hominissuis*-infected macrophages produced increased levels of IL-1β, IL-6, TNF-α, and IL-10 whereas IL-12p70, IL-8, MCP-1, and MIP1a were induced by both *M. intracellulare* and MAH (Z. Feng et al., 2020). MAH-infected human monocyte-derived macrophages expressed M2-like macrophage-related genes, which induced a Th2 response. However, TNF, IL1B and CXCL10, which associated with M1 macrophage polarization, were also upregulated (Sharbati et al., 2011). MAH upregulated miRNA expression and interfered with the regulation of apoptosis. The downregulation of CASP3 and CASP7 was mediated by let-7e/miR-29a in human MDMs (Sharbati et al., 2011). In a mouse model, reduced Th1 responses increased the susceptibility to systemic MAH infection, and Th17 development induced excessive neutrophilic pulmonary inflammation by controlling cytokine and NO levels (Matsuyama et al., 2014). The robust Th17 response could provide fuel for the growth of granulomas and the development of tuberculosis by inducing inflammation and neutrophil recruitment (Cardona & Cardona, 2019). Therefore, a mouse model infected with MAH was examined and revealed that the Th17 response could play a pathological role and induce neutrophilic inflammation under Th1-diminished conditions (Matsuyama et al., 2014). In contrast, some reports have indicated that attenuation of Th17 immunity might contribute to host vulnerability or pathogen evasion in MAC-PD by impairing neutrophil recruitment and granulopoiesis (A. Lim, Allison, Price, &

Waterer, 2010; Wu et al., 2019). MAC-PD patients showed a lower frequency of Th17 cells but a higher frequency of Th2 cells and Tregs than control individuals (S. Han, Ko, Shin, & Jhun, 2020). In addition, MAC induced a decrease in Th1 cytokines compared with that in healthy controls (Kumar, 2017), and PBMCs from patients with active pulmonary MAC produced less IFN-γ, IL-12, and TNF-α than those from control individuals (Vankayalapati et al., 2001). IFN-γ and TNF-α levels were reduced in MAC-stimulated PBMCs from patients with MAC-PD (Y. S. Kwon et al., 2007; Shu et al., 2017).

M. intracellulare-infected mouse bone marrow-derived macrophages exhibited Th1 and Th2 cytokines downregulation but markedly increased the production of IL-17A and IL-22 by increasing Th17 cell expansion (Tatano et al., 2014). This study showed a novel macrophage population that was functionally distinguishable from M1 and M2 macrophage subsets and possessed unique phenotypes. *M. intracellulare*-infected BMDMs expressed high levels of IL-12, IL-1β, IL-6, TNF-α, NOS 2, CCR7, IL-10, CD163, Ym1, and Arg-1 and low levels of mannose receptor and Fizz. This new macrophage population suppressed T cell functions, including proliferation by downregulating IL-2 receptor expression and proinflammatory cytokine production, markedly suppressing cellular immunity in the advanced stages of mycobacteriosis (Tomioka et al., 2012; VanHeyningen, Collins, & Russell, 1997). In addition, the immunosuppressive activity of the macrophages was mediated by reactive nitrogen intermediates, prostaglandin E2, TGF-β, and phosphatidylserine produced by these cells (Maw, Shimizu, Sato, & Tomioka, 1997; Tomioka, Saito, & Yamada, 1990;

Tomioka, Sato, Maw, & Saito, 1995; Tomioka et al., 2012). These findings indicate potent suppression of T cell mitogenesis in vitro and in vivo (Murray & Wynn, 2011; Sica & Mantovani, 2012). In addition, pulmonary MAC patients infected with *M. intracellulare* exhibited higher concentrations of IL-10 but lower concentrations of IFN-γ, IL-12, and TNF-α in PBMCs stimulated by mycobacteria. Thus, these findings suggest that IFN-γ, TNF-α, and IL-12 protect against MAC, whereas IL-10 is immunosuppressive (Vankayalapati et al., 2001). However, the bacterial burden of *M. intracellulare* was less than that of *M. avium*, which is inconsistent with the clinical findings that isolation of *M. intracellulare* is more likely to be predictive of lung disease and that this strain is associated with more severe presentation and worse outcome (X. Y. Han, Tarrand, Infante, Jacobson, & Truong, 2005; Koh et al., 2012). In contrast, BALB/c mice are more capable of controlling infection with rapidly growing mycobacteria than *M. intracellulare*, as indicated by distinct granuloma formation in livers (Silva et al., 2010).

Other intracellular bacteria also induced granulomatous lesions with a Th17 response in dogs. *Brucella canis* as a zoonotic agent, is the main cause of canine brucellosis and mild human brucellosis (Atluri, Xavier, De Jong, Den Hartigh, & Tsolis, 2011; Hollett, 2006). *B. canis* infection causes granulomatous lesions in several organs and is the main cause of reproductive disorders (Ledbetter, Landry, Stokol, Kern, & Messick, 2009). The cellular immune response elicited by *B. canis* is different in humans and dogs (Pujol, Borie, Montoya, Ferreira, & Vernal, 2019). The Th1 response is triggered by human MoDCs, whereas canine MoDCs induce

Th1/Th17 responses, and increased $CD4^+$ T cells simultaneously produce IFN-γ and IL-17A. The differences in cellular responses may contribute to host susceptibility and virulence differences between these two hosts. Th1 lymphocytes are efficient and protect against *Brucella* infection, and the development of this cellular response in human cells could partly explain the increased host resistance to *B. canis* infection. In contrast, Th17 polarization could contribute to the development of granulomatous lesions during canine brucellosis, which occurs during tuberculosis infections (Lombard et al., 2016). Furthermore, although IL-17A production contributes to the elimination of some intracellular bacteria, such as *L. monocytogenes* or *S. enterica*, this effect is mainly mediated by granulocyte recruitment (Conlan, 1997), which is ineffective against infection with *Brucella* spp. due to its high resistance to neutrophil-mediated killing (Keleher & Skyberg, 2016). Moreover, the development of a Th17 response affects host susceptibility and the virulence of *Brucella* spp., impairing an effective Th1 response. Patients with active brucellosis have increased blood levels of IL-17A, which decrease at the end of antibiotic treatment (Sofian et al., 2016).

Thus, this study was similar to studies that examined the production of IL-17 after infection with the *Mycobacterium avium* complex and intracellular bacteria. These results will help explain why most reported cases in dogs showed granulomatous inflammation after mycobacterial disease progression induced by MAC members (Barandiaran et al., 2017; Campora et al., 2011; Etienne et al., 2013; Ghielmetti & Giger, 2020; Haist et al., 2008). In addition, the development of the Th17 response

might induce the growth of granulomas and affect host susceptibility in dogs. Therefore, this study revealed that *M. intracellulare* could be a causative agent of canine mycobacteriosis caused by MAC as well as *M. avium* subsp. *hominissuis*.

M. intracellulare is mainly distributed in the environment and new species are still being identified. New species and subspecies pose new threats to disease control. In this study, genetic diversity within newly isolated *M. intracellulare* from the soil in animal shelters and parks was investigated to help control potential threats. The isolates of *M. intracellulare* revealed genetic diversity and evolution in relation to virulence factors as associated with mammalian cell entry and the type VII secretion system. The immune response induced by *M. intracellulare* isolates in murine alveolar macrophages indicated differences between environmental and clinical isolates. The number of macrophages infected with *M. intracellulare* ATCC13950 decreased, while that of *M. intracellulare* isolates-infected macrophages increased. In addition, the number of viable cells among ATCC13950-infected macrophages increased but decreased dramatically in response to the isolates. Macrophages also exhibited M2 morphology in *M. intracellulare* ATCC13950-infected macrophages. In contrast, most isolates induced macrophage differentiation to the M1 phenotype. This result might reveal differences in clinical and environmental isolates in relation to chronic inflammation (Le et al., 2020; Parisi et al., 2018). Nonetheless, S1-36A, S1-32, and S2-8 clustered with *M. intracellulare* ATCC13950 phylogenetically, and the cytokine profiling was also similar to that of the type strain. Therefore, environmental isolates may pose a potential risk to hosts, as do clinical isolates. In

particular, B1-4 was previously identified as *M. intracellulare* by conventional methods but was identified as *M. chimaera* through whole genome sequencing in this study. Thus, it is important to understand genetic variations and identify the distribution of new species of MAC. This study will contribute to improving understanding of the pathogenesis of MAC and control the potential risk of infection in dogs.

General Conclusion

Nontuberculous mycobacteria (NTM) are opportunistic bacteria that are easily acquired from the environment, such as soil and water. *Mycobacterium avium* complex (MAC) is the most common cause of pulmonary NTM infection. *M. avium* and *M. intracellulare* are representative MAC pathogens and have been isolated from a wide range of hosts including humans and dogs. Dogs with mycobacteriosis caused by MAC usually have poor prognoses due to the difficulty of diagnosis and nonspecific clinical signs. However, the underlying mechanisms of MAC infection in dogs have not yet been studied. In this study, the canine immune response to MAC infection was investigated with *M. avium* subsp. *hominissuis* (MAH) and *M. intracellulare*. In addition, the genetic diversity of newly isolated *M. intracellulare* strains was investigated by whole genome sequencing.

1. Transcriptome analysis of canine peripheral blood mononuclear cells showed that *M. avium* subsp. *hominissuis* induces Th1 and Th17 immune responses and can replicate within canine macrophages by avoiding apoptosis signaling.

2. Coculture systems of canine lymphocytes and macrophages indicated that Th17 cells predominantly responded to *M. intracellulare* infection through M1-like macrophage activation while Th1 cells decreased over time.

3. The comparative analysis of *M. intracellulare* isolates revealed the difference between the type strain and environmental isolates with respect to antibiotic susceptibility, virulence factors, and induction of the host immune response.

The comparative analysis of host immune responses to MAC infection will promote a better understanding of the mechanism of infection in dogs. Pangenome analysis provides genetic information that can be used to elucidate the virulence and pathogenesis of MAC. This study might open new insight into understanding MAC infection in dogs and helping to control the potential public health risk of zoonosis between dogs and humans.

References

Abdallah, A. M., Savage, N. D., Van Zon, M., Wilson, L., Vandenbroucke-Grauls, C. M., Van Der Wel, N. N., . . . Bitter, W. (2008). The ESX-5 secretion system of Mycobacterium marinum modulates the macrophage response. *The Journal of Immunology, 181*(10), 7166-7175.

Alikhan, N.-F., Petty, N. K., Zakour, N. L. B., & Beatson, S. A. (2011). BLAST Ring Image Generator (BRIG): simple prokaryote genome comparisons. *BMC Genomics, 12*(1), 1-10.

Appelberg, R., Leal, I. S., Pais, T. F., Pedrosa, J., & Flórido, M. (2000). Differences in resistance of C57BL/6 and C57BL/10 mice to infection by Mycobacterium avium are independent of gamma interferon. *Infection and Immunity, 68*(1), 19-23.

Ariel, O., Gendron, D., Dudemaine, P.-L., Gévry, N., Ibeagha-Awemu, E. M., & Bissonnette, N. (2020). Transcriptome profiling of bovine macrophages infected by Mycobacterium avium spp. paratuberculosis depicts foam cell and innate immune tolerance phenotypes. *Frontiers in Immunology, 10*, 2874.

Ates, L. S., Ummels, R., Commandeur, S., van der Weerd, R., Sparrius, M., Weerdenburg, E., . . . Abdallah, A. M. (2015). Essential role of the ESX-5 secretion system in outer membrane permeability of pathogenic mycobacteria. *Plos Genetics, 11*(5), e1005190.

Atluri, V. L., Xavier, M. N., De Jong, M. F., Den Hartigh, A. B., & Tsolis, R. M. (2011). Interactions of the human pathogenic Brucella species with their hosts. *Annual Review of Microbiology, 65*, 523-541.

Augenstreich, J., Arbues, A., Simeone, R., Haanappel, E., Wegener, A., Sayes, F., . . . Guilhot, C. (2017). ESX-1 and phthiocerol dimycocerosates of Mycobacterium tuberculosis act in concert to cause phagosomal rupture and host cell apoptosis. *Cellular Microbiology, 19*(7), e12726.

Bang, D., Herlin, T., Stegger, M., Andersen, A. B., Torkko, P., Tortoli, E., & Thomsen, V. O. (2008). Mycobacterium arosiense sp. nov., a slowly growing, scotochromogenic species causing osteomyelitis in an immunocompromised child. *International Journal of Systematic and Evolutionary Microbiology, 58*(10), 2398-2402.

Bannantine, J. P., Conde, C., Bayles, D. O., Branger, M., & Biet, F. (2020). Genetic diversity among Mycobacterium avium subspecies revealed by analysis of complete genome sequences. *Frontiers in Microbiology, 11*, 1701.

Barandiaran, S., Martinez Vivot, M., Falzoni, E., Marfil, M. J., Perez Tort, G., Rovatti, P., . . . Duchene, A. (2017). Mycobacterioses in dogs and cats from Buenos Aires, Argentina. *Journal of Veterinary Diagnostic Investigation, 29*(5), 729-732.

Bauer, N., Burkhardt, S., Kirsch, A., Weiss, R., Moritz, A., & Baumgaertner, W. (2002). Lymphadenopathy and diarrhea in a Miniature Schnauzer. *Veterinary Clinical Pathology, 31*(2), 61-64.

Beckwith, K. S., Beckwith, M. S., Ullmann, S., Sætra, R. S., Kim, H., Marstad, A., . . . Niederweis, M. (2020). Plasma membrane damage causes NLRP3 activation and pyroptosis during Mycobacterium tuberculosis infection. *Nature Communications, 11*(1), 1-18.

Behar, S. M., Divangahi, M., & Remold, H. G. (2010). Evasion of innate immunity by Mycobacterium tuberculosis: is death an exit strategy? *Nature Reviews Microbiology, 8*(9), 668.

Bermudez, L. E., & Young, L. S. (1994). Factors affecting invasion of HT-29 and HEp-2 epithelial cells by organisms of the Mycobacterium avium complex. *Infection and Immunity, 62*(5), 2021-2026.

Bonovska, M., Tzvetkov, Y., Najdenski, H., & Bachvarova, Y. (2005). PCR for detection of Mycobacterium tuberculosis in experimentally infected dogs. *Journal of Veterinary Medicine, Series B, 52*(4), 165-170.

Boyle, D. P., Zembower, T. R., & Qi, C. (2016). Relapse versus reinfection of

Mycobacterium avium complex pulmonary disease. Patient characteristics and macrolide susceptibility. *Annals of the American Thoracic Society, 13*(11), 1956-1961.

Boyle, D. P., Zembower, T. R., Reddy, S., & Qi, C. (2015). Comparison of clinical features, virulence, and relapse among Mycobacterium avium complex species. *American Journal of Respiratory and Critical Care Medicine, 191*(11), 1310-1317.

Busman-Sahay, K. O., Walrath, T., Huber, S., & O'Connor Jr, W. (2015). Cytokine crowdsourcing: multicellular production of TH17-associated cytokines. *Journal of Leukocyte Biology, 97*(3), 499-510.

Cambier, C., Falkow, S., & Ramakrishnan, L. (2014). Host evasion and exploitation schemes of Mycobacterium tuberculosis. *Cell, 159*(7), 1497-1509.

Campora, L., Corazza, M., Zullino, C., Ebani, V. V., & Abramo, F. (2011). Mycobacterium avium subspecies hominissuis disseminated infection in a Basset Hound dog. *Journal of Veterinary Diagnostic Investigation, 23*(5), 1083-1087.

Cardona, P., & Cardona, P.-J. (2019). Regulatory T cells in Mycobacterium tuberculosis infection. *Frontiers in Immunology, 10*, 2139.

Carpenter, J., Myers, A., Conner, M., Schelling, S., Kennedy, F., & Reimann, K. (1988). Tuberculosis in five basset hounds. *Journal of the American Veterinary Medical Association, 192*(11), 1563-1568.

Castejon, M., Menéndez, M. C., Comas, I., Vicente, A., & Garcia, M. J. (2018). Whole-genome sequence analysis of the Mycobacterium avium complex and proposal of the transfer of Mycobacterium yongonense to Mycobacterium intracellulare subsp. yongonense subsp. nov. *International Journal of Systematic and Evolutionary Microbiology, 68*(6), 1998-2005.

Chang, H., Zhao, F., Xie, X., Liao, Y., Song, Y., Liu, C., . . . Wang, Y. (2019). PPARα suppresses Th17 cell differentiation through IL-6/STAT3/RORγt pathway in experimental autoimmune myocarditis. *Experimental Cell Research, 375*(1),

22-30.

Chaudhari, N. M., Gupta, V. K., & Dutta, C. (2016). BPGA-an ultra-fast pan-genome analysis pipeline. *Scientific Reports, 6*(1), 1-10.

Chawla, A. (2010). Control of macrophage activation and function by PPARs. *Circulation Research, 106*(10), 1559-1569.

Chen, L., Yang, J., Yu, J., Yao, Z., Sun, L., Shen, Y., & Jin, Q. (2005). VFDB: a reference database for bacterial virulence factors. *Nucleic Acids Research, 33*(suppl_1), D325-D328.

Chen, M., Gan, H., & Remold, H. G. (2006). A mechanism of virulence: virulent Mycobacterium tuberculosis strain H37Rv, but not attenuated H37Ra, causes significant mitochondrial inner membrane disruption in macrophages leading to necrosis. *The Journal of Immunology, 176*(6), 3707-3716.

Cole, S., Eiglmeier, K., Parkhill, J., James, K., Thomson, N., Wheeler, P., . . . Harris, D. (2001). Massive gene decay in the leprosy bacillus. *Nature, 409*(6823), 1007-1011.

Conlan, J. W. (1997). Critical roles of neutrophils in host defense against experimental systemic infections of mice by Listeria monocytogenes, Salmonella typhimurium, and Yersinia enterocolitica. *Infection and Immunity, 65*(2), 630-635.

Cruz, A., Ludovico, P., Torrado, E., Gama, J. B., Sousa, J., Gaifem, J., . . . Pedrosa, J. (2015). IL-17A promotes intracellular growth of Mycobacterium by inhibiting apoptosis of infected macrophages. *Frontiers in Immunology, 6*, 498.

Cruz, A., Torrado, E., Carmona, J., Fraga, A. G., Costa, P., Rodrigues, F., . . . Saraiva, M. (2015). BCG vaccination-induced long-lasting control of Mycobacterium tuberculosis correlates with the accumulation of a novel population of CD4+ IL-17+ TNF+ IL-2+ T cells. *Vaccine, 33*(1), 85-91.

Cucchi, E., Bernini, S., Chinosi, S., Mazzocchi, D., Vicini, B., & Bertazzolo, W. (2009). Mycobacterium avium complex infection in a dog. *Veterinaria*

(Cremona), 23(4), 59-63.

Daley, C. L. (2017). Mycobacterium avium complex disease. *Microbiology Spectrum, 5*(2), 5.2. 29.

Darling, A. C., Mau, B., Blattner, F. R., & Perna, N. T. (2004). Mauve: multiple alignment of conserved genomic sequence with rearrangements. *Genome Research, 14*(7), 1394-1403.

de la Paz Santangelo, M., Blanco, F., Campos, E., Soria, M., Bianco, M. V., Klepp, L., . . . Bigi, F. (2009). Mce2R from Mycobacterium tuberculosis represses the expression of the mce2 operon. *Tuberculosis, 89*(1), 22-28.

Delirezh, N., Shojaeefar, E., Parvin, P., & Asadi, B. (2013). Comparison the effects of two monocyte isolation methods, plastic adherence and magnetic activated cell sorting methods, on phagocytic activity of generated dendritic cells. *Cell Journal (Yakhteh), 15*(3), 218.

Dey, A., Verma, A. K., & Chatterji, D. (2010). Role of an RNA polymerase interacting protein, MsRbpA, from Mycobacterium smegmatis in phenotypic tolerance to rifampicin. *Microbiology, 156*(3), 873-883.

Dey, A., Verma, A. K., & Chatterji, D. (2011). Molecular insights into the mechanism of phenotypic tolerance to rifampicin conferred on mycobacterial RNA polymerase by MsRbpA. *Microbiology, 157*(7), 2056-2071.

Diel, R., Nienhaus, A., Ringshausen, F. C., Richter, E., Welte, T., Rabe, K. F., & Loddenkemper, R. (2018). Microbiologic outcome of interventions against Mycobacterium avium complex pulmonary disease: a systematic review. *Chest, 153*(4), 888-921.

Domingo-Gonzalez, R., Prince, O., Cooper, A., & Khader, S. A. (2017). Cytokines and chemokines in Mycobacterium tuberculosis infection. *Tuberculosis and the Tubercle Bacillus*, 33-72.

Early, J., Fischer, K., & Bermudez, L. E. (2011). Mycobacterium avium uses apoptotic macrophages as tools for spreading. *Microbial Pathogenesis, 50*(2), 132-139.

Edgar, R. (2010). Usearch. Lawrence Berkeley National Lab.(LBNL), Berkeley, CA (United States)

Epperson, L. E., Timke, M., Hasan, N. A., Godo, P., Durbin, D., Helstrom, N. K., . . . Salfinger, M. (2018). Evaluation of a novel MALDI Biotyper algorithm to distinguish Mycobacterium intracellulare from Mycobacterium chimaera. *Frontiers in Microbiology, 9*, 3140.

Etienne, C. L., Granat, F., Trumel, C., Raymond-Letron, I., Lucas, M. N., Boucraut-Baralon, C., . . . Delverdier, M. (2013). A mycobacterial coinfection in a dog suspected on blood smear. *Veterinary Clinical Pathology, 42*(4), 516-521.

Falkinham, J. O. (2015). Environmental sources of nontuberculous mycobacteria. *Clinics in Chest Medicine, 36*(1), 35-41.

Fedrizzi, T., Meehan, C. J., Grottola, A., Giacobazzi, E., Serpini, G. F., Tagliazucchi, S., . . . De Sanctis, V. (2017). Genomic characterization of nontuberculous mycobacteria. *Scientific Reports, 7*(1), 1-14.

Feng, L., Mundy, J. E., Stevenson, C. E., Mitchenall, L. A., Lawson, D. M., Mi, K., & Maxwell, A. (2021). The pentapeptide-repeat protein, MfpA, interacts with mycobacterial DNA gyrase as a DNA T-segment mimic. *Proceedings of the National Academy of Sciences, 118*(11).

Feng, Z., Bai, X., Wang, T., Garcia, C., Bai, A., Li, L., . . . Chan, E. D. (2020). Differential responses by human macrophages to infection with Mycobacterium tuberculosis and non-tuberculous mycobacteria. *Frontiers in Microbiology, 11*, 116.

Friend, S., Russell, E., Hartley, W., & Everist, P. (1979). Infection of a dog with Mycobacterium avium serotype II. *Veterinary Pathology, 16*(3), 381-384.

Galperin, M. Y., Makarova, K. S., Wolf, Y. I., & Koonin, E. V. (2015). Expanded microbial genome coverage and improved protein family annotation in the COG database. *Nucleic Acids Research, 43*(D1), D261-D269.

Gentleman, R. C., Carey, V. J., Bates, D. M., Bolstad, B., Dettling, M., Dudoit, S., . . . Gentry, J. (2004). Bioconductor: open software development for

computational biology and bioinformatics. *Genome Biology, 5*(10), R80.

Ghielmetti, G., & Giger, U. (2020). Mycobacterium avium: an Emerging Pathogen for Dog Breeds with Hereditary Immunodeficiencies. *Current Clinical Microbiology Reports*, 1-14.

Girard-Misguich, F., Laencina, L., Dubois, V., Le Moigne, V., Kremer, L., Maljessi, L., . . . Herrmann, J.-L. (2018). The most ancestral mycobacterial ESX-4 secretion system is essential for intracellular growth of Mycobacterium abscessus within environmental and human phagocytes. *Medecine Sciences: M/S, 34*(10), 795-797.

Glawischnig, W., Steineck, T., & Spergser, J. (2006). Infections caused by Mycobacterium avium subspecies avium, hominissuis, and paratuberculosis in free-ranging red deer (Cervus elaphus hippelaphus) in Austria, 2001–2004. *Journal of Wildlife Diseases, 42*(4), 724-731.

Gopal, R., Lin, Y., Obermajer, N., Slight, S., Nuthalapati, N., Ahmed, M., . . . Khader, S. A. (2012). IL-23-dependent IL-17 drives Th1-cell responses following Mycobacterium bovis BCG vaccination. *European Journal of Immunology, 42*(2), 364-373.

Gorla, P., Plocinska, R., Sarva, K., Satsangi, A. T., Pandeeti, E., Donnelly, R., . . . Madiraju, M. V. (2018). MtrA response regulator controls cell division and cell wall metabolism and affects susceptibility of mycobacteria to the first line antituberculosis drugs. *Frontiers in Microbiology, 9*, 2839.

Goto-Koshino, Y., Ohno, K., Nakajima, M., Mochizuki, H., Kanemoto, H., & Tsujimoto, H. (2011). A rapid and simple method to obtain canine peripheral blood-derived macrophages. *Journal of Veterinary Medical Science*, 1101270448-1101270448.

Greene, C. E. (2006). *Infectious Diseases of the Dog and Cat*: WB Saunders\Elsevier Science.

Griffith, D. E., Aksamit, T., Brown-Elliott, B. A., Catanzaro, A., Daley, C., Gordin, F., . . . Iademarco, M. F. (2007). An official ATS/IDSA statement: diagnosis,

treatment, and prevention of nontuberculous mycobacterial diseases. *American Journal of Respiratory and Critical Care Medicine, 175*(4), 367-416.

Gupta, S. K., Padmanabhan, B. R., Diene, S. M., Lopez-Rojas, R., Kempf, M., Landraud, L., & Rolain, J.-M. (2014). ARG-ANNOT, a new bioinformatic tool to discover antibiotic resistance genes in bacterial genomes. *Antimicrobial Agents and Chemotherapy, 58*(1), 212-220.

Haist, V., Seehusen, F., Moser, I., Hotzel, H., Deschl, U., Baumgärtner, W., & Wohlsein, P. (2008). Mycobacterium avium subsp. hominissuis infection in 2 pet dogs, Germany. *Emerging Infectious Diseases, 14*(6), 988.

Han, S., Ko, Y., Shin, S. J., & Jhun, B. W. (2020). Characteristics of Circulating CD4+ T Cell Subsets in Patients with Mycobacterium avium Complex Pulmonary Disease. *Journal of Clinical Medicine, 9*(5), 1331.

Han, X. Y., Tarrand, J. J., Infante, R., Jacobson, K. L., & Truong, M. (2005). Clinical significance and epidemiologic analyses of Mycobacterium avium and Mycobacterium intracellulare among patients without AIDS. *Journal of Clinical Microbiology, 43*(9), 4407-4412.

Hartley, G., Faulhaber, E., Caldwell, A., Coy, J., Kurihara, J., Guth, A., . . . Dow, S. (2017). Immune regulation of canine tumour and macrophage PD-L1 expression. *Veterinary and Comparative Oncology, 15*(2), 534-549.

Harvey, K. L., Jarocki, V. M., Charles, I. G., & Djordjevic, S. P. (2019). The diverse functional roles of elongation factor Tu (EF-Tu) in microbial pathogenesis. *Frontiers in Microbiology, 10*, 2351.

Haverkamp, M., Van Dissel, J., & Holland, S. (2006). Human host genetic factors in nontuberculous mycobacterial infection: lessons from single gene disorders affecting innate and adaptive immunity and lessons from molecular defects in interferon-γ-dependent signaling. *Microbes and Infection, 8*(4), 1157-1166.

Heinrich, F., Lehmbecker, A., Raddatz, B. B., Kegler, K., Tipold, A., Stein, V. M., . . .

Ulrich, R. (2017). Morphologic, phenotypic, and transcriptomic characterization of classically and alternatively activated canine blood-derived macrophages in vitro. *PloS One, 12*(8), e0183572.

Henkle, E., Hedberg, K., Schafer, S. D., & Winthrop, K. L. (2017). Surveillance of extrapulmonary nontuberculous mycobacteria infections, Oregon, USA, 2007–2012. *Emerging Infectious Diseases, 23*(10), 1627.

Hobi, S., Bettenay, S., Majzoub, M., Mueller, R., & Moser, I. (2015). Mycobacterium avium subspecies hominissuis infection in a dog from Germany with multifocal alopecia, exfoliative dermatitis, hypercalcaemia and subsequent sebaceous atrophy. *Veterinary Record Case Reports, 3*(1), e000168.

Hollett, R. B. (2006). Canine brucellosis: outbreaks and compliance. *Theriogenology, 66*(3), 575-587.

Horn, B., Forshaw, D., Cousins, D., & Irwin, P. (2000). Disseminated Mycobacterium avium infection in a dog with chronic diarrhoea. *Australian Veterinary Journal, 78*(5), 320-325.

Hubbard, A. K., & Giardina, C. (2000). Regulation of ICAM-1 expression in mouse macrophages. *Inflammation, 24*(2), 115-125.

Huchzermeyer, M.-F. T. H., & Michel, A. (2001). intracellulare infection in mammals. *Rev. Sci. Tech. Off. int. Epiz, 20*(1), 204-218.

Hunt, M., De Silva, N., Otto, T. D., Parkhill, J., Keane, J. A., & Harris, S. R. (2015). Circlator: automated circularization of genome assemblies using long sequencing reads. *Genome Biology, 16*(1), 1-10.

Ichikawa, K., van Ingen, J., Koh, W.-J., Wagner, D., Salfinger, M., Inagaki, T., . . . Yamada, K. (2015). Genetic diversity of clinical Mycobacterium avium subsp. hominissuis and Mycobacterium intracellulare isolates causing pulmonary diseases recovered from different geographical regions. *Infection, Genetics and Evolution, 36*, 250-255.

Inderlied, C., Kemper, C., & Bermudez, L. (1993). The Mycobacterium avium complex. *Clinical Microbiology Reviews, 6*(3), 266-310.

Jasenosky, L. D., Scriba, T. J., Hanekom, W. A., & Goldfeld, A. E. (2015). T cells and adaptive immunity to Mycobacterium tuberculosis in humans. *Immunological Reviews, 264*(1), 74-87.

Jia, B., Raphenya, A. R., Alcock, B., Waglechner, N., Guo, P., Tsang, K. K., . . . Sharma, A. N. (2016). CARD 2017: expansion and model-centric curation of the comprehensive antibiotic resistance database. *Nucleic Acids Research*, gkw1004.

Johansen, T. B., Olsen, I., Jensen, M. R., Dahle, U. R., Holstad, G., & Djønne, B. (2007). New probes used for IS 1245 and IS 1311 restriction fragment length polymorphism of Mycobacterium avium subsp. avium and Mycobacterium avium subsp. hominissuis isolates of human and animal origin in Norway. *BMC Microbiology, 7*(1), 1-9.

Jones, B. E., Lo, C. R., Liu, H., Pradhan, Z., Garcia, L., Srinivasan, A., . . . Czaja, M. J. (2000). Role of caspases and NF-κB signaling in hydrogen peroxide-and superoxide-induced hepatocyte apoptosis. *American Journal of Physiology-Gastrointestinal and Liver Physiology, 278*(5), G693-G699.

Kabara, E., & Coussens, P. M. (2012). Infection of primary bovine macrophages with Mycobacterium avium subspecies paratuberculosis suppresses host cell apoptosis. *Frontiers in Microbiology, 3*, 215.

Kannan, N., Haug, M., Steigedal, M., & Flo, T. H. (2020). Mycobacterium smegmatis Vaccine Vector Elicits CD4+ Th17 and CD8+ Tc17 T Cells With Therapeutic Potential to Infections With Mycobacterium avium. *Frontiers in Immunology, 11*, 1116.

Kasperbauer, S. H., & Daley, C. L. (2008, October). Diagnosis and treatment of infections due to Mycobacterium avium complex. In Seminars in respiratory and critical care medicine (Vol. 29, No. 05, pp. 569-576). © Thieme Medical Publishers.

Keane, J., Gershon, S., Wise, R. P., Mirabile-Levens, E., Kasznica, J., Schwieterman, W. D., . . . Braun, M. M. (2001). Tuberculosis associated with infliximab, a

tumor necrosis factor α–neutralizing agent. *New England Journal of Medicine, 345*(15), 1098-1104.

Keleher, L. L., & Skyberg, J. A. (2016). Activation of bovine neutrophils by Brucella spp. *Veterinary Immunology and Immunopathology, 177*, 1-6.

Kendall, B. A., & Winthrop, K. L. (2013, February). Update on the epidemiology of pulmonary nontuberculous mycobacterial infections. In Seminars in respiratory and critical care medicine (Vol. 34, No. 01, pp. 087-094). Thieme Medical Publishers.

Kim, B.-J., Math, R. K., Jeon, C. O., Yu, H.-K., Park, Y.-G., Kook, Y.-H., & Kim, B.-J. (2013). Mycobacterium yongonense sp. nov., a slow-growing non-chromogenic species closely related to Mycobacterium intracellulare. *International Journal of Systematic and Evolutionary Microbiology, 63*(Pt_1), 192-199.

Kim, D.-Y., Cho, D.-Y., Newton, J., Gerdes, J., & Richter, E. (1994). Granulomatous myelitis due to Mycobacterium avium in a dog. *Veterinary Pathology, 31*(4), 491-493.

Kim, M.-C., Kim, J., Kang, W., Jang, Y., & Kim, Y. (2016). Systemic infection of Mycobacterium avium subspecies hominissuis and fungus in a pet dog. *Journal of Veterinary Medical Science, 78*(1), 157-160.

Kim, S.-Y., Park, H. Y., Jeong, B.-H., Jeon, K., Huh, H. J., Ki, C.-S., . . . Koh, W.-J. (2015). Molecular analysis of clinical isolates previously diagnosed as Mycobacterium intracellulare reveals incidental findings of "Mycobacterium indicus pranii" genotypes in human lung infection. *BMC Infectious Diseases, 15*(1), 1-11.

Kim, S.-Y., Shin, S. H., Moon, S. M., Yang, B., Kim, H., Kwon, O. J., . . . Shin, S. J. (2017). Distribution and clinical significance of Mycobacterium avium complex species isolated from respiratory specimens. *Diagnostic Microbiology and Infectious Disease, 88*(2), 125-137.

Kim, S., Park, H.-E., Park, W. B., Kim, S. Y., Park, H.-T., & Yoo, H. S. (2021).

Mycobacterium avium Modulates the Protective Immune Response in Canine Peripheral Blood Mononuclear Cells. *Frontiers in Cellular and Infection Microbiology, 10*, 840.

Klotz, D., Barth, S. A., Baumgärtner, W., & Hewicker-Trautwein, M. (2018). Mycobacterium avium subsp. hominissuis Infection in a Domestic Rabbit, Germany. *Emerging Infectious Diseases, 24*(3), 596.

Klotz, L., Burgdorf, S., Dani, I., Saijo, K., Flossdorf, J., Hucke, S., . . . Mayer, G. (2009). The nuclear receptor PPARγ selectively inhibits Th17 differentiation in a T cell–intrinsic fashion and suppresses CNS autoimmunity. *Journal of Experimental Medicine, 206*(10), 2079-2089.

Ko, R.-E., Moon, S. M., Ahn, S., Jhun, B. W., Jeon, K., Kwon, O. J., . . . Koh, W.-J. (2018). Changing epidemiology of nontuberculous mycobacterial lung diseases in a tertiary referral hospital in Korea between 2001 and 2015. *Journal of Korean Medical Science, 33*(8).

Koh, W.-J., Jeong, B.-H., Jeon, K., Lee, N. Y., Lee, K. S., Woo, S. Y., . . . Kwon, O. J. (2012). Clinical significance of the differentiation between Mycobacterium avium and Mycobacterium intracellulare in M avium complex lung disease. *Chest, 142*(6), 1482-1488.

Kolmogorov, M., Yuan, J., Lin, Y., & Pevzner, P. A. (2019). Assembly of long, error-prone reads using repeat graphs. *Nature Biotechnology, 37*(5), 540-546.

Kontos, V., Papadogiannakis, E., Mantziaras, G., Styliara, M., & Kanavaki, S. (2014). A case of disseminated Mycobacterium avium infection in a dog in Greece. *Case Reports in Veterinary Medicine, 2014*.

Koren, S., Walenz, B. P., Berlin, K., Miller, J. R., Bergman, N. H., & Phillippy, A. M. (2017). Canu: scalable and accurate long-read assembly via adaptive k-mer weighting and repeat separation. *Genome Research, 27*(5), 722-736.

Kozakiewicz, L., Chen, Y., Xu, J., Wang, Y., Dunussi-Joannopoulos, K., Ou, Q., . . . Chan, J. (2013). B cells regulate neutrophilia during Mycobacterium tuberculosis infection and BCG vaccination by modulating the interleukin-

17 response. *PLoS Pathogens, 9*(7), e1003472.

Krämer, A., Green, J., Pollard Jr, J., & Tugendreich, S. (2013). Causal analysis approaches in ingenuity pathway analysis. *Bioinformatics, 30*(4), 523-530.

Kriz, P., Jahn, P., Bezdekova, B., Blahutkova, M., Mrlik, V., Slana, I., & Pavlik, I. (2010). Mycobacterium avium subsp. hominissuis infection in horses. *Emerging Infectious Diseases, 16*(8), 1328.

Kumar, P. (2017). IFNγ-producing CD4+ T lymphocytes: the double-edged swords in tuberculosis. *Clinical and Translational Medicine, 6*(1), 1-7.

Kwon, Y.-S., & Koh, W.-J. (2016). Diagnosis and treatment of nontuberculous mycobacterial lung disease. *Journal of Korean Medical Science, 31*(5), 649-659.

Kwon, Y.-S., Koh, W.-J., & Daley, C. L. (2019). Treatment of Mycobacterium avium complex pulmonary disease. *Tuberculosis and Respiratory Diseases, 82*(1), 15-26.

Kwon, Y. S., Kim, E. J., Lee, S.-H., Suh, G. Y., Chung, M. P., Kim, H., . . . Koh, W.-J. (2007). Decreased cytokine production in patients with nontuberculous mycobacterial lung disease. *Lung, 185*(6), 337.

Laencina, L., Dubois, V., Le Moigne, V., Viljoen, A., Majlessi, L., Pritchard, J., . . . Gaillard, J.-L. (2018). Identification of genes required for Mycobacterium abscessus growth in vivo with a prominent role of the ESX-4 locus. *Proceedings of the National Academy of Sciences, 115*(5), E1002-E1011.

Lam, A., Foster, D., Martin, P., Spielman, D., Chee, H., Strong, M., . . . Malik, R. (2012). Treatment of Mycobacterium avium infection in a dog. *Australian Veterinary Practitioner, 42*(2), 234-239.

Langmead, B., & Salzberg, S. L. (2012). Fast gapped-read alignment with Bowtie 2. *Nature Methods, 9*(4), 357.

Larsen, M. H., Biermann, K., Tandberg, S., Hsu, T., & Jacobs Jr, W. R. (2007). Genetic manipulation of Mycobacterium tuberculosis. *Current Protocols in Microbiology, 6*(1), 10A. 12.11-10A. 12.21.

Le, Y., Cao, W., Zhou, L., Fan, X., Liu, Q., Liu, F., . . . Rao, Y. (2020). Infection of mycobacterium tuberculosis promotes both M1/M2 polarization and MMP production in cigarette smoke-exposed macrophages. *Frontiers in Immunology, 11*, 1902.

Ledbetter, E. C., Landry, M. P., Stokol, T., Kern, T. J., & Messick, J. B. (2009). Brucella canis endophthalmitis in 3 dogs: clinical features, diagnosis, and treatment. *Veterinary Ophthalmology, 12*(3), 183-191.

Lee, D.-G., Woo, J.-W., Kwok, S.-K., Cho, M.-L., & Park, S.-H. (2013). MRP8 promotes Th17 differentiation via upregulation of IL-6 production by fibroblast-like synoviocytes in rheumatoid arthritis. *Experimental and Molecular Medicine, 45*(4), e20-e20.

Lee, Y., Awasthi, A., Yosef, N., Quintana, F. J., Xiao, S., Peters, A., . . . Hafler, D. A. (2012). Induction and molecular signature of pathogenic TH 17 cells. *Nature Immunology, 13*(10), 991-999.

Li, G., Zhang, J., Guo, Q., Jiang, Y., Wei, J., Zhao, L.-l., . . . Wan, K. (2015). Efflux pump gene expression in multidrug-resistant Mycobacterium tuberculosis clinical isolates. *PloS One, 10*(2), e0119013.

Li, G., Zhang, J., Guo, Q., Wei, J., Jiang, Y., Zhao, X., . . . Wan, K. (2015). Study of efflux pump gene expression in rifampicin-monoresistant Mycobacterium tuberculosis clinical isolates. *The Journal of Antibiotics, 68*(7), 431-435.

Li, Q., Gu, Y., Tu, Q., Wang, K., Gu, X., & Ren, T. (2016). Blockade of interleukin-17 restrains the development of acute lung injury. *Scandinavian Journal of Immunology, 83*(3), 203-211.

Li, Y., Wei, C., Xu, H., Jia, J., Wei, Z., Guo, R., . . . Qi, X. (2018). The immunoregulation of Th17 in host against intracellular bacterial infection. *Mediators of Inflammation, 2018*.

Lim, A., Allison, C., Price, P., & Waterer, G. (2010). Susceptibility to pulmonary disease due to Mycobacterium avium–intracellulare complex may reflect low IL-17 and high IL-10 responses rather than Th1 deficiency. *Clinical*

Immunology, 137(2), 296-302.

Lim, J., Park, H.-T., Ko, S., Park, H.-E., Lee, G., Kim, S., . . . Kim, D. (2021). Genomic diversity of Mycobacterium avium subsp. paratuberculosis: pangenomic approach for highlighting unique genomic features with newly constructed complete genomes. *Veterinary Research, 52*(1), 1-15.

Lin, Y., Yuan, J., Kolmogorov, M., Shen, M. W., Chaisson, M., & Pevzner, P. A. (2016). Assembly of long error-prone reads using de Bruijn graphs. *Proceedings of the National Academy of Sciences, 113*(52), E8396-E8405.

Liu, H., Xiong, X., Zhai, W., Zhu, T., Zhu, X., Zhu, Y., . . . Chen, H. (2020). Upregulation of cytokines and differentiation of Th17 and Treg by dendritic cells: central role of prostaglandin E2 induced by Mycobacterium bovis. *Microorganisms, 8*(2), 195.

Lombard, R., Doz, E., Carreras, F., Epardaud, M., Le Vern, Y., Buzoni-Gatel, D., & Winter, N. (2016). IL-17RA in non-hematopoietic cells controls CXCL-1 and 5 critical to recruit neutrophils to the lung of mycobacteria-infected mice during the adaptive immune response. *PloS One, 11*(2), e0149455.

Lovering, A. L., Safadi, S. S., & Strynadka, N. C. (2012). Structural perspective of peptidoglycan biosynthesis and assembly. *Annual Review of Biochemistry, 81*, 451-478.

Lugo-Villarino, G., Vérollet, C., Maridonneau-Parini, I., & Neyrolles, O. (2011). Macrophage polarization: convergence point targeted by mycobacterium tuberculosis and HIV. *Frontiers in Immunology, 2*, 43.

Lyadova, I., & Panteleev, A. (2015). Th1 and Th17 cells in tuberculosis: protection, pathology, and biomarkers. *Mediators of Inflammation, 2015*.

Machado, D., Couto, I., Perdigão, J., Rodrigues, L., Portugal, I., Baptista, P., . . . Viveiros, M. (2012). Contribution of efflux to the emergence of isoniazid and multidrug resistance in Mycobacterium tuberculosis. *PloS One, 7*(4), e34538.

Madarame, H., Saito, M., Ogihara, K., Ochiai, H., Oba, M., Omatsu, T., . . . Mizutani,

T. (2017). Mycobacterium avium subsp. hominissuis menigoencephalitis in a cat. *Veterinary Microbiology, 204*, 43-45.

Maiga, M., Siddiqui, S., Diallo, S., Diarra, B., Traoré, B., Shea, Y. R., . . . Kassambara, H. (2012). Failure to recognize nontuberculous mycobacteria leads to misdiagnosis of chronic pulmonary tuberculosis. *PloS One, 7*(5), e36902.

Malik, R., Smits, B., Reppas, G., Laprie, C., O'Brien, C., & Fyfe, J. (2013). Ulcerated and nonulcerated nontuberculous cutaneous mycobacterial granulomas in cats and dogs. *Veterinary Dermatology, 24*(1), 146-e133.

Marianelli, C., Ape, D., & Rossi Mori, F. (2020). Isolation, Molecular Typing, and Antibiotic Susceptibility Testing of Mycobacterium avium Subspecies hominissuis From a Dog With Generalized Mycobacteriosis. *Frontiers in Veterinary Science, 7*, 927.

Marjanovic, O., Miyata, T., Goodridge, A., Kendall, L. V., & Riley, L. W. (2010). Mce2 operon mutant strain of Mycobacterium tuberculosis is attenuated in C57BL/6 mice. *Tuberculosis, 90*(1), 50-56.

Martín-Casabona, N., Bahrmand, A., Bennedsen, J., Østergaard Thomsen, V., Curcio, M., Fauville-Dufaux, M., . . . Köksalan, K. (2004). Non-tuberculous mycobacteria: patterns of isolation. A multi-country retrospective survey. *The International Journal of Tuberculosis and Lung Disease, 8*(10), 1186-1193.

Martínez-Colón, G. J., & Moore, B. B. (2018). Prostaglandin E2 as a regulator of immunity to pathogens. *Pharmacology and Therapeutics, 185*, 135-146.

Matsuyama, M., Ishii, Y., Yageta, Y., Ohtsuka, S., Ano, S., Matsuno, Y., . . . Ogawa, K. (2014). Role of Th1/Th17 balance regulated by T-bet in a mouse model of Mycobacterium avium complex disease. *The Journal of Immunology, 192*(4), 1707-1717.

Maw, W. W., Shimizu, T., Sato, K., & Tomioka, H. (1997). Further study on the roles of the effector molecules of immunosuppressive macrophages induced by

mycobacterial infection in expression of their suppressor function against mitogen-stimulated T cell proliferation. *Clinical and Experimental Immunology, 108*(1), 26-33.

McWhorter, F. Y., Wang, T., Nguyen, P., Chung, T., & Liu, W. F. (2013). Modulation of macrophage phenotype by cell shape. *Proceedings of the National Academy of Sciences, 110*(43), 17253-17258.

Miller, M., Greene, C., & Brix, A. (1995). Disseminated Mycobacterium avium--intracellulare complex infection in a miniature schnauzer. *Journal of the American Animal Hospital Association, 31*(3), 213-216.

Mittal, E., Skowyra, M. L., Uwase, G., Tinaztepe, E., Mehra, A., Köster, S., . . . Philips, J. A. (2018). Mycobacterium tuberculosis type VII secretion system effectors differentially impact the ESCRT endomembrane damage response. *mBio, 9*(6), e01765-01718.

Monahan, I. M., Betts, J., Banerjee, D. K., & Butcher, P. D. (2001). Differential expression of mycobacterial proteins following phagocytosis by macrophages. *Microbiology, 147*(2), 459-471.

Murcia, M. I., Tortoli, E., Menendez, M. C., Palenque, E., & Garcia, M. J. (2006). Mycobacterium colombiense sp. nov., a novel member of the Mycobacterium avium complex and description of MAC-X as a new ITS genetic variant. *International Journal of Systematic and Evolutionary Microbiology, 56*(9), 2049-2054.

Murray, P. J., Allen, J. E., Biswas, S. K., Fisher, E. A., Gilroy, D. W., Goerdt, S., . . . Lawrence, T. (2014). Macrophage activation and polarization: nomenclature and experimental guidelines. *Immunity, 41*(1), 14-20.

Murray, P. J., & Wynn, T. A. (2011). Protective and pathogenic functions of macrophage subsets. *Nature Reviews Immunology, 11*(11), 723-737.

Namkoong, H., Kurashima, A., Morimoto, K., Hoshino, Y., Hasegawa, N., Ato, M., & Mitarai, S. (2016). Epidemiology of pulmonary nontuberculous mycobacterial disease, Japan.

Nash, K. A., Andini, N., Zhang, Y., Brown-Elliott, B. A., & Wallace Jr, R. J. (2006). Intrinsic macrolide resistance in rapidly growing mycobacteria. *Antimicrobial Agents and Chemotherapy, 50*(10), 3476-3478.

Newton-Foot, M., Warren, R. M., Sampson, S. L., Van Helden, P. D., & van Pittius, N. C. G. (2016). The plasmid-mediated evolution of the mycobacterial ESX (Type VII) secretion systems. *BMC Evolutionary Biology, 16*(1), 1-12.

Noël, W., Raes, G., Ghassabeh, G. H., De Baetselier, P., & Beschin, A. (2004). Alternatively activated macrophages during parasite infections. *Trends in Parasitology, 20*(3), 126-133.

O'Sullivan, M. P., O'Leary, S., Kelly, D. M., & Keane, J. (2007). A caspase-independent pathway mediates macrophage cell death in response to Mycobacterium tuberculosis infection. *Infection and Immunity, 75*(4), 1984-1993.

O'Toole, D., Tharp, S., Thomsen, B., Tan, E., & Payeur, J. (2005). Fatal mycobacteriosis with hepatosplenomegaly in a young dog due to Mycobacterium avium. *Journal of Veterinary Diagnostic Investigation, 17*(2), 200-204.

Olea-Popelka, F., Muwonge, A., Perera, A., Dean, A. S., Mumford, E., Erlacher-Vindel, E., . . . El Idrissi, A. (2017). Zoonotic tuberculosis in human beings caused by Mycobacterium bovis—a call for action. *The Lancet Infectious Diseases, 17*(1), e21-e25.

Ostadkarampour, M., Eklund, A., Moller, D., Glader, P., Olgart Höglund, C., Lindén, A., . . . Wahlström, J. (2014). Higher levels of interleukin IL-17 and antigen-specific IL-17 responses in pulmonary sarcoidosis patients with L öfgren's syndrome. *Clinical and Experimental Immunology, 178*(2), 342-352.

Ouyang, W., Kolls, J. K., & Zheng, Y. (2008). The biological functions of T helper 17 cell effector cytokines in inflammation. *Immunity, 28*(4), 454-467.

Page, A. J., Cummins, C. A., Hunt, M., Wong, V. K., Reuter, S., Holden, M. T., . . . Parkhill, J. (2015). Roary: rapid large-scale prokaryote pan genome analysis.

Bioinformatics, 31(22), 3691-3693.

Parisi, L., Gini, E., Baci, D., Tremolati, M., Fanuli, M., Bassani, B., . . . Mortara, L. (2018). Macrophage polarization in chronic inflammatory diseases: killers or builders? *Journal of Immunology Research, 2018*.

Park, H.-E., Kim, S., Shim, S., Park, H.-T., Park, W. B., Im, Y. B., & Yoo, H. S. (2020). 16S and 23S rRNA Gene Mutation Independent Multidrug Resistance of Non-Tuberculous Mycobacteria Isolated from South Korean Soil. *Microorganisms, 8*(8), 1114.

Patel, S. Y., Ding, L., Brown, M. R., Lantz, L., Gay, T., Cohen, S., . . . Holland, S. M. (2005). Anti-IFN-γ autoantibodies in disseminated nontuberculous mycobacterial infections. *The Journal of Immunology, 175*(7), 4769-4776.

Pavlik, I., Svastova, P., Bartl, J., Dvorska, L., & Rychlik, I. (2000). Relationship between IS901 in theMycobacterium avium Complex Strains Isolated from Birds, Animals, Humans, and the Environment and Virulence for Poultry. *Clinical and Diagnostic Laboratory Immunology, 7*(2), 212-217.

Portal-Celhay, C., Tufariello, J. M., Srivastava, S., Zahra, A., Klevorn, T., Grace, P. S., . . . Jacobs, W. R. (2016). Mycobacterium tuberculosis EsxH inhibits ESCRT-dependent CD4+ T-cell activation. *Nature Microbiology, 2*(2), 1-9.

Pranada, A. B., Witt, E., Bienia, M., Kostrzewa, M., & Timke, M. (2017). Accurate differentiation of Mycobacterium chimaera from Mycobacterium intracellulare by MALDI-TOF MS analysis. *Journal of Medical Microbiology, 66*(5), 670-677.

Prevots, D. R., & Marras, T. K. (2015). Epidemiology of human pulmonary infection with nontuberculous mycobacteria: a review. *Clinics in Chest Medicine, 36*(1), 13-34.

Pujol, M., Borie, C., Montoya, M., Ferreira, A., & Vernal, R. (2019). Brucella canis induces canine CD4+ T cells multi-cytokine Th1/Th17 production via dendritic cell activation. *Comparative Immunology, Microbiology and Infectious Diseases, 62*, 68-75.

Qiang, L., Wang, J., Zhang, Y., Ge, P., Chai, Q., Li, B., . . . Liu, C. H. (2019). Mycobacterium tuberculosis Mce2E suppresses the macrophage innate immune response and promotes epithelial cell proliferation. *Cellular & Molecular Immunology, 16*(4), 380-391.

Quinlan, A. R., & Hall, I. M. (2010). BEDTools: a flexible suite of utilities for comparing genomic features. *Bioinformatics, 26*(6), 841-842.

Rai, D., & Mehra, S. (2021). The Mycobacterial Efflux Pump EfpA Can Induce High Drug Tolerance to Many Antituberculosis Drugs, Including Moxifloxacin, in Mycobacterium smegmatis. *Antimicrobial Agents and Chemotherapy, 65*(11), e00262-00221.

Ramesh, R., Kozhaya, L., McKevitt, K., Djuretic, I. M., Carlson, T. J., Quintero, M. A., . . . Sundrud, M. S. (2014). Pro-inflammatory human Th17 cells selectively express P-glycoprotein and are refractory to glucocorticoids. *Journal of Experimental Medicine, 211*(1), 89-104.

Refai, A., Gritli, S., Barbouche, M.-R., & Essafi, M. (2018). Mycobacterium tuberculosis virulent factor ESAT-6 drives macrophage differentiation toward the pro-inflammatory M1 phenotype and subsequently switches it to the anti-inflammatory M2 phenotype. *Frontiers in Cellular and Infection Microbiology, 8*, 327.

Rivera-Calzada, A., Famelis, N., Llorca, O., & Geibel, S. (2021). Type VII secretion systems: structure, functions and transport models. *Nature Reviews Microbiology*, 1-18.

Rojas, M., Barrera, L. F., & García, L. F. (1998). Induction of apoptosis in murine macrophages by Mycobacterium tuberculosis is reactive oxygen intermediates-independent. *Biochemical and Biophysical Research Communications, 247*(2), 436-442.

Roy, S., Schmeier, S., Kaczkowski, B., Arner, E., Alam, T., Ozturk, M., . . . Itoh, M. (2018). Transcriptional landscape of Mycobacterium tuberculosis infection in macrophages. *Scientific Reports, 8*(1), 1-13.

Runyon, E. (1965). Pathogenic mycobacteria. *Bibliotheca Tuberculosea, 21*, 235-287.

Ryu, Y. J., Koh, W.-J., & Daley, C. L. (2016). Diagnosis and treatment of nontuberculous mycobacterial lung disease: clinicians' perspectives. *Tuberculosis and Respiratory Diseases, 79*(2), 74-84.

Saha, B., Prasanna, S. J., Chandrasekar, B., & Nandi, D. (2010). Gene modulation and immunoregulatory roles of Interferonγ. *Cytokine, 50*(1), 1-14.

Sajid, A., Arora, G., Gupta, M., Singhal, A., Chakraborty, K., Nandicoori, V. K., & Singh, Y. (2011). Interaction of Mycobacterium tuberculosis elongation factor Tu with GTP is regulated by phosphorylation. *Journal of Bacteriology, 193*(19), 5347-5358.

Salah, I. B., Cayrou, C., Raoult, D., & Drancourt, M. (2009). Mycobacterium marseillense sp. nov., Mycobacterium timonense sp. nov. and Mycobacterium bouchedurhonense sp. nov., members of the Mycobacterium avium complex. *International Journal of Systematic and Evolutionary Microbiology, 59*(11), 2803-2808.

Saleeb, P., & Olivier, K. N. (2010). Pulmonary nontuberculous mycobacterial disease: new insights into risk factors for susceptibility, epidemiology, and approaches to management in immunocompetent and immunocompromised patients. *Current Infectious Disease Reports, 12*(3), 198-203.

Sangari, F. J., Goodman, J., & Bermudez, L. E. (2000). Mycobacterium avium enters intestinal epithelial cells through the apical membrane, but not by the basolateral surface, activates small GTPase Rho and, once within epithelial cells, expresses an invasive phenotype. *Cellular Microbiology, 2*(6), 561-568.

Sassetti, C. M., Boyd, D. H., & Rubin, E. J. (2003). Genes required for mycobacterial growth defined by high density mutagenesis. *Molecular Microbiology, 48*(1), 77-84.

Sayers, S., Li, L., Ong, E., Deng, S., Fu, G., Lin, Y., . . . Zhao, B. (2019). Victors: a

web-based knowledge base of virulence factors in human and animal pathogens. *Nucleic Acids Research, 47*(D1), D693-D700.

Schinköthe, J., Möbius, P., Köhler, H., & Liebler-Tenorio, E. (2016). Experimental infection of goats with Mycobacterium avium subsp. hominissuis: a model for comparative tuberculosis research. *Journal of Comparative Pathology, 155*(2-3), 218-230.

Scott, N. R., Swanson, R. V., Al-Hammadi, N., Domingo-Gonzalez, R., Rangel-Moreno, J., Kriel, B. A., . . . Mehra, S. (2020). S100A8/A9 regulates CD11b expression and neutrophil recruitment during chronic tuberculosis. *The Journal of Clinical Investigation, 130*(6), 3098-3112.

Seemann, T. (2014). Prokka: rapid prokaryotic genome annotation. *Bioinformatics, 30*(14), 2068-2069.

Serafini, A., Boldrin, F., Palù, G., & Manganelli, R. (2009). Characterization of a Mycobacterium tuberculosis ESX-3 conditional mutant: essentiality and rescue by iron and zinc. *Journal of Bacteriology, 191*(20), 6340-6344.

Shackelford, C. C., & Reed, W. M. (1989). Disseminated Mycobacterium avium infection in a dog. *Journal of Veterinary Diagnostic Investigation, 1*(3), 273-275.

Sharbati, J., Lewin, A., Kutz-Lohroff, B., Kamal, E., Einspanier, R., & Sharbati, S. (2011). Integrated microRNA-mRNA-analysis of human monocyte derived macrophages upon Mycobacterium avium subsp. hominissuis infection. *PloS One, 6*(5), e20258.

Shen, H., & Chen, Z. W. (2018). The crucial roles of Th17-related cytokines/signal pathways in M. tuberculosis infection. *Cellular & Molecular Immunology, 15*(3), 216.

Shin, J.-I., Shin, S. J., & Shin, M.-K. (2020). Differential genotyping of Mycobacterium avium complex and its implications in clinical and environmental epidemiology. *Microorganisms, 8*(1), 98.

Shinohara, H., Yano, S., Bucana, C. D., & Fidler, I. J. (2000). Induction of chemokine

secretion and enhancement of contact-dependent macrophage cytotoxicity by engineered expression of granulocyte-macrophage colony-stimulating factor in human colon cancer cells. *The Journal of Immunology, 164*(5), 2728-2737.

Shiomi, A., Usui, T., & Mimori, T. (2016). GM-CSF as a therapeutic target in autoimmune diseases. *Inflammation and Regeneration, 36*(1), 1-9.

Shu, C.-C., Wang, J.-Y., Wu, M.-F., Lai, H.-C., Chiang, B.-L., & Yu, C.-J. (2018). Interleukin 23/interleukin 17 axis activated by Mycobacterium avium complex (MAC) is attenuated in patients with MAC-lung disease. *Tuberculosis, 110*, 7-14.

Shu, C.-C., Wang, J.-Y., Wu, M.-F., Wu, C.-T., Lai, H.-C., Lee, L.-N., . . . Yu, C.-J. (2017). Attenuation of lymphocyte immune responses during Mycobacterium avium complex-induced lung disease due to increasing expression of programmed death-1 on lymphocytes. *Scientific Reports, 7*(1), 1-12.

Sica, A., & Mantovani, A. (2012). Macrophage plasticity and polarization: in vivo veritas. *The Journal of Clinical Investigation, 122*(3), 787-795.

Silva, T. R. M. d., Petersen, A. L. d. O. A., Santos, T. d. A., Almeida, T. F. d., Freitas, L. A. R. d., & Veras, P. S. T. (2010). Control of Mycobacterium fortuitum and Mycobacterium intracellulare infections with respect to distinct granuloma formations in livers of BALB/c mice. *Memorias do Instituto Oswaldo Cruz, 105*, 642-648.

Simeone, R., Bobard, A., Lippmann, J., Bitter, W., Majlessi, L., Brosch, R., & Enninga, J. (2012). Phagosomal rupture by Mycobacterium tuberculosis results in toxicity and host cell death. *PLoS Pathogens, 8*(2), e1002507.

Singh, P., Benjak, A., Schuenemann, V. J., Herbig, A., Avanzi, C., Busso, P., . . . Cole, S. T. (2015). Insight into the evolution and origin of leprosy bacilli from the genome sequence of Mycobacterium lepromatosis. *Proceedings of the National Academy of Sciences, 112*(14), 4459-4464.

Sofian, M., Ramezani, A., Mousavi, A., Banifazl, M., Cherei, S., Cherei, A., & Aghakhani, A. (2016). Interlukine-17 and TGF-ß levels in patients with acute brucellosisbefore and after treatment. *Turkish Journal of Medical Sciences, 46*(5), 1348-1352.

Sreevatsan, S., Pan, X., Stockbauer, K. E., Williams, D. L., Kreiswirth, B. N., & Musser, J. M. (1996). Characterization of rpsL and rrs mutations in streptomycin-resistant Mycobacterium tuberculosis isolates from diverse geographic localities. *Antimicrobial Agents and Chemotherapy, 40*(4), 1024-1026.

Stark, M. A., Huo, Y., Burcin, T. L., Morris, M. A., Olson, T. S., & Ley, K. (2005). Phagocytosis of apoptotic neutrophils regulates granulopoiesis via IL-23 and IL-17. *Immunity, 22*(3), 285-294.

Stout, J. E., Koh, W.-J., & Yew, W. W. (2016). Update on pulmonary disease due to non-tuberculous mycobacteria. *International Journal of Infectious Diseases, 45*, 123-134.

Tatano, Y., Shimizu, T., & Tomioka, H. (2014). Unique macrophages different from M1/M2 macrophages inhibit T cell mitogenesis while upregulating Th17 polarization. *Scientific Reports, 4*(1), 1-11.

Tateishi, Y., Ozeki, Y., Nishiyama, A., Miki, M., Maekura, R., Fukushima, Y., . . . Matsumoto, S. (2021). Comparative genomic analysis of Mycobacterium intracellulare: implications for clinical taxonomic classification in pulmonary Mycobacterium avium-intracellulare complex disease. *BMC Microbiology, 21*(1), 1-15.

Thegerström, J., Jönsson, B., Brudin, L., Olsen, B., Wold, A. E., Ernerudh, J., & Friman, V. (2012). Mycobacterium avium subsp. avium and subsp. hominissuis give different cytokine responses after in vitro stimulation of human blood mononuclear cells. *PloS One, 7*(4), e34391.

Thiriot, J. D., Martinez-Martinez, Y. B., Endsley, J. J., & Torres, A. G. (2020). Hacking the host: exploitation of macrophage polarization by intracellular

bacterial pathogens. *Pathogens and Disease, 78*(1), ftaa009.

Thorel, M., Huchzermeyer, H., & Michel, A. (2001). Mycobacterium avium and Mycobacterium intracellulare infection in mammals. *Revue Scientifique et Technique (International Office of Epizootics), 20*(1), 204-218.

Tomioka, H., Saito, H., Sato, K., & Dawson, D. J. (1993). Comparison of the virulence for mice of Mycobacterium avium and Mycobacterium intracellulare identified by DNA probe test. *Microbiology and Immunology, 37*(4), 259-264.

Tomioka, H., Saito, H., & Yamada, Y. (1990). Characteristics of immunosuppressive macrophages induced in spleen cells by Mycobacterium avium complex infections in mice. *Microbiology, 136*(5), 965-973.

Tomioka, H., Sato, K., Maw, W. W., & Saito, H. (1995). The role of tumor necrosis factor, interferon-γ, Transforming growth factor-β, and nitric oxide in the expression of immunosuppressive functions of splenic macrophages induced by Mycobacterium avium complex infection. *Journal of Leukocyte Biology, 58*(6), 704-712.

Tomioka, H., Tatano, Y., Maw, W. W., Sano, C., Kanehiro, Y., & Shimizu, T. (2012). Characteristics of suppressor macrophages induced by mycobacterial and protozoal infections in relation to alternatively activated M2 macrophages. *Clinical and Developmental Immunology, 2012*.

Torrado, E., & Cooper, A. M. (2010). IL-17 and Th17 cells in tuberculosis. *Cytokine and Growth Factor Reviews, 21*(6), 455-462.

Tortoli, E., Pecorari, M., Fabio, G., Messinò, M., & Fabio, A. (2010). Commercial DNA probes for mycobacteria incorrectly identify a number of less frequently encountered species. *Journal of Clinical Microbiology, 48*(1), 307-310.

Tortoli, E., Rindi, L., Garcia, M. J., Chiaradonna, P., Dei, R., Garzelli, C., . . . Mariottini, A. (2004). Proposal to elevate the genetic variant MAC-A, included in the Mycobacterium avium complex, to species rank as

Mycobacterium chimaera sp. nov. *International Journal of Systematic and Evolutionary Microbiology, 54*(4), 1277-1285.

Tosi, M. F., Stark, J. M., Smith, C. W., Hamedani, A., Gruenert, D. C., & Infeld, M. D. (1992). Induction of ICAM-1 expression on human airway epithelial cells by inflmmatory cytokines: effect of neutrophil-epithelial cells adhesion. *American Journal of Respiratory Cell and Molecular Biology, 7*, 214-221.

Treede, I., Jakobsen, L., Kirpekar, F., Vester, B., Weitnauer, G., Bechthold, A., & Douthwaite, S. (2003). The avilamycin resistance determinants AviRa and AviRb methylate 23S rRNA at the guanosine 2535 base and the uridine 2479 ribose. *Molecular Microbiology, 49*(2), 309-318.

Tufariello, J. M., Chapman, J. R., Kerantzas, C. A., Wong, K.-W., Vilchèze, C., Jones, C. M., . . . Fenyö, D. (2016). Separable roles for Mycobacterium tuberculosis ESX-3 effectors in iron acquisition and virulence. *Proceedings of the National Academy of Sciences, 113*(3), E348-E357.

Uchiya, K.-i., Tomida, S., Nakagawa, T., Asahi, S., Nikai, T., & Ogawa, K. (2017). Comparative genome analyses of Mycobacterium avium reveal genomic features of its subspecies and strains that cause progression of pulmonary disease. *Scientific Reports, 7*(1), 1-14.

Ushach, I., & Zlotnik, A. (2016). Biological role of granulocyte macrophage colony-stimulating factor (GM-CSF) and macrophage colony-stimulating factor (M-CSF) on cells of the myeloid lineage. *Journal of Leukocyte Biology, 100*(3), 481-489.

van Ingen, J. (2015). Microbiological diagnosis of pulmonary disease caused by nontuberculous mycobacteria. *Clinics in Chest Medicine, 36*, 43-54.

van Ingen, J., Boeree, M. J., Kösters, K., Wieland, A., Tortoli, E., Dekhuijzen, P. R., & van Soolingen, D. (2009). Proposal to elevate Mycobacterium avium complex ITS sequevar MAC-Q to Mycobacterium vulneris sp. nov. *International Journal of Systematic and Evolutionary Microbiology, 59*(9), 2277-2282.

Van Ingen, J., Hoefsloot, W., Buijtels, P., Tortoli, E., Supply, P., Dekhuijzen, P., . . . Van Soolingen, D. (2012). Characterization of a novel variant of Mycobacterium chimaera. *Journal of Medical Microbiology, 61*(9), 1234-1239.

van Ingen, J., Kohl, T. A., Kranzer, K., Hasse, B., Keller, P. M., Szafrańska, A. K., . . . Sommerstein, R. (2017). Global outbreak of severe Mycobacterium chimaera disease after cardiac surgery: a molecular epidemiological study. *The Lancet Infectious Diseases, 17*(10), 1033-1041.

van Ingen, J., Lindeboom, J. A., Hartwig, N. G., de Zwaan, R., Tortoli, E., Dekhuijzen, P. R., . . . van Soolingen, D. (2009). Mycobacterium mantenii sp. nov., a pathogenic, slowly growing, scotochromogenic species. *International Journal of Systematic and Evolutionary Microbiology, 59*(11), 2782-2787.

van Ingen, J., Turenne, C. Y., Tortoli, E., Wallace Jr, R. J., & Brown-Elliott, B. A. (2018). A definition of the Mycobacterium avium complex for taxonomical and clinical purposes, a review. *International Journal of Systematic and Evolutionary Microbiology, 68*(11), 3666-3677.

VanHeyningen, T. K., Collins, H. L., & Russell, D. G. (1997). IL-6 produced by macrophages infected with Mycobacterium species suppresses T cell responses. *The Journal of Immunology, 158*(1), 330-337.

Vankayalapati, R., Wizel, B., Samten, B., Griffith, D. E., Shams, H., Galland, M. R., . . . Barnes, P. F. (2001). Cytokine profiles in immunocompetent persons infected with Mycobacterium avium complex. *The Journal of Infectious Diseases, 183*(3), 478-484.

Vázquez, N., Rekka, S., Gliozzi, M., Feng, C. G., Amarnath, S., Orenstein, J. M., & Wahl, S. M. (2012). Modulation of innate host factors by Mycobacterium avium complex in human macrophages includes interleukin 17. *The Journal of Infectious Diseases, 206*(8), 1206-1217.

Vereyken, E. J., Heijnen, P. D., Baron, W., de Vries, E. H., Dijkstra, C. D., &

Teunissen, C. E. (2011). Classically and alternatively activated bone marrow derived macrophages differ in cytoskeletal functions and migration towards specific CNS cell types. *Journal of Neuroinflammation, 8*(1), 1-16.

Verreck, F. A., de Boer, T., Langenberg, D. M., van der Zanden, L., & Ottenhoff, T. H. (2006). Phenotypic and functional profiling of human proinflammatory type-1 and anti-inflammatory type-2 macrophages in response to microbial antigens and IFN-γ-and CD40L-mediated costimulation. *Journal of Leukocyte Biology, 79*(2), 285-293.

Vila-del Sol, V., Punzón, C., & Fresno, M. (2008). IFN-γ-induced TNF-α expression is regulated by interferon regulatory factors 1 and 8 in mouse macrophages. *The Journal of Immunology, 181*(7), 4461-4470.

Waldo, S. W., Li, Y., Buono, C., Zhao, B., Billings, E. M., Chang, J., & Kruth, H. S. (2008). Heterogeneity of human macrophages in culture and in atherosclerotic plaques. *The American Journal of Pathology, 172*(4), 1112-1126.

Wallace Jr, R. J., Iakhiaeva, E., Williams, M. D., Brown-Elliott, B. A., Vasireddy, S., Vasireddy, R., . . . Kwait, R. (2013). Absence of Mycobacterium intracellulare and presence of Mycobacterium chimaera in household water and biofilm samples of patients in the United States with Mycobacterium avium complex respiratory disease. *Journal of Clinical Microbiology, 51*(6), 1747-1752.

Wang, X., Barnes, P. F., Huang, F., Alvarez, I. B., Neuenschwander, P. F., Sherman, D. R., & Samten, B. (2012). Early secreted antigenic target of 6-kDa protein of Mycobacterium tuberculosis primes dendritic cells to stimulate Th17 and inhibit Th1 immune responses. *The Journal of Immunology, 189*(6), 3092-3103.

Wattam, A. R., Davis, J. J., Assaf, R., Boisvert, S., Brettin, T., Bun, C., . . . Gabbard, J. L. (2017). Improvements to PATRIC, the all-bacterial bioinformatics database and analysis resource center. *Nucleic Acids Research, 45*(D1),

D535-D542.

Weaver, C. T., Elson, C. O., Fouser, L. A., & Kolls, J. K. (2013). The Th17 pathway and inflammatory diseases of the intestines, lungs, and skin. *Annual Review of Pathology: Mechanisms of Disease, 8*, 477-512.

Wellenberg, G., De Haas, P., Van Ingen, J., Van Soolingen, D., & Visser, I. (2010). Multiple strains of Mycobacterium avium subspecies hominissuis infections associated with aborted fetuses and wasting in pigs. *Veterinary Record, 167*(12), 451-454.

Wheat, W., Chow, L., Kuzmik, A., Soontararak, S., Kurihara, J., Lappin, M., & Dow, S. (2019). Local immune and microbiological responses to mucosal administration of a Liposome-TLR agonist immunotherapeutic in dogs. *BMC Veterinary Research, 15*(1), 1-13.

Wu, U.-I., & Holland, S. M. (2015). Host susceptibility to non-tuberculous mycobacterial infections. *The Lancet Infectious Diseases, 15*(8), 968-980.

Wu, U. I., Olivier, K. N., Kuhns, D. B., Fink, D. L., Sampaio, E. P., Zelazny, A. M., ... & Holland, S. M. (2019, December). Patients with idiopathic pulmonary nontuberculous mycobacterial disease have normal Th1/Th2 cytokine responses but diminished Th17 cytokine and enhanced granulocyte-macrophage colony-stimulating factor production. In Open forum infectious diseases (Vol. 6, No. 12, p. ofz484). US: Oxford University Press.

Xu, L., Cui, G., Jia, H., Zhu, Y., Ding, Y., Chen, J., . . . Li, L. (2016). Decreased IL-17 during treatment of sputum smear-positive pulmonary tuberculosis due to increased regulatory T cells and IL-10. *Journal of Translational Medicine, 14*(1), 179.

Xu, L., Wu, D., Liu, L., Zheng, Q., Song, Y., Ye, L., . . . Ma, Y. (2014). Characterization of mycobacterial UDP-N-acetylglucosamine enolpyruvyle transferase (MurA). *Research in Microbiology, 165*(2), 91-101.

Yang, F.-C., Chiu, P.-Y., Chen, Y., Mak, T. W., & Chen, N.-J. (2019). TREM-1-dependent M1 macrophage polarization restores intestinal epithelium

damaged by DSS-induced colitis by activating IL-22-producing innate lymphoid cells. *Journal of Biomedical Science, 26*(1), 1-14.

Yang, M., Liu, J., Piao, C., Shao, J., & Du, J. (2015). ICAM-1 suppresses tumor metastasis by inhibiting macrophage M2 polarization through blockade of efferocytosis. *Cell Death & Disease, 6*(6), e1780-e1780.

Yano, H., Iwamoto, T., Nishiuchi, Y., Nakajima, C., Starkova, D. A., Mokrousov, I., . . . Nakanishi, N. (2017). Population structure and local adaptation of MAC lung disease agent Mycobacterium avium subsp. hominissuis. *Genome Biology and Evolution, 9*(9), 2403-2417.

Yoshida, Y. O., Umemura, M., Yahagi, A., O'Brien, R. L., Ikuta, K., Kishihara, K., . . . Matsuzaki, G. (2010). Essential role of IL-17A in the formation of a mycobacterial infection-induced granuloma in the lung. *The Journal of Immunology, 184*(8), 4414-4422.

Zeiss, C. J., Jardine, J., & Huchzermeyer, H. (1994). A case of disseminated tuberculosis in a dog caused by Mycobacterium avium-intracellulare. *American Animal Hospital Association (USA)*.

Zhang, F., & Xie, J.-P. (2011). Mammalian cell entry gene family of Mycobacterium tuberculosis. *Molecular and Cellular Biochemistry, 352*(1), 1-10.

Zhang, Y.-L., Han, D. H., Kim, D.-Y., Lee, C. H., & Rhee, C.-S. (2017). Role of Interleukin-17A on the chemotactic responses to ccl7 in a murine allergic rhinitis model. *PloS One, 12*(1), e0169353.

Zhang, Z., Pang, Y., Wang, Y., Cohen, C., Zhao, Y., & Liu, C. (2015). Differences in risk factors and drug susceptibility between Mycobacterium avium and Mycobacterium intracellulare lung diseases in China. *International Journal of Antimicrobial Agents, 45*(5), 491-495.

Zirlik, A., Maier, C., Gerdes, N., MacFarlane, L., Soosairajah, J., Bavendiek, U., . . . Missiou, A. (2007). CD40 ligand mediates inflammation independently of CD40 by interaction with Mac-1. *Circulation, 115*(12), 1571.

국문초록

개에서의 *Mycobacterium avium* complex 감염에 대한 숙주 면역반응 규명

김 수 지

(지도교수: 유 한 상, D.V.M., Ph.D.)

서울대학교 대학원

수의학과 수의병인생물학 및 예방수의학 전공

비결핵 항산균 (nontuberculous mycobacteria, NTM)은 토양 및 자연수 등 자연 환경에 널리 분포하고 있는 기회 감염균이다. *M. avium* 및 *M. intracellulare*는 NTM 폐질환을 일으키는 주요 원인균으로 *Mycobacterium avium* complex (MAC)의 대표적인 균주이다. MAC는 사람을 포함하여 다양한 동물에서 감염이 보고되었으며 개에서는 산발적인 발생이 보고되고 있다. MAC에 감염된 개의 경우 대부분 예후가 좋지 않아 안락사되거나

사망하였다. 또한, MAC 감염에 대한 개에서의 인수공통감염병의 가능성은 현재까지 밝혀진 바가 없지만 MTBC (*Mycobacterium tuberculosis* complex)중 *M. tuberculosis*, *M. bovis* 및 *M. microti* 등은 개에서 사람으로의 전파가 보고된 바 있다. 현재 가축과 야생동물에 의한 MAC의 감염 보고 또한 증가하고 있기 때문에 MAC 감염에 대한 개에서의 면역 반응을 조사하는 것은 진단 및 치료와 더불어 사람과 개 사이의 잠재적인 인수공통 감염을 제어하는 데에도 필수적인 요소라고 판단된다.

개에서의 MAC 감염은 주로 *M. avium* subsp. *hominissuis* (MAH)가 원인균으로 지목되어 왔다. 이에 본 연구에서는 개의 MAH 감염에 대한 숙주 면역반응을 개 말초 혈액 단핵세포 (peripheral blood mononuclear cells; PBMCs)의 전사체 분석을 통해 확인하였다. 전사체 분석은 MAH 감염시 Th1 및 Th17 반응과 관련한 T 세포 면역 반응이 유도됨을 보여주었다. Th1 관련 유전자의 발현은 감염 초기에 확인된 반면, Th17 관련 유전자의 발현은 감염 12시간 이후에 확인되었다. 또한 24시간 감염 이후 큰포식세포 (Macrophages) 내에서 세포 사멸 관련 유전자의 발현이 감소되었으며 MAH가 증식함을 확인하였다. 본 연구를 통해 MAH 가 개 말초 혈액 단핵세포에 침입시 Th1 및 Th17 면역 반응을 유도하고 세포 사멸 기작을 피하며 개의 큰포식세포 내에서 생존할 수 있음을 확인하였다.

개에서의 MAC 감염에 대한 원인균은 MAH 가 주로 지목되어 왔지만

대부분의 감염 사례에서는 종 또는 아종이 정확히 확인되지 않았다. 이는 샘플 수집의 어려움, 불특정 임상 징후 및 긴 잠복 기간으로 인하여 원인균 동정이 어렵기 때문인 것으로 생각된다. 그러나 MAC는 종마다 병원성이 다르고 항생제 내성이 다양하기 때문에 감염 시 원인균을 확인하는 것이 치료에 매우 중요하다. 따라서 본 연구에서는 MAH 와 더불어 반려견에서 감염 가능성이 높을 것으로 예상되는 *M. intracellulare* 감염에 대한 개에서의 숙주 면역 반응을 조사하였다. 개의 자가 단핵구 유래 큰포식세포 (monocyte-derived macrophages; MDMs) 및 림프구의 공동 배양을 통해 *M. intracellulare* 감염에 대한 숙주 면역 반응을 확인하였다. 전사체 분석 결과는 *M. intracellulare* 침입시 개 MDMs이 M1 유사 큰포식세포로 분화하고 Th1 및 Th17 세포의 분화를 유도하는 사이토카인을 분비하는 것을 보여주었다. 또한 감염된 MDMs 과 개 림프구의 공동 배양을 통해 Th17 세포가 *M. intracellulare* 감염시 우세하게 반응함을 확인하였다. 따라서 본 연구를 통해 *M. intracellulare* 감염 시 개의 큰포식세포 활성화에 의해 Th17 반응이 유도됨을 확인할 수 있다.

현재까지도 MAC의 새로운 종과 아종은 여전히 밝혀지고 있으며 이는 질병 통제에 새로운 위협이 되고 있다. 이러한 신종은 항생제 내성, 숙주 특이성 및 병원성과 관련한 유전적 다양성을 나타낸다. 따라서 MAC 감염에 의한 질병의 통제를 위해서는 신종 균주의 유전적 특성을 이해하는

것이 필수적이다. 현재 전장 유전체 분석의 발달로 MAC의 유전학적인 특성이 밝혀지고 있지만 아직까지도 *M. intracellulare*는 다른 MAC 종에 비해 관련 정보가 매우 부족한 실정이다. 국내 동물 보호소 및 반려동물 출입 가능 공원에서 새롭게 분리된 *M. intracellulare* 가 각 분리주 별로 다양한 항생제 감수성을 가지고 있음이 확인되었다. 이에 본 연구에서는 SMRT (single-molecule real-time) 시퀀싱을 통해 *M. intracellulare* 국내 분리주들의 유전적 특성을 조사하였다. *M. intracellulare* 분리주의 전장유전체 비교 분석은 Mammalian cell entry 및 Type VII secretion system 와 관련한 병원성 인자들의 유전적 다양성을 나타내었다. 또한 이러한 분리주들의 유전적인 차이는 마우스 폐 큰포식세포에서의 사이토카인 유도 및 세포 내 생존에서도 차이를 나타내었다. 따라서 환경 분리주의 유전적 변이는 토양과 같이 환경에 쉽게 노출되는 반려견에게 새로운 위협이 될 수 있을 것으로 판단된다.

개에서의 MAC 감염이 꾸준히 보고됨에 따라 MAC에 대한 개에서의 숙주 면역반응 분석은 질병의 예방 및 치료법 개발에 큰 도움이 될 것이다. 또한, 전장 유전체 비교 분석은 MAC 환경 분리주의 특이적인 병원성 인자 및 유전적 특성을 이해하는 데 필수적인 요소이다. 따라서 본 연구는 개에서의 MAC의 병원성 및 감수성을 이해하고 잠재적인 인수공통감염병 전파를 억제하는 데에 기여할 수 있을 것으로 생각된다.

핵심어: *Mycobacterium avium* complex, 세포성 면역반응, 개, 전장 유전체 분석, 전사체 분석

학번: 2016-21760

감사의 글

많은 분들의 도움 덕분에 지난 6년간의 학위 과정을 마무리할 수 있었습니다. 대학원 생활 동안 제가 힘들 때 격려해주시고 소중한 추억을 함께 만들어 주신 모든 분들께 고마움을 전하고 싶습니다. 부족한 저를 학생으로 맞아주시고 가르쳐주신 지도교수님 유한상 교수님께 깊은 존경과 감사의 마음을 드립니다. 교수님의 아낌없는 격려와 가르침 덕분에 연구자로서 성장할 수 있었습니다. 또한, 바쁘신 일정에도 학위논문의 완성을 위해 조언해주시고 심사해주신 양수진 교수님, 허은미 교수님, 신성재 교수님, 신민경 교수님께 진심으로 감사드립니다.

처음 전염병학교실에 들어와 실험의 기초를 가르쳐주신 정명환 교수님, 본 학위논문의 처음과 끝을 함께해주신 박현의 박사님께도 감사를 전하고 싶습니다. 학위 과정 동안 긍정적인 마음가짐을 가르쳐 주시며 항상 응원해주셨던 Kuastros 박사님, 좋은 연구를 고민할 수 있도록 도와주셨던 박홍태 박사님께도 감사드립니다. 긴 학위 과정 동안 많은 연구를 함께하며 도와주셨던 임영빈 박사님, 박우빈 오빠, 심수진 박사님, 오명환 오빠, 소상희 언니께도 감사드립니다. 연구실 생활 동안 소중한 친구가 되어주었던 Salome, Lalina, 그리고 실습생 첫날부터 학위과정의 마지막까지 항상 응원해주신 세진언니께도 감사의 말씀을 드립니다. 학위과정동안 든든한 버팀목이 되어주었던 성운 오빠와 수민이 앞으로 전염병학교실을 이끌어 갈 준호, 운기에게도 감사를 전합니다. 저를 연구자의 길로 이끌어주신 한국외국어대학교 미생물생태학 실험실의 조기성 교수님, 정요찬 교수님, 김하늘 언니, 강희영 오빠, 이범일 오빠께도 진심으로 감사드립니다.

마지막으로 항상 저를 지지해주시고 응원해주시는 존경하는 저의 아버지, 어머니, 사랑하는 우리 언니와 모든 가족들분들께 진심으로 감사드립니다. 더불어 오랜 시간 동안 좋은 연구자로서 인생의 친구로서 힘들때마다 함께해준 유석오빠께도 감사드립니다. 다시 한번 힘이 되어주신 모든 분들께 머리 숙여 깊은 감사의 인사를 올립니다.